IESCA-2012

PRE-MEETING FIELD TRIP GUIDE-4

Late Cenozoic Extensional Tectonics and Sedimentation in Central and Northern Menderes Massif, Western Turkey*

by
Prof. Dr. İbrahim Çemen
Dr. E. Yalçın Ersoy
Prof. Dr. Cahit Helvacı
Dr. Özgür Karaoğlu
Dr. Zeynep Öner

** Portions of this field guide article is reprinted from Çemen et al. (2006), Karaoğlu et al. (2010), Öner and Dilek (2011), Karaoğlu and Helvacı (2012) and Ersoy et al. (2010, 2011, 2012a) (Please see the references for full citation)*

CONTENTS

FIELD TRIP ROUTE and DESCRIPTION of the STOPS

Day 1 - 29 September 2012, Saturday

İzmir, Manisa, Selendi, Güre, Uşak, Güre, Kula, Salihli, Alaşehir

The purpose of the first day is to have a detailed understanding of NE-SW-trending basins of the Northern Menderes Massif. Stratigraphy and tectonics of these basins will be discussed at stops in several keys outcrops of the basinal sediments. The contacts between the metamorphic basement rocks and overlying sedimentary rocks will be examined in several locations. The Kula Volcanics will be examined and their structural/tectonic importance will be discussed along several outcrops. The field trip route and the stops are indicated on Figure 10.

The road Akhisar-Gördes and STOP-1:

Along this route, Early Miocene sedimentary succession of the Gördes Basin can be seen. From the west to east, the basement rocks belong to İzmir-Ankara Zone can be traced. Further east, the sedimentary features of the Early Miocne Kızıldam and Köprübaşı formations will be examined (see also Figure 12). In the centre of the basin, the rhyolitic plugs cutting the basin fill will be examined (Figures 40 and 41) (**STOP-1**).

The road Gördes-Borlu and STOP-2:

This road section presents the metamorphic rocks of the Menderes Massif between the Gördes and Demirci basins (Figure 10). The middle Miocene Borlu and Köprübaşı formations will be traced (**STOP-2**).

The road Borlu-Demirci and STOP-3:

Along this route, faciess characteristics of the İnay Group in the Demirci Basin can be traced. Also, the left-lateral srike-slip fault segments of the Güneşli fault zone cutting the Asitepe volcanics can be examined (See Figure 35) (**STOP-3**).

The road Demirci-Simav and STOP-4 and STOP-5:

To the north of the Demirci, the unconformable contact between the İnay Group and Hacıbekir Group will be examined (see Figure 14a) (**STOP-4**). Here, the southern margin of the Simav half-graben, cutting the Neogene sewuence of the Demirci basin can be well traced (Figure 36). Along the road, the facies characteristics of the Hacıbekir Group will be examined. In the NW-margin of the Demirci Basin, the Simav detachment fault between the Lower Miocene Hacıbekir Group and the metamorphic rocks of the Menderes Massif can be seen (Figure 28) (**STOP-5**).

The road Simav-Güre and STOP-6:

This road section presents the well-preserved outcrops of the Yeniköy Formation of the Hacıbekir Group in the north of the Güre Basin. To the south along this route, the İnay Group can also be seen. Araund the Yenikent village, the İnay Group is cut by tha Yeniköy dikes of the Payamtepe volcanics (**STOP 6**).

The road Güre-Kula and STOP-7:

Along this route, the lamproitic outcrops of the Payamtepe volcanics (the Güre lamproite) can be seen.

The road Güre-Kula and STOP-8 and STOP-9:

Along this road section, the facies characteristics of the İnay Group in the Selendi basin can be examined. At the Gediz Bridge on the İzmir-Ankara road, the contact tectonic between the silicified ophiolitic rocks of the İzmir-Ankara zone and the metamorphic rocks of the Menderes Massif will be examined (See Figure 19) (**STOP-8**). Here, the tectonic contact is unconformably overlain by the Middle Miocene İnay Group. The cinder cones of the Kula volcanics will also be seen around the Kula (**STOP-9**).

Day 2 - 30 September 2012, Sunday

Alaşehir, Buldan, Denizli, Pamukören, Başçayır, Aydın

Alaşehir detachment and associated structures will be examined in several locations along the southern Margin of the Alaşehir Graben. The Basinal sediments of the Alaşehir Graben will be compared to the sediments in the NE-Trending basins and in the Denizli basin. The Turgutlu and Salihli Granodiorites will be examined. The Horzum Turtleback fault surface will be visited and its importance in the tectonics of Western Turkey will be discussed. The Büyük Menderes Detachment surface will also be examined along several outcrops north of the Village of Başçayır. Back to İzmir.

STOP-1. View Of The Alasehir Detachment Fault Along ~NW-SE-Trending (Basin-Parallel) Salihli-Alaşehir Main Road

General view of the N-Dipping, low-angle Alasehir detachment fault along the NW-SE direction.

The detachment fault surface is usually dipping to the NE or NW. It forms dome-shape morphology at the surface defined as turtle-back fault surfaces. Drainage system in the Alasehir supradetachment basin above the Alasehir detachment is mainly controlled by intrabasinal extensional fault generations and main stream valleys occur in E-W and N-S- direction due to extension-perpendicular and extension-parallel structure forming since Early Miocene continues extension. Approximately N-S-trending valleys cross-cutting the detachment surface define the deep incisions in the morphology, representing extension-parallel hinge structures. Some of these structures are well defined oblique rotational faults and accommodate differential uplift and extension rates throughout the entire basin and continue to the north. They display a significant role on the intrabasinal fault kinematics and the depositional processes due to vertical-axis rotation and differential uplift in their fault blocks, controlling the formation of local unconformities during the sedimentation in the Alasehir Basin.

STOP-2. View Of The Alasehir Detachment, Basin-Prependicular Faults, Supradetachment Basin Strata Along ~NE-SW-Trending (Basin Perpendicular) Yesilkavak-Degirmendere Road.

Along the road going up to higher elevations on the footwall of the detachment fault, we can have another closer view of the Alasehir detachment and extension-parallel hinge faults and extension-perpendicular high-angle normal faults. Buff-color, alluvial/fluvial clastic sediments represent the younger units of the basinal strata and unconformably overlie the older, red-colored Early-Middle Miocene units. This angular unconformity is a result of rotational deformation due to synchronous activity of different type of extensional faults, i.e. ~E-W-striking, high-angle normal faults (resulting in horizontal axis rotation, back-tilting), ~N-S-striking, rotational oblique faults (resulting in vertical axis rotation and changes in strike and dip orientations in the E-W direction). At this stop, we can see one of the main high-angle normal faults, representing the tectonic contact between Plio-Quaternary Yenipazar-Asartepe formations and Early Miocene Acidere formation. These high-angle normal faults get progressively younger towards north and form step-like structure in the basin.

STOP-3 General View Of The Alasehir Basin Along ~N-S View Around The Cakaldogan Village Road (Optional)

Along the Cakaldogan village road, we can see the Alasehir basin in ~N-S view and main high-angle normal faults occurred as basin-parallel. Modern Alasehir graben is observable at the further north and its boundary with Plio-Quaternary Yenipazar-Asartepe formations is defined by the seismically active, Alasehir-Derekoy-Yenipazar fault (most recent EQ activity 1969 Alasehir Earthquake of 6.5 magnitude). Buff-colored, alluvial-fluvial Yenipazar and Asartepe units represent depositional environment change from local lacustrine to axial alluvial fan environment in this time period. Red-colored Acidere and Gobekli formations characterize alluvio-fluvial depositional environment and occurrence of debris flow deposits due to accelerated seismic activity on high-angle normal faults in Early Miocene- Early Pliocene times. The wide stream valley trending in N-S direction (towards us on the picture) is most likely one of the high-angle, rotational hinge faults extending within the basin strata and into the Menderes massif. These transverse drainage systems were the main transporter of the sedimentary material sourced from the uplifting footwall of the Alasehir detachment fault. The bluish, altered rocks seen at the bottom of the photo are cataclastic rocks covering ~100 m zone above the detachment fault. At this stop, various footwall rocks such as cataclasite, mylonite, ultramylonite

STOP-4. View Of Dome-Shaped Geometry Of The Alasehir Detachment And Extensional Structures Around Horzumalayaka (Or Karadut)

The fault plane and slickenline measurements from the footwall of the Alasehir detachment fault show that the dip direction of the detachment surface is mainly northeast, indicating large-scale dome-shaped morphological feature. The oldest basin strata dipping southerlyy towards the detachment fault, indicating fault movement during and after sedimentation.

STOP-5. General View Of The Alasehir Supradetachment Basin and the Alasehir Detachment Fault From The South Of Kurudere Town Near Alasehir.

This is one of the best spots to see syn-extensional sedimentary rocks dipping into the detachment fault surface at the south of the basin and high-angle normal faults cutting the intrabasinal rocks in the ~E-W direction and result in back-tilting and rotation. The plain in the right-hand side of the image is the modern Alasehir graben, which is bounded to the south by the youngest and seismically active, high-angle normal fault, capable of generating earthquake of M=7 or bigger.

1. Introduction

Since the early 1900's, western Anatolia and the Aegean region have been recognized as being formed by crustal extension. High-angle crustal penetrating, normal faults were discovered and documented in the region throughout the early and middle parts of the 20th Century (e.g., Phillipson, 1910-1915; Erinc, 1955). The discovery of low-angle normal faults (e.g., Wright and Troxel, 1973; Wernicke, 1981) and recognition of metamorphic core complexes in the Basins and Ranges province of North America (e.g., Davis, 1980) changed our understanding of the geometry and evolution of extensional features worldwide and assisted modern geological studies in extended terranes. Although the metamorphic core complex origin of the Central Menderes Massif has been generally accepted today (e.g., Bozkurt and Park, 1994; Hetzel et al., 1995a, 1995b; Emre and Sözbilir, 1997; Gessner et al., 2001; Ring and Collins 2005), the origin, timing of initiation, geometry, and evolution of the major extensional features in western Anatolia remain controversial.

Models proposed for the origin of extension in western Anatolia include (1) tectonic escape (e.g., Dewey and Şengör, 1979; Şengör, 1979, Şengör and Yılmaz, 1981, Şengör et al., 1985) and its modification, the lateral extrusion (Çemen et al., 1993, 1999), (2) back-arc extension (e.g., McKenzie, 1978; Le Pichon and Angelier, 1979; 1981) in response to subduction roll back (e.g., Meulenkamp et al., 1988; Spakman et al., 1988), and (3) orogenic collapse (e.g., Dewey, 1988; Seyitoğlu and Scott, 1996; Dilek and Whitney, 2000). These models imply different timing for initiation of extension in western Anatolia. Tectonic escape models require initiation of extension in the Tortonian (Late Miocene) commensurate with westward movement of the Anatolian plate along the North Anatolian Fault System (Figure 1), whereas back-arc extension and subduction roll back models suggest that the extension started in Early Miocene as subduction along the Hellenic arc shifted southwest. The orogenic collapse model suggests that extension might have started as early as the Oligocene after Eocene thickening subsided.

Radiometric age determinations have been used in attempts to solve this controversy. Hetzel et al. (1995a,b) proposed that extension along the Alaşehir (or Gediz) Detachment began in the Early Miocene (19.5±1.4 Ma) based on the $^{40}Ar/^{39}Ar$ amphibole age from a "syn-extensional" granodiorite that they interpreted as intruding prior to brittle deformation along the detachment surface. This widely cited age (e.g., Hetzel et al., 1995b; Seyitoğlu and Scott, 1996; Gessner et al., 2001a; Lips et al., 2001) is the sole evidence for Early Miocene extension. However, the extensional origin of the granodiorite is controversial. Yılmaz et al. (2000) interpreted it as the product of crustal thickening during the formation of the Izmir-Ankara suture zone. In addition, the age spectrum and correlation diagram show that the amphibole is affected by excess argon, so its apparent age may be spuriously old, implying a younger age for initial extension.

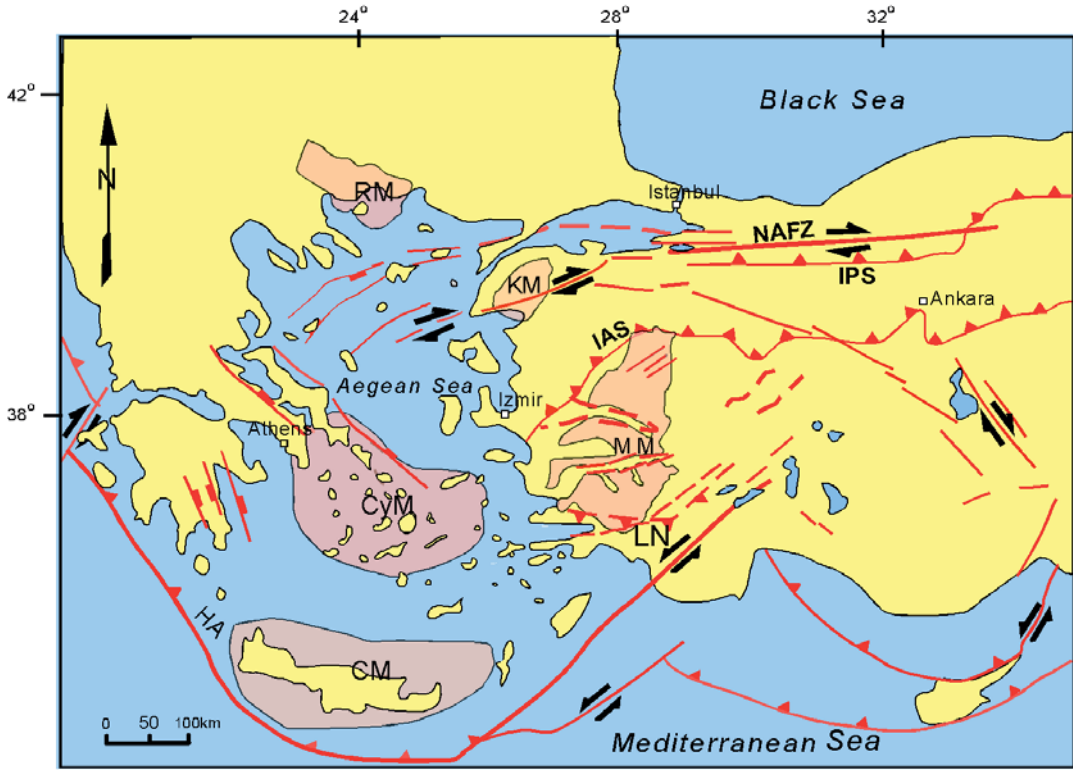

Figure 1. The simplified map of the Aegean extensional province showing major tectonic features and metamorphic massifs (From Çemen et al., 2006).

A bivergent rolling hinge model for the Central Menderes Massif was developed based on the two oppositely dipping Alaşehir and Büyük Menderes Detachments (Figure 2) (Gessner et al., 2001a). In this model, the two detachments developed as high normal faults in Early Miocene. The Alaşehir Graben of the Central Menderes Massif may have formed by a process similar to the rolling hinge/flexural bending model of extension proposed for the Death Valley Graben of the Basins and Range province (see Seyitoğlu et al., 2002; e.g., Hamilton, 1988; Wernicke et al., 1988; Wernicke, 1988; Holm et al., 1992; Wernicke, 1992).

Ring et al., (2003) proposed that extension in western Anatolia has been initiated in the Late Oligocene, along two oppositely dipping symmetric, deep-seated detachment surfaces that unroofed the high-grade metamorphic rocks of the Menderes Massif in the Late Miocene, similar to the flexural rotation-deep seated normal fault model processes (e.g. Buck, 1988). They also proposed that a second episode of extension started around the Miocene-Pliocene boundary, again along two oppositely dipping symmetric, deep-seated high-angle normal faults. Alternatively, extension in the Menderes Massif may have initiated by a north-dipping listric main breakaway in the Late Oligocene as proposed by Seyitoğlu et al., (2004). In this scenario, the Alaşehir and Büyük Menderes Detachments initiated in the Early Miocene as high-angle normal faults and became low angle normal faults in response to footwall rotation as Cenozoic extension has continued (Seyitoglu et al., 2002 and 2004). Based on their Monazite ages, Catlos and Çemen (2005) also proposed that extension in western Anatolia may have occurred in two uninterrupted, continuous stages. The first stage started in the Oligocene and lasted until the Early Miocene. The second stage started in the Early Miocene and continues at present.

Purvis and Robertson (2004) proposed a "pulsed extension" model for western Turkey. This model suggests that the Cenozoic extension in western Turkey has been produced in three phases. They related the first two-phases to rollback of the Aegean subduction zone and the third phase to the tectonic escape of Anatolia.

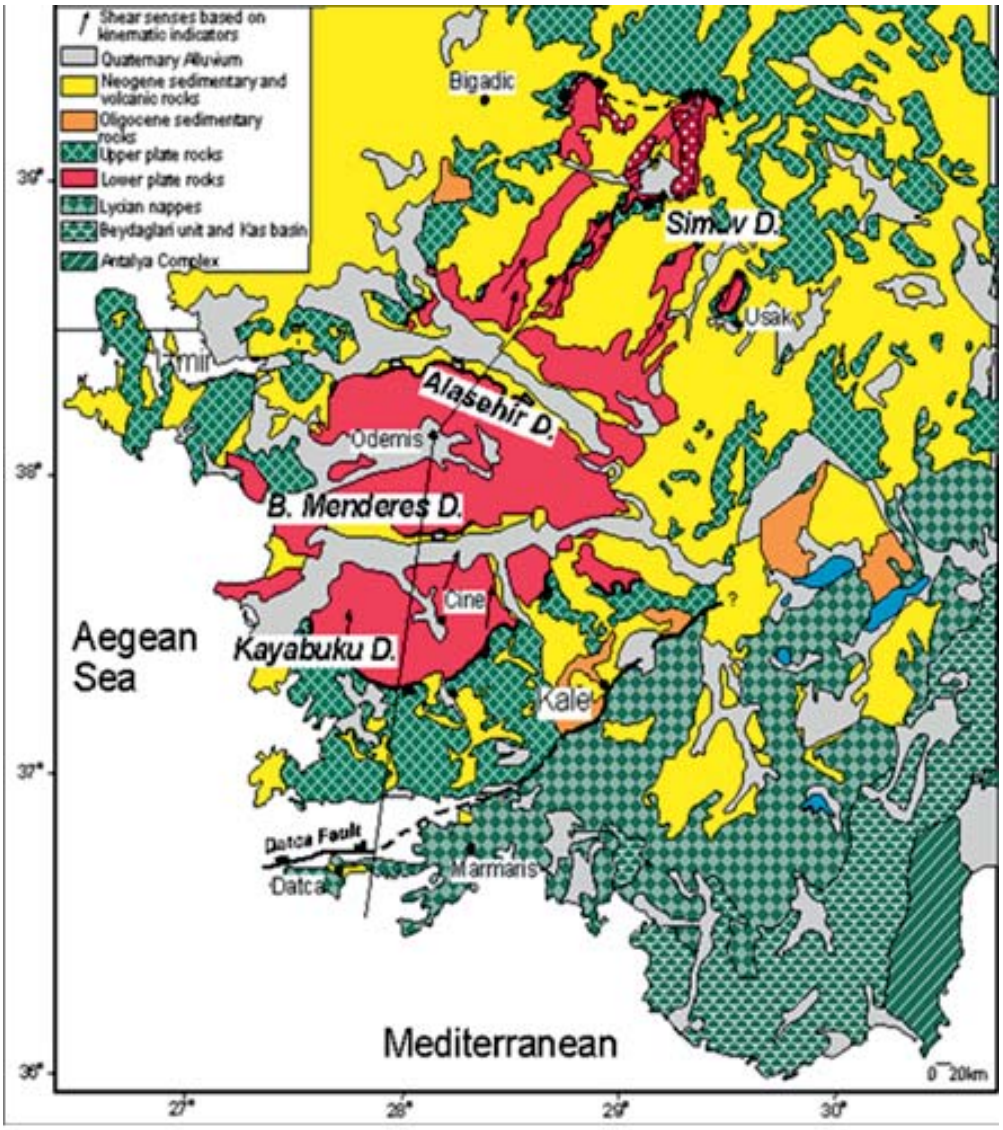

Figure 2. Simplified geologic map illustrating major tectonic features and lithostratigraphic units in western Anatolia, (from Çemen et al., 2006).

2. Tectonic Setting of The Western Anatolia

The geology of Western Anatolia is characterized by late Tertiary volcano-sedimentary deposits covering a basement that includes several continental fragments and suture zones. The basement units comprise; (1) the Menderes and Cycladic massifs, (2) the İzmir-Ankara Zone (comprising; (a) the Bornova flysch zone, (b) the Afyon zone, and (c) the Tavşanlı zone, (3) the rocks of the Sakarya Continent to the north, and (4) the Lycian Nappes to the south (e.g., Şengör and Yılmaz, 1981; Figures 1 and 2). The İzmir-Ankara zone was formed by late Paleocene to early Eocene closure of the northern branch of the Neo-Tethys Ocean between the Sakarya continent and the Anatolide block, with the latter including the Menderes Massif and the Lycian Nappes (e.g., Şengör and Yılmaz, 1981; Okay et al., 2001).

2.1. Menderes Massif

The Menderes Massif is a large metamorphic massif with an exhumed ellipsoidal shape. The massif has traditionally been divided into two sequences: a "*core"* composed of augen gneisses, metagranites, schists, paragneisses and metagabbros; and a "cover" composed of schists, quartzites, amphibolites, phyllites and marbles (Akkök, 1983; Şengör et al., 1984; Candan et al., 1997, 2001; 2011). The core of high-grade metamorphic rocks was thought to have deformed during the Pan-African orogeny (Cambro-Ordovician; Şengör et al., 1984), whereas the cover contains Paleozoic schist and Mesozoic-Cenozoic marble that experienced regional metamorphism during the Alpine orogeny (Sengör et al., 1984). More recent field studies document the presence of nappes that formed during the formation of the Izmir-Ankara suture zone (see Ring et al., 1999; Gessner et al., 2001b). The Bayindir nappe is structurally lowest, and consists of Paleozoic-Mesozoic rocks, deformed and metamorphosed at least once in the Cenozoic. This metamorphism, often referred to as the "Main Menderes Metamorphism," is commonly assumed to be Paleocene-Eocene in age and to have been pervasive throughout the massif. The overlying Bozdag nappe is composed of metapelite with intercalated amphibolite, eclogite, and marble lenses. The Cine nappe is made up of orthogneiss and paragneiss with intercalated metabasite. The Selimiye nappe, Cycladic blueschists, and Lycian nappes overlie the Cine and Bozdag nappes and contain high-P, low-T assemblages (e.g., Mg-carpholite) (e.g., Oberhänsli et al., 1998). The Menderes Massif is tectonically overlain by several nappes of the İzmir-Ankara Zone to the west and north, and by the Lycian nappes mainly to the south and east. In the west, the nappes are generally composed of graywackes and limestones with ophiolitic rocks of the Bornova flysch zone, while to the northeast, they are metaclastics, metabasites, and recrystallized limestones of the Afyon zone (Figures 1 and 2).

In the following sections, we summarize the previous work done to understand the geologic history of the Menderes Massif via geochronology, thermobarometry, and field observations. Other structural, metamorphic, and geochronologic summaries include: Bozkurt and Oberhansli (2001), Gessner et al. (2001b), Regnier et al. (2003), and Rimmele et al. (2003).

2.1.1. Geochronology and Thermobarometry

In the Northern Menderes Massif, rocks experienced peak metamorphic conditions of ~5.3 kbar to ~9.2 kbar and ~572°C to ~712°C, which have been correlated to metamorphism during the Pan African orogeny (Candan et al., 2001), or perhaps, corresponding to the closure of the northern Karakaya marginal basin (e.g., Akkok, 1983). The presence of Late Cambrian metamorphism or magmatism in the Northern Menderes Massif are based on six whole rock Rb-Sr analyses which yield 471±9 Ma (Satır and Friedrichsen, 1986) and in situ ion microprobe ^{207}Pb-^{206}Pb zircon ages that average 508±92 Ma (Catlos and Çemen, 2005) (Table 1). However, the pressure-temperature (P-T) conditions could record more recent metamorphism, as Th-Pb ion microprobe ages of monazites from the Bozdağ and Cine nappes in the Northern Menderes Massif range from 52.9±5.7 Ma to 26.9±0.6 Ma (Table 2; Catlos and Çemen, 2005). K-Ar and ^{40}Ar/^{39}Ar ages of muscovite and biotite are

are Early to Middle Miocene, which have been typically related to regional metamorphism. Apatite and zircon fission track ages in the Northern Menderes Massif average 19.5±1.3 Ma (Gessner et al., 2001a; Ring et al., 2003), suggesting that the rocks were near the surface by the Early Miocene.

Table 1. Matrix 207Pb-206Pb ion microprobe zirzon age data from Gördes massif (Catlos and Cemen, 2005).

Grain_spot[a]	Age[b] (Ma) (± 1σ)	%^{206}Pb*[c] (± 1σ)
5_1	558 (62)	96.8 (0.1)
4_1	499 (134)	98.5 (0.3)
3_1	493 (79)	99.5 (0.2)
2_1	481 (78)	99.5 (0.2)

The Central Menderes Massif consists largely of three major lithological units: gneiss, schist, and marble (e.g., Akkök, 1983; Gessner et al., 2001a). The gneiss underlies the schist and marble, and is composed of porphyroblastic and augen gneisses with minor amounts of banded gneiss and massive granite gneisses, whereas the schist contains garnet-mica schist, quartzite, and augen schist, and is intruded by the Dede Dağı granite which contains lenses of serpentinite (e.g., Akkök, 1983). The northern segment of the Central Menderes Massif may have experienced a more complicated history than the southern segment due to its proximity to the Pontides and Anatolide-Tauride platform. The schist and marble in the north have been speculated to have experienced three major phases of metamorphism (Akkök, 1983).

The first major phase which occurred during the Cambro-Ordovician (Pan African) is recorded by U-Pb zircon and Th-Pb monazite ages (Hetzel et al., 1998; Catlos and Çemen, 2005). During this time, rocks from the massif may have reached eclogite conditions as high as ~730°C and ~15.1 kbar (Candan et al., 2001; Ring et al., 2001). However, depending on location, this event may have also resulted in more moderate greenschist facies as low as ~4.9 kbar and ~512°C (Candan et al., 2001).

Table 2. Monazite age data from Gördes massif (Catlos and Cemen, 2005).

Grain-spot[a]	Location[b]	Th–Pb age (± 1σ) (Ma)	ThO_2^+/Th^{+c} (± 1σ)	%^{207}Pb*[d] (± 1σ)	208Pb*/Th^{+c} (± 1σ)
59-19-124b					
4-1	i	39.7 (0.9)	3.339 (0.020)	95.1 (1.0)	1.966E-03 (4.488E-05)
5-1	i	37.9 (1.1)	3.047 (0.023)	96.5 (0.6)	1.877E-03 (5.406E-05)
3-1	i	36.1 (0.8)	3.447 (0.034)	95.7 (0.7)	1.788E-03 (4.033E-05)
1-1	m	32.8 (0.5)	3.864 (0.020)	96.8 (0.5)	1.625E-03 (2.286E-05)
01-26					
1_1	i	36.0 (0.6)	4.130 (0.011)	96.8 (0.5)	1.784E-03 (3.170E-05)
3_2	m	41.4 (1.3)	3.007 (0.013)	92.4 (0.9)	2.050E-03 (6.568E-05)
2_1	m	38.4 (0.8)	3.499 (0.048)	92.3 (1.0)	1.903E-03 (4.086E-05)
3_1	m	33.6 (0.7)	3.873 (0.023)	90.9 (1.2)	1.664E-03 (3.356E-05)
5_1	m	33.6 (0.8)	3.364 (0.007)	95.8 (0.6)	1.662E-03 (3.879E-05)
5_1	m	33.0 (0.5)	2.487 (0.006)	91.5 (0.9)	1.444E-03 (1.685E0–5)
4_1	m	29.6 (1.1)	3.416 (0.021)	74.5 (2.4)	1.463E-03 (5.458E-05)
6_2	m	29.2 (0.3)	2.913 (0.006)	91.8 (0.7)	1.444E-03 (1.685E-05)
6_1	m	28.2 (0.4)	2.814 (0.009)	86.9 (0.9)	1.398E-03 (1.806E-05)
30					
5_1	m	52.9 (5.7)	2.395 (0.016)	88.2 (1.4)	2.619E-03 (2.823E-04)
4_1	m	43.2 (3.6)	2.558 (0.019)	91.0 (1.1)	2.140E-03 (1.767E-04)
2_1	m	42.7 (0.9)	3.453 (0.010)	93.4 (0.7)	2.116E-03 (4.318E-05)
3_1	m	41.4 (1.7)	3.007 (0.010)	94.2 (0.7)	2.050E-03 (8.273E-05)
1_1	m	40.1 (0.9)	3.400 (0.011)	96.0 (0.8)	1.985E-03 (4.534E-05)
6_3	m	35.1 (0.3)	2.424 (0.005)	93.5 (0.4)	1.739E-03 (1.702E-05)
5_2	m	27.9 (1.0)	4.824 (0.058)	75.9 (1.7)	1.380E-03 (4.880E-05)
6_2	m	26.9 (0.6)	4.420 (0.015)	86.4 (0.9)	1.330E-03 (3.114E-05)

Calibration: $y = (0.078 \pm 0.002)x + 1.196 \pm 0.045$, $r^2 = 0.988$, $ThO_2^+/Th^+ = 2.729 \pm 0.014$[f]

The second phase occurred during Late Cretaceous-Early Eocene (Alpine) regional metamorphism (Akkök, 1983; Ring et al., 2001). Blueschist metamorphism occurred at 39.6±0.4 Ma (Okay et al., 1998) along the western peninsula of the Menderes Massif, in which rocks experienced ~10 kbar and <470°C (Candan et al., 1997).

The third phase, which occurred during the Early to Late Miocene, is a retrograde metamorphic event (e.g., Akkök, 1983). Muscovite $^{40}Ar/^{39}Ar$ ages of a rock from the north dipping Alaşehir Detachment of the Central Menderes Massif yields 7±1 Ma indicating the reactivation of the detachment fault, whereas the south-dipping Büyük Menderes Detachment muscovite grains record $^{40}Ar/^{39}Ar$ ages that are Oligocene to Early Miocene (Gessner et al., 2001a; Lips et al., 2001; Ring et al., 2003). Other granodiorites from the northern massif yield Late Miocene ages (Gessner et al., 2001a; Ring et al., 2003).

As with the Central and Northern Menderes Massifs, the Southern Menderes Massif contains evidence of a Cambro-Ordovician, Eocene-Oligocene to Late Miocene geologic history. Peak P-T conditions ascribed to the Pan African orogeny range from ~8 kbar to ~12 kbar at ~440ºC to ~643ºC (Candan et al., 2001; Regnier et al., 2003; Rimmele et al., 2003). However, these conditions are no different than those that have been ascribed to Late Cretaceous-Early Eocene regional metamorphism (~4 kbar to ~12 kbar and ~430ºC to ~675ºC; Whitney and Bozkurt, 2002; Regnier et al., 2003). Oxygen isotope temperatures of ~514ºC to ~529ºC have been reported from the range (Satır and Taubald, 2001), although the origin of the event that created these conditions remains unknown.

The difficulty in ascribing peak P-T conditions achieved by rocks within the Menderes Massif to specific events underscores the region's complicated tectonometamorphic history. Catlos and Çemen (2005) report both Cambro-Ordovician and Eocene-Oligocene monazite inclusions in Menderes Massif garnets, indicating that garnet growth events occurred during both the Pan African and Alpine orogenies. Garnet-based thermobarometric methods are typically used to generate the P-T estimations (e.g., Ashworth and Evirgen, 1984; 1985), and rocks in the massif may have experienced multiple episodes of deformation (Catlos and Çemen, 2005), which can affect mineral compositions and thus, the reported P-T conditions.

2.1.2. Structural Geology

The tectonic contacts between the tectono-stratigraphic units, described above, have long been interpreted as thrusts. However, after the discovery of low-angle normal faults between; (a) the core and the cover rocks of the Menderes Massif (Bozkurt and Park, 1994); (b) the metamorphic rocks of the Menderes Massif and the non-metamorphic rocks of the İzmir-Ankara zone (Lips et al., 2001; Işık and Tekeli, 2001); and (c) the metamorphic rocks of the Menderes Massif and the Neogene volcano-sedimentary units (Hetzel et al., 1995; Emre, 1996; Emre and Sözbilir, 1997; Purvis and Robertson, 2004; Ersoy et al., 2010), it is now widely accepted that the massif was exhumed along low-angle normal detachment faults or shear zones. Field studies in the Northern, Central and Southern Menderes Massif document the presence of four low-angle detachment surfaces (Figure 2). They are, from north to south, the Simav detachment fault (SDF, Işık and Tekeli, 2001; Işık et al., 2003), Alaşehir (Gediz or Kuzey) Gediz detachment fault (GDF; Emre, 1996; Ring et al., 1999a; Ring et al., 2003; Lips et al., 2001; Gessner et al., 2001b; Bozkurt and Sözbilir, 2004; Seyitoglu et al., 2000; 2002 and 2004; Çiftçi and Bozkurt, 2009), Büyük Menderes (Güney) detachment fault (Emre and Sözbilir 1997; Lips et al., 2001; Gessner et al., 2001a,b), and Kayabükü detachment fault or Selimiye shear zone (SSZ; Bozkurt and Park, 1994; Régnier et al., 2003, 2007; Bozkurt, 2007). In this section, we describe the geometry and shear-sense indicators of these structural features.

The Simav Detachment Fault lies in the northern part of the Menderes Massif (Işık and Tekeli, 2001; Işık et al., 2003, 2004; Ersoy et al., 2010; Figure 2). The Simav Detachment Fault separates Pan-African–Paleozoic rocks containing migmatitic banded gneiss, biotite gneiss, high-grade schist, marble, and amphibolite in its footwall from low-grade Upper Paleozoic metamorphic rocks,

Mesozoic limestone, and ophiolitic mélange in its hanging wall. The footwall rocks experienced low to medium greenschist-facies conditions. Kinematic indicators that developed during cooling and uplift of the footwall indicate top to the north-northeast shear sense (Işık et al., 2003). Mylonitic stretching lineations consistently indicate top to the north shear-sense direction. Kinematic data also show that trends of the lineations range from N10°E to N30°E. Considering that mylonitic lineations form parallel to the direction of extension, the measurements define well-developed N10°E to N30°E directed extension (see Çemen et al., 2006).

Systematic strike and dip measurements of foliation surfaces in the Northern Menderes Massif indicate the presence of major antiformal and synformal structures. Çemen et al (2006) mapped these antiformal and synformal structures in the Usak area (Figures 3, 4 and 5) and determined that their axial surface traces have a northeastward trend. In the Northern Menderes Massif, the hinge lines of mesoscopic folds have a trend parallel to the axial surfaces of the major folds. The hinge lines of the major and minor folds trend between N10°E to N30°E (Figure 5) and are parallel to the trend of the stretching lineations (Figure 5). This geometry suggests a genetic relationship between the stretching lineations and small and large folds. These folds were probably formed by the contractional component of the N30E directed extension since their axes are parallel to the extension direction. Footwall rocks of the Simav Detachment are intruded by the syn-extensional Koyunoba and Egrigöz granodiorites during early stages of extension in the Early Miocene (Işık et al., 2003b; 2004; Ring et al., 2003).

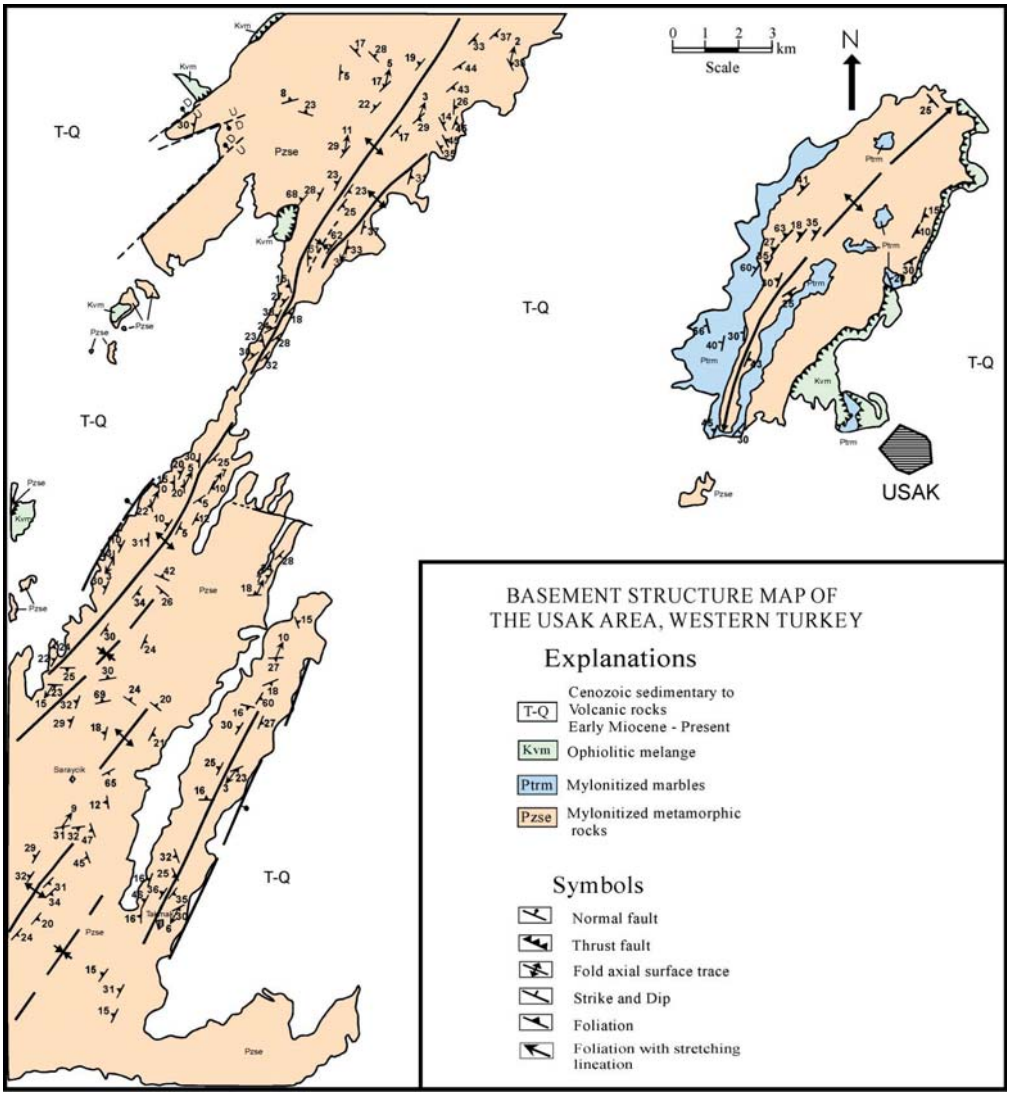

Figure 3. Simplified Basement structure map of the Uşak-Güre area showing large antiforms and synforms trending N10°E to N30°E.

Figure 4. Field photo showing an extension parallel antiform and synform pair to the north of the town of Kula, looking northward. The hinge lines of the antiform and synform trend about N30E parallel to small scale anform and synforms superimposed onto the large folds. The ductile stretching lineation direction (~N30°E) is parallel to the hinge lines of these folds.

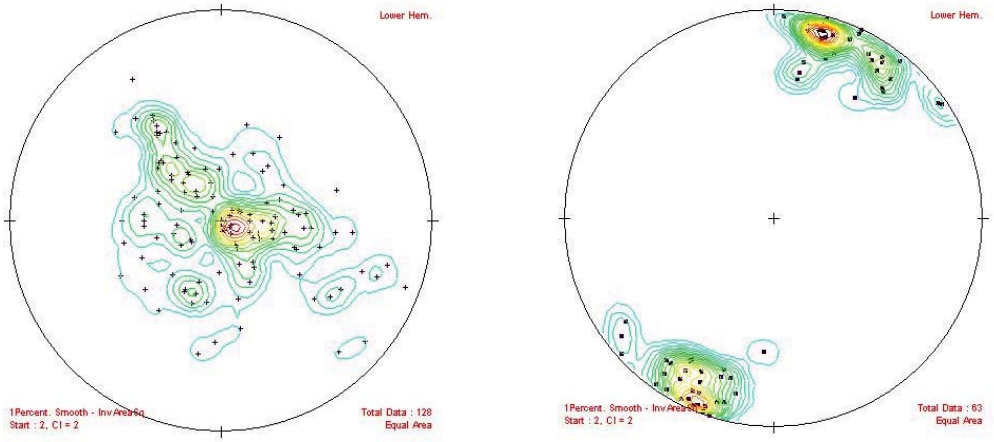

Figure 5. (A) 1 % contouring of the poles to the foliation planes of small scale folds in the Northern Menderes Massif. The fold axes are striking approximately N30E. (B) 1 % contouring of trend and plunge of the extensional stretching lineations in the Northern Menderes Massif. The trend of the lineations is also about N30E, parallel to the fold axes, indicating that they are formed in the same stress field (See text for explanation).

Field-oriented geological studies in the Central Menderes Massif indicate the presence of the north-dipping Alaşehir and the south-dipping low-angle Büyük Menderes Detachment surfaces on the northern and southern margin of the Central Menderes Massif, respectively (Figure 2) (e.g., Hetzel, 1995a; Emre, 1996, Seyitoğlu et al., 2000; Gessner et al., 2001). In the Central Menderes Massif, Hetzel et al. (1995b) and Gessner et al. (2001b) reported the presence of an overall dome-shaped foliation pattern and north-northeast trending stretching lineations parallel to the stretching lineations of the Northern Menderes Massif. The asymmetry of shear bands and quartz c-axis

fabrics on either side of the structural dome record a top to the north-northeast shear sense across the Alaşehir Detachment and a top to the north and south-southwest shear sense along the Büyük Menderes Detachment surface, although top to the NE shear sense indicators along the Büyük Menderes Detachment are also present (see Hetzel et al., 1995b; Gessner, 2001b). Based primarily on the presence of a north-dipping detachment surface with top to the north-northeast shear indicators and a south-dipping detachment surface containing both top to the north and top to the south shear sense indicators, Gessner et al. (2001a) proposed a bivergent rolling hinge detachment system as a mechanism of exhumation of the Central Menderes Massif in western Turkey.

The footwall of the Alaşehir Detachment is composed of gneiss, schist, quartzite marble intruded by synextensional Salihli and Turgutlu granitoids (Hetzel et al., 1995b). The Alasehir supradetachment basin, developed in the hanging wall of the Alaşehir Detachment contains Neogene sediments. Ductile deformation in the footwall of the detachment produced mylonitic foliation and stretching lineations. Kinematic indicators include mesoscopic and microscopic features, such as mica fish, S-C, and C' fabric, oblique foliation, and fractured and displaced grains. A brittle deformational stage of the shear zone is defined by development of cataclastic rocks (Işık et al., 2003a).

The footwalls of both the Simav and Alaşehir Detachments contain well developed ductilely deformed fault rocks displaying top to the north ductile shear sense indicators that are progressively overprinted by top-to-the NNE brittle deformation (Emre, 1996; Kocyigit et al., 1999; Sozbilir, 2001; Isik et al., 2003a, Öner et al., 2009). The granitoids show a gradual change structurally upward from undeformed granodiorite to protomylonite, mylonite, and ultramylonite with extensional mylonitic foliation and lineation. The metamorphic rocks are also mylonitized structurally upward. The deformed granitoid, in turn, grades into a cataclastic zone with the uppermost part composed of the brittlely deformed rocks of the Alaşehir Detachment. This gradual upward change from the undeformed granitoid to brittlely deformed detachment surface suggests that the Cenozoic extension resulted in a ductile deformation at depth and, as the crust adjusted to the removal of rocks in the hanging wall of the detachment, ductility deformed rocks were brought to shallower depths where they were brittlely deformed (Işık et al., 2003a). Both ductile and brittle shear sense indicators along the Alaşehir Detachment surface show top to the north-northeast shearing, suggesting that the northeasterly directed Cenozoic extension produced a large regional extensional shear zone at depth.

The southern margin of the Alaşehir Graben (Figure 2) is locally bounded by a turtleback fault surface known as the Horzum Turtleback (Çemen et al., 2005). The turtleback is a part of the Alaşehir Detachment, which contains mylonitic lineations trending between N10°E to N30°E. Striations along the detachment surface also trend between N10°E to N30°E and overprint the mylonitic lineations. These observations suggest a structural relationship between the Alaşehir Detachment, which contains the Horzum Turtleback in its footwall, and the Simav Detachment surface, which contains large-scale antiformal structures of the Northern Menderes Massif in its footwall (Figure 1). Çemen et al. (2005) suggest that the Horzum Turtleback is a large-scale, extension-perpendicular antiformal fold similar in origin to the Death Valley turtlebacks.

The Büyük Menderes Detachment surface is well exposed along the northern margin of the Büyük Menderes Graben. The fault generally strikes N50°E to N50°W and dips about 15° to 30° southward. It separates a sequence of high-grade metamorphic gneisses and a Lower-Miocene sedimentary rock succession in its hanging wall from marble intercalated, mylonitized schists in its footwall (Göğüş et al., 2003 and Göğüş, 2004).

The hanging wall of the Büyük Menderes Detachment consists of quartzofeldspathic gneiss and Early-Miocene sedimentary rocks of the Haskoy formation. The gneiss has an assemblage of K-feldspar + quartz + plagioclase + muscovite + biotite ± garnet. Quartz grains typically form elongate domains and polycrystalline ribbons suggesting that they experienced ductile conditions. Feldspars commonly have reaction rims of biotite and muscovite, and plagioclase is altered into sericite. Biotite is typically altered to foliation parallel chlorite. Foliations in the gneiss sequence are characterized by recrystallized quartz, feldspar and biotite (Göğüş, 2004).

The presence of high-grade metamorphic gneiss in the hanging wall of the Büyük Menderes detachment has been problematic. The detachment was first mapped by Emre and Sözbilir (1997) as a normal fault surface. They named it as the Başçayır Detachment because it is well exposed in the vicinity of the Başçayır village. Gessner et al (2001) also interpreted this surface as a low angle normal fault. Okay (2001) mapped the Büyük Menderes Detachment surface as a thrust fault based on the apparent older over younger field relationship. He proposed the presence of a large recumbent fold (the Menderes Fold) formed during pre-extension tectonism in the region. Okay, (2001 and 2002) suggested that the high-grade gneiss were brought over the marble intercalated mylonitized schists by a low angle thrust fault during the Eocene contractional tectonics in the region. However, Gessner et al. (2002) pointed out that within a structure similar to the Menderes massif fold-thrust fault and low-angle normal fault geometries can be found together. Consequently, a low angle normal fault can show older over younger geometry. Moreover, the presence of a) extensional stretching lineations along the detachment surface; and b) Miocene sedimentary rocks overlying the high-grade metamorphic gneiss in the hanging wall of the Büyük Menderes Detachment suggest extensional low angle faulting.

The Büyük Menderes Detachment surface is typically marked by cataclastic rocks and is well-exposed in the vicinity of the Başçayir Village (Figures 6 and 7). Cataclastic zones are commonly more than 1 m thick and grade into fractured rock adjacent to the fault. Most of the cataclastic rocks are composed of fractured marble, which is derived from the non-mylonitic marble-intercalated schists of the footwall (Figure 7).

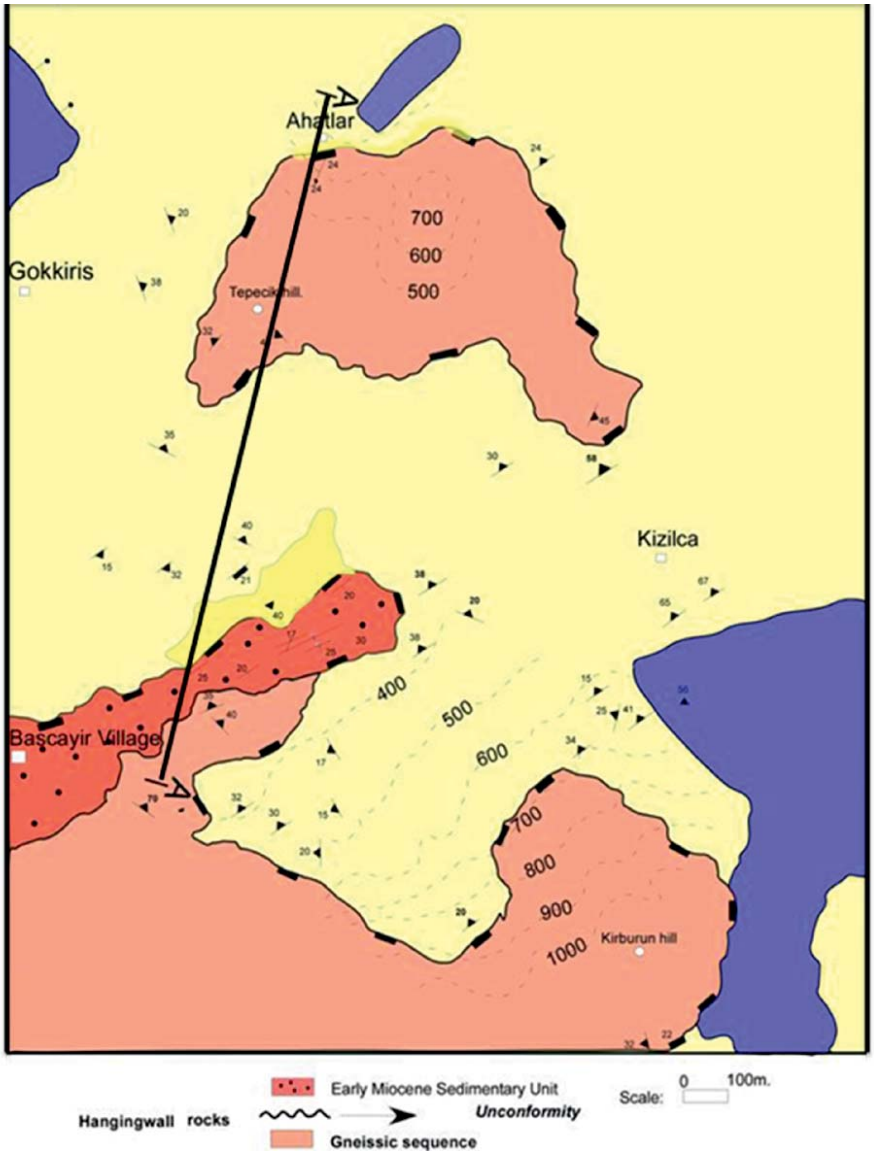

Figure 6. Geologic map of the Büyük Menderes Detachment area in the vicinity of Bascayir village. Cross-section is given in Figure 7 (from Göğüş, 2004).

At structurally lower levels, the fault rocks are ductilely deformed and display S-C and S-C asymmetric structures, schistosity, asymmetric mica fish, isoclinal folds, and asymmetric porphyroclasts. These features suggest top to the north sense of shear. Northward directed ductile shear sense indicators are overprinted by southward-directed ductile shear sense indicators, such as asymmetric porphyroclasts, mica fish, and asymmetric quartzite. These ductile features are overprinted by top to the-south brittle shear sense indicators, including Riedel shears (Figure 7).

These findings suggest that the Büyük Menderes Detachment may have developed in more than one stage; earlier ductile extension with top to the north sense of tectonic transport, overprinted by top to the south tectonic transport again under ductile conditions. The top to the south tectonic transport must have continued as the footwall rocks reached the higher crustal levels to produce brittle top to the south shear sense indicators (Göğüş et al., 2003 and Göğüş, 2004). The footwall rocks are made of foliated micaschists and marbles (Figure 7), with micas showing undulose extinction, indicative of intracrystalline cataclasis.

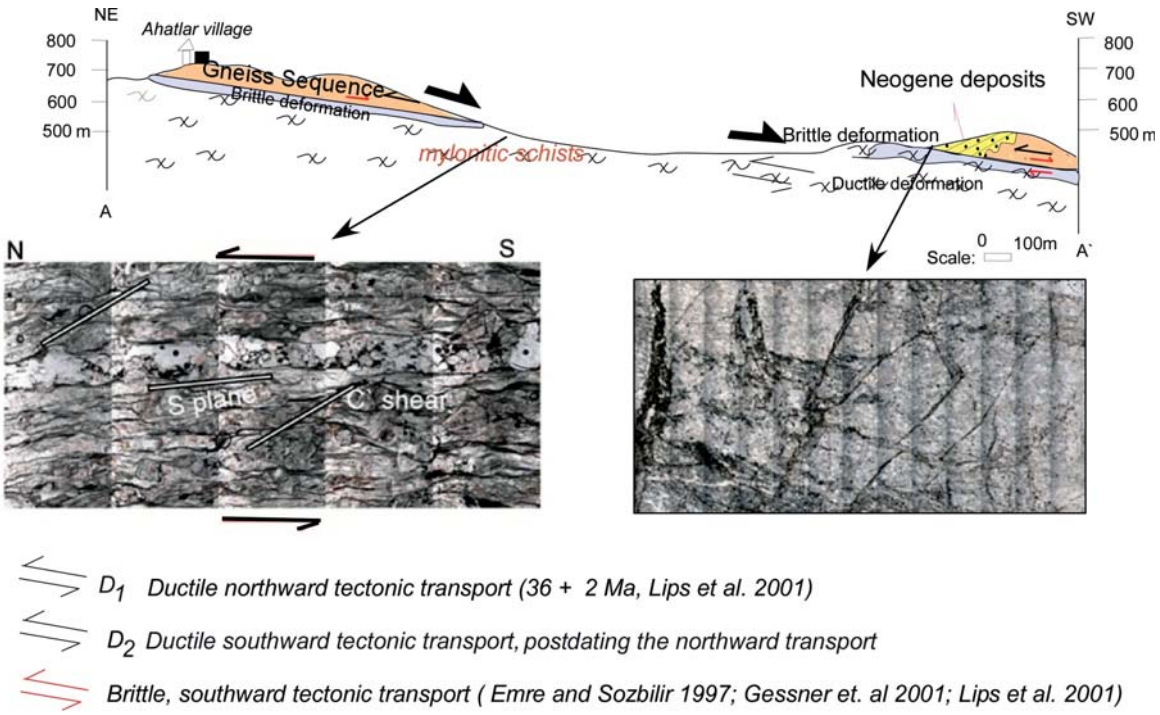

Figure 7. Geologic cross-section along line A-A' and two photomicrographs showing top to the north ductile shear sense indicators, overprinted by top to the south ductile and brittle shear sense indicators (from Göğüş, 2004).

In the Southern Menderes Massif, coarse-grained augen gneisses are separated from pelitic schists by a major extensional shear zone, termed the Kayabükü Shear Zone, that exhibits a moderately dipping mylonitic foliation and a north-northeast to south-southwest trending mineral lineations (Bozkurt and Park, 1994; Hetzel and Reischmann, 1996; Işık et al., 2003b). The augen gneisses display various kinematic indicators (e.g. S-C fabric, extensional shear cleavage, asymmetric feldspar porphyroclasts, and oblique quartz grain-shape foliation) suggesting top to the south, down-dip sense of shearing (e.g., Bozkurt and Park, 1994).

Preliminary investigation and data collection along the Kayabuku Deatchment surface suggest that the surface is characterized by mostly top to the north ductile shear-sense indicators (Işık et al., 2003b). The detachment surface also contains secondary top to south shear sense indicators that overprinted the top to the north shear indicators (Işık et al., 2003b) that may have formed during the back-slippage along the shear zone. However, further systematic analyses of shear-sense indicators along the Kayabükü Detachments are necessary to ascertain the validity of this hypothesis.

3. Ne–Sw-Trending Basins

3.1. Stratigraphy

The late Tertiary volcano-sedimentary basins in Western Anatolia (the eastern part of the Aegean Extensional Province) can be grouped as follows: (a) the Oligocene–Miocene molasse basins (Sözbilir, 2002, Çemen et al., 2006); (b) the Neogene volcano-sedimentary basins (Ercan et al., 1978; Şengör, 1987; Seyitoğlu and Scott, 1991, 1994a; Helvacı, 1995; Helvacı and Yağmurlu, 1995; Seyitoğlu, 1997a; Helvacı and Alonso, 2000; Yılmaz et al., 2000; Purvis and Robertson, 2004; Ersoy et al., 2010; 2011); and (c) the Pliocene-Quaternary E–W-trending grabens (e.g., Cohen et al., 1995; Emre, 1996; Hakyemez et al., 1999; Bozkurt and Sözbilir, 2004; Çiftçi and Bozkurt, 2009).

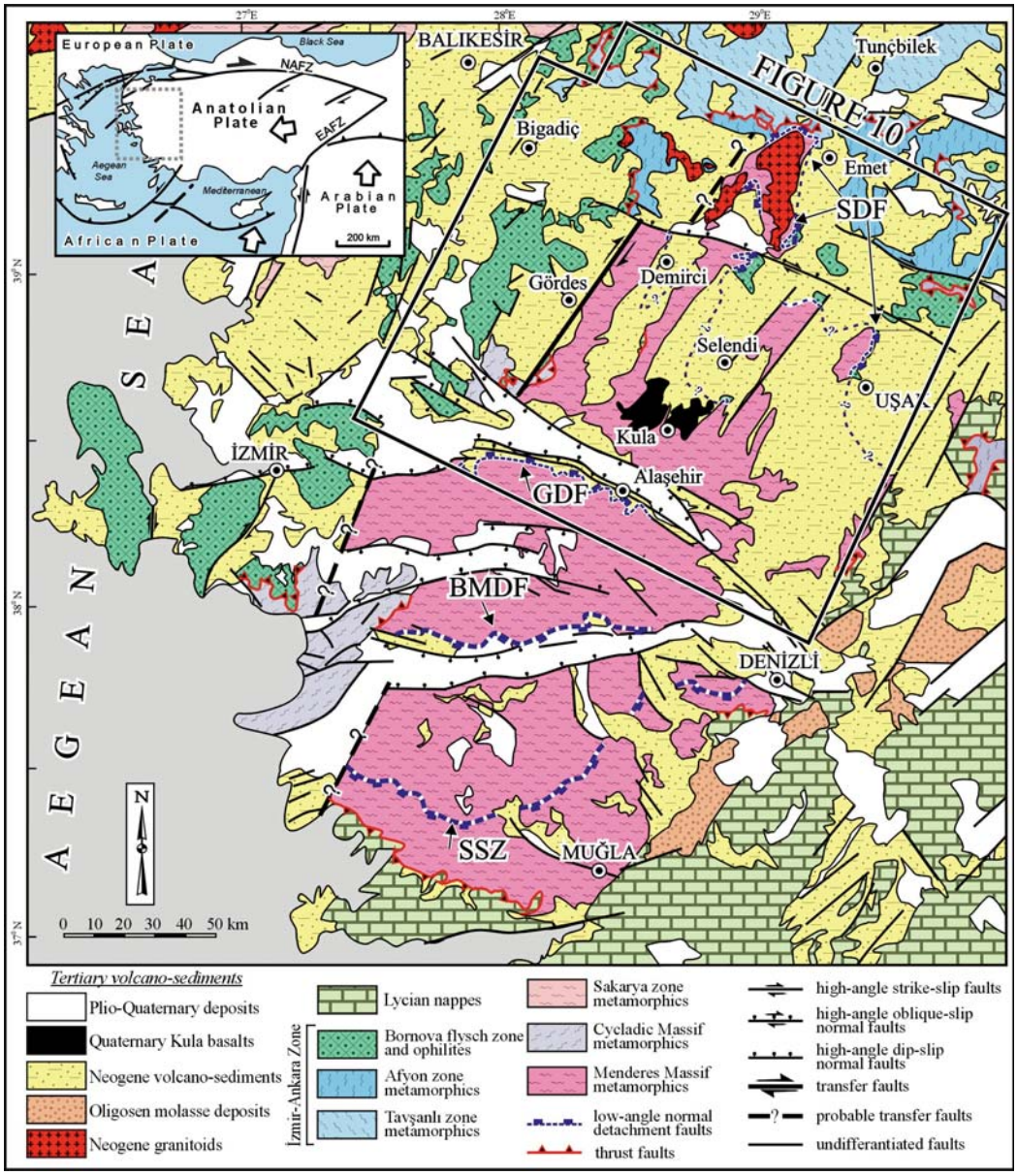

Figure 8. Generalized geological map of western Anatolia, showing the main tectono-stratigraphic units and tectonic elements (modified from Geological Map of Turkey (1:500000), 2002). NAFZ-North Anatolian Fault Zone, EAFZ-East Anatolian Fault Zone, SDF-Simav detachment fault, GDF-Gediz detachment fault, BMDF-Büyük Menderes detachment fault, SSZ-Selimiye shear zone (from Ersoy et al., 2011).

The Neogene volcano-sedimentary deposits, which are located on the northern part of the Menderes Massif, were mainly developed in NE–SW-trending basins that are cut and displaced by nearly E–W-trending active high-angle normal faults bounding the Pliocene-Quaternary grabens. The NE–SW-trending Miocene basins in the region are, from west to east, the Bigadiç (Helvacı, 1995; Helvacı and Yağmurlu, 1995; Erkül et al., 2005a,b), Soma (İnci, 1998; Ersoy et al., 2012b), Gördes (Seyitoğlu and Scott, 1994a,b; Purvis and Robertson, 2004), Demirci (Yılmaz et al., 2000), Akdere (Seyitoğlu, 1997b); Emet (Helvacı, 1986; Seyitoğlu et al., 1997); Selendi (Ercan et al., 1983; Seyitoğlu, 1997a; Westaway et al., 2004; Purvis and Robertson 2004; Ersoy and Helvacı, 2007; Ersoy et al., 2010) and Uşak-Güre basins (Ercan et al., 1978; Seyitoğlu, 1997a; Westaway et al., 2004; Seyitoğlu et al., 2009; Karaoğlu et al., 2010; Karaoğlu and Helvacı, 2012a,b). The E–W-trending Pliocene-Quaternary grabens include, the Simav half-graben (Seyitoğlu, 1997b), and the Gediz (Cohen et al., 1995; Emre, 1996; Hakyemez et al., 1999; Bozkurt and Sözbilir, 2004; Çiftçi and Bozkurt, 2009), Küçük Menderes (Rojay et al., 2005; Emre and Sözbilir, 2007), and Büyük Menderes (Hakyemez et al., 1999) grabens which are actively deformed by basin-facing normal faults (Figures 1, 2 and 8).

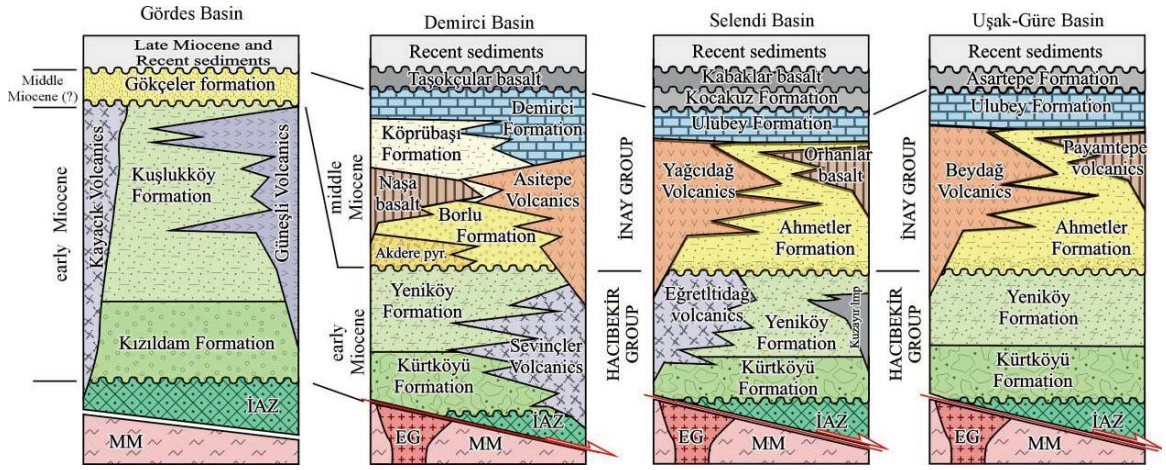

Figure 9. Generalized stratigraphic columnar sections of the NE–SW-trending Gördes, Demirci, Selendi and Uşak-Güre basins (from Ersoy et al., 2011).

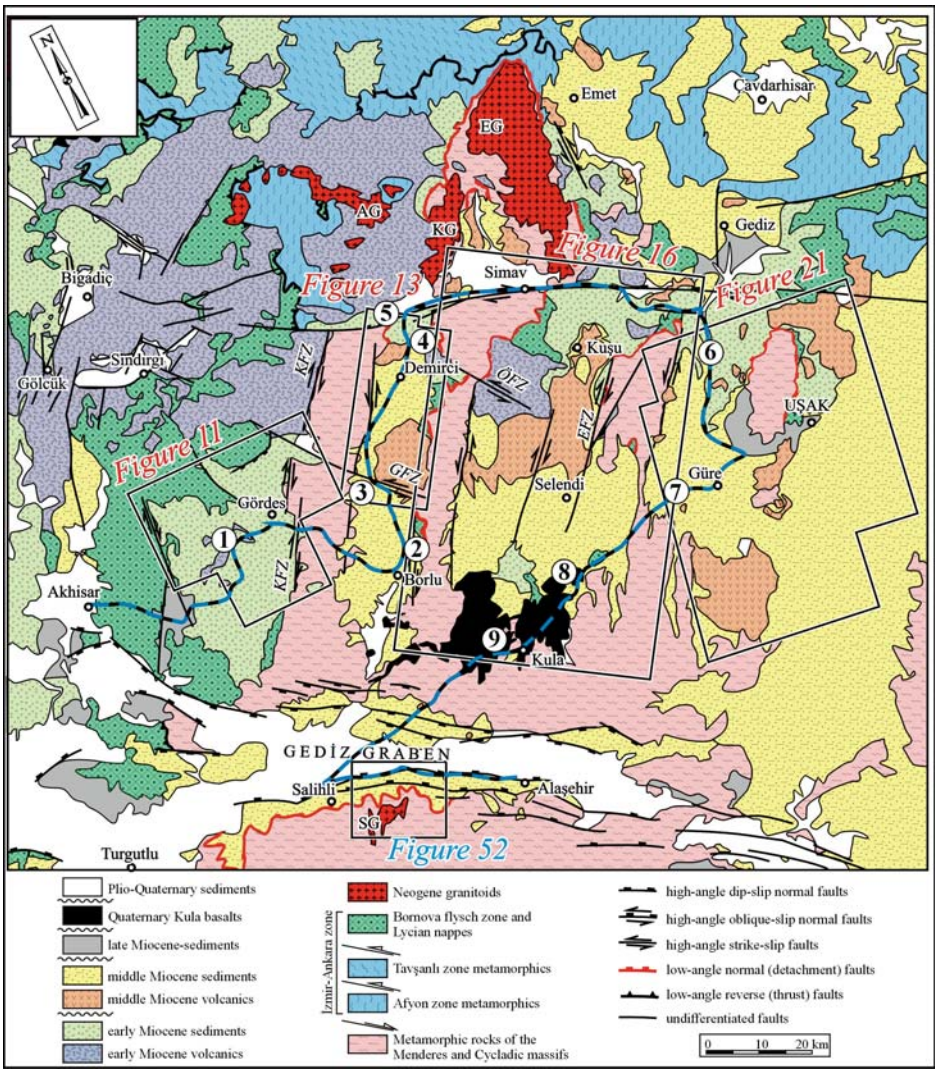

Figure 10. Generalized geological map of the NE–SW-trending Neogene basins (Compiled from Geological Map of Turkey (1:500000), 2002; Okay and Tüysüz, 1999; Koçyiğit et al., 1999; Sözbilir, 2001; Işık and Tekeli, 2001; Ersoy et al., 2010). EG-Eğrigöz granitoid, KG-Koyunoba granitoid, AG-Alaçam granitoid, SG-Salihli granitoids, KFZ-Kızıldam fault zone, GFZ-Güneşli fault zone, ÖFZ-Ören fault zone, EFZ-Eskin fault zone. Also shown are the locations of the detailed geological maps given below (from Ersoy et al., 2011). The field trip route for the first day (from Akhisar to Alaşehir) is indicated by blue-black line. The stops along this route are indicated by numbers in circles.

3.1.1. Gördes Basin

Gördes basin is confined by the Menderes Massif to the east and by ophiolitic mélange units of the Bornova flysch zone to the west (Figure 9), and has been studied by Nebert (1961), Yağmurlu (1984), Seyitoğlu and Scott (1994a,b) and Purvis and Robertson (2004, 2005) and Ersoy et al. (2011). The stratigraphy of the basin begins with Kızıldam Formation which is conformably overlain by the Kuşlukköyü Formation. The Kuşlukköyü Formation interfingers with the Güneşli Volcanics and are also cut by the Kayacık Volcanics in the center of the basin (Figures 10 and 11). These units are unconformably overlain by the Gökçeler Formation and late Miocene to Recent sediments.

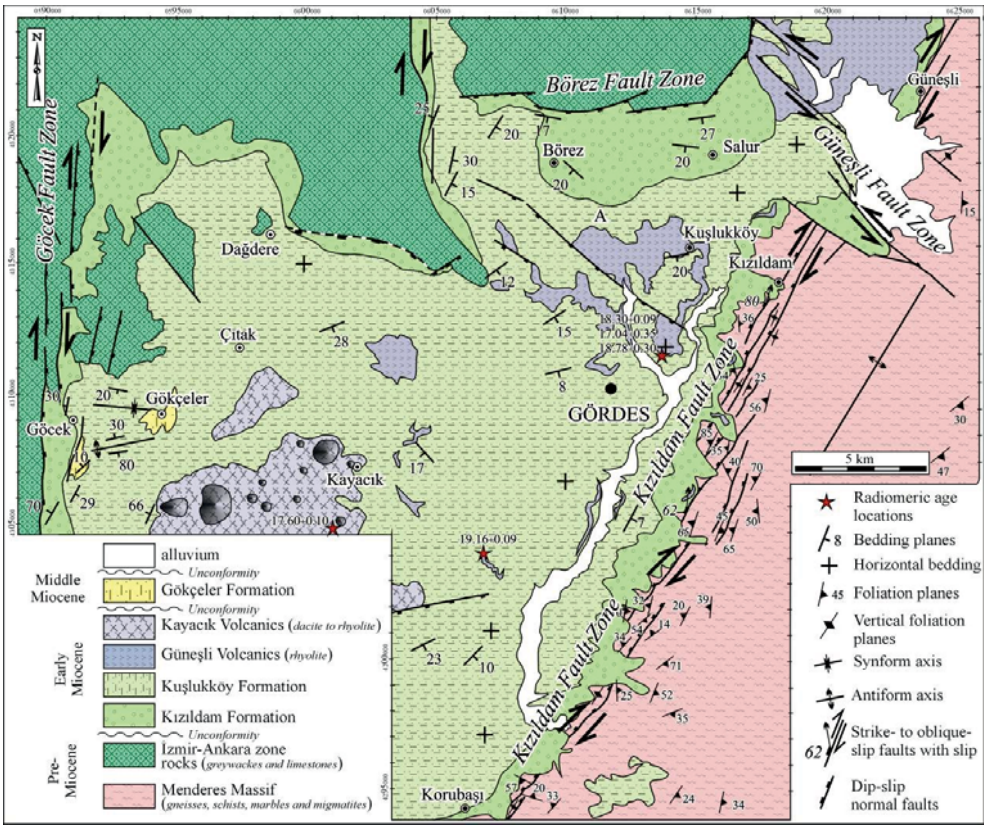

Figure 11. Detailed geological map of the NE–SW-trending Gördes basins (from Ersoy et al., 2011).

The Kızıldam Formation crops out along the basin-bounding faults in Gördes basin. In the eastern margin of Gördes basin, the Kızıldam Formation is made up of reddish-brown conglomerates of alluvial fan origin, which are mainly derived from the underlying metamorphic rocks of the Menderes Massif (Seyitoğlu and Scott, 1994a,b; Ersoy et al., 2011). Here, the Kızıldam Formation unconformably overlies the metamorphic rocks. In the western part of Gördes basin, the Kızıldam Formation starts with well-lithified carbonate-cemented conglomerates with mainly limestone-dominated clasts derived from the rocks of the İzmir-Ankara suture zone (Figure 12a). The Kuşlukköy Formation (Seyitoğlu and Scott, 1994a,b; Ersoy et al., 2011) crops out in a large area throughout the Gördes basin and is composed of conglomerate–sandstone and sandstone–claystone alternations of fluvio-lacustrine origin (Figure 12b). The upper section of the Kuşlukköy Formation is represented by marl and limestone to the north of the Korubaşı village. The Güneşli Volcanics cover a large area to the north of the basin and are cut by the E–W-trending oblique-slip normal faults of the Simav half-graben. This unit is composed of several pink to white colored rhyolitic dykes and lava flows and associated rhyolitic pyroclastic rocks to the north of the Gördes basin. The Kayacık Volcanics crop out in the center of Gördes basin. They are composed of mainly green colored dacitic to rhyolitic volcanic necks and associated lava flows and minor pyroclastic rocks interfingering with the Kuşlukköy Formation.

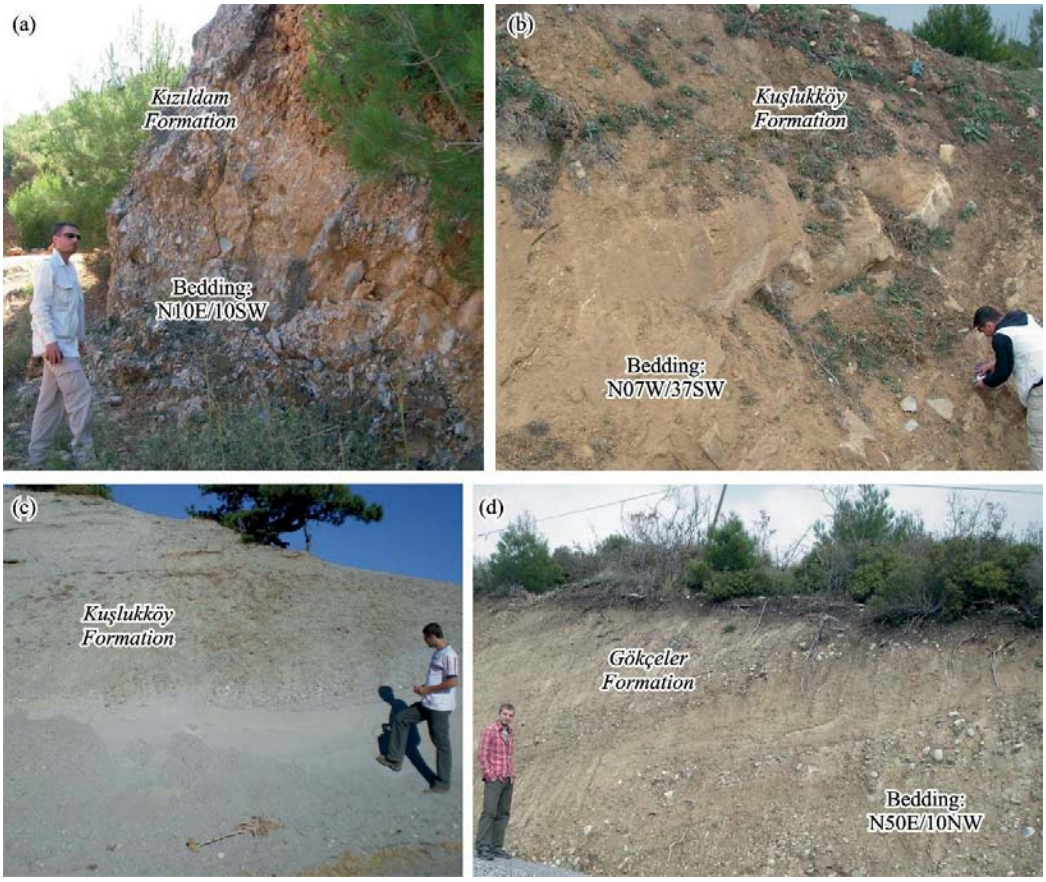

Figure 12. Field photographs from Gördes basin: (a) the Kızıldam Formation composed of well-lithified conglomerates derived mainly from limestone rocks of the İzmir-Ankara zone at the western margin of the basin; sandstone–mudstone alternations (b) and tuffaceous sandstone–siltstone (c) alternations of the Kuşlukköy Formation, (d) pebblestone–sandstone alternations of the Gökçeler Formation (from Ersoy et al., 2011).

The Gökçeler Formation crops out in a limited area at the western margin of Gördes basin. The unit is best observed along the road-section from Gökçeler to Kayacık village. The unit is composed of conglomerates, pebblestones, sandstones, siltstones and marls which have a fluvio-lacustrine origin (Figure 12d). The conglomerates at the base of the unit include several conglomerate blocks derived from the underlying Kızıldam Formation (Ersoy et al., 2011).

3.1.2. Demirci Basin

The Demirci Basin is located to the east of the Gördes Basin (Figures 8, 9 and 13) and is cut into two sub-basins by the Plio-Quaternary Simav half-graben (İnci, 1984; Yılmaz et al., 2000; Ersoy et al., 2011). The stratigraphy of the Demirci basin contains two distinct units separated by a basin-wide angular unconformity (İnci, 1984; Ersoy et al., 2011). The older one is correlated with the Hacıbekir Group in the adjacent Selendi and Uşak-Güre basins (Ercan et al., 1978, 1983), and the younger volcano-sedimentary unit unconformably overlies the Hacıbekir Group and can be correlated with the İnay Group in the adjacent Selendi basin (Ersoy et al., 2010; 2011). The Hacıbekir Group in Demirci basin is composed of the Kürtköyü and Yeniköy formations and the rhyolitic volcanic rocks of Sevinçler Volcanics. The İnay Group comprises the Akdere pyroclastics, sedimentary rocks of the Borlu, Köprübaşı, and Demirci formations which are interfingered by andesitic–dacitic Asitepe Volcanics and the Naşa basalt to the northern part of the basin (Figure 10).

The Kürtköyü Formation crops out in the northern part of Demirci basin, and is composed of reddish-brown to pale yellow boulder conglomerates (with blocks of up to 1 m), pebblestones, cobblestones and sandstones mainly derived from the Menderes Massif metamorphics and the Eğrigöz granitoid. The conglomerates of the unit overlie the metamorphic rocks along a low-angle tectonic contact,

similar to that observed in Selendi basin (Ersoy et al., 2010). The Yeniköy Formation is composed of yellowish sandstones and mudstones with local laminated limestone and marls, and mainly crop out in the north of Demirci basin. The contact relationship between the Yeniköy and Kürtköyü formations is best traced along the Demirci-Simav road-section. The Yeniköy Formation is cut by dacitic–rhyolitic dykes and volcanic necks and is also conformably overlain by rhyolitic pyroclastics and lava flows of the Sevinçler Volcanics. Stratigraphic and geochemical data from the dacitic–rhyolitic lavas of the Sevinçler Volcanics indicate that they are correlated with the Lower Miocene Eğreltidağ Volcanics that crops out in the northern part of the Selendi basin (Ersoy and Helvacı, 2007; Ersoy et al., 2010).

In Demirci basin, the İnay Group is composed of Akdere pyroclastics, conglomerates of the Borlu Formation, sandstone–siltstone alternations of the Köprübaşı Formation, and shales, marls and limestones of the Demirci Formation. These sedimentary rocks are interfingered with the andesitic–dacitic lava flows and pyroclastics of the Asitepe Volcanics. In the northern flank of the Simav half-graben, the İnay Group consists of Akdere pyroclastics, conglomerates and sandstones of the Borlu and Köprübaşı formations, and the Naşa basalt.

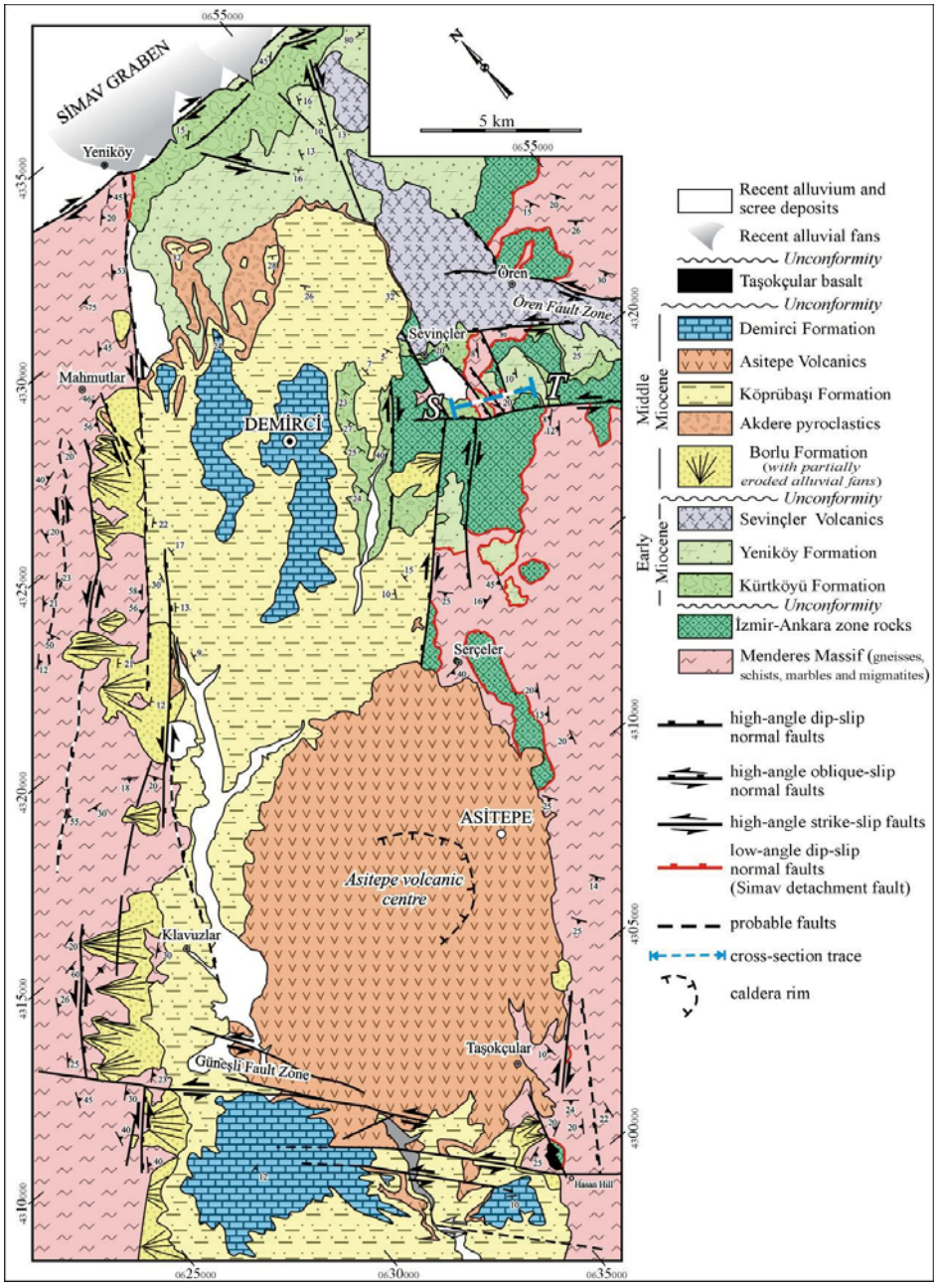

Figure 13. Detailed geological map of the Demirci basin (from Ersoy et al., 2011).

The Borlu Formation of the İnay Group is composed of boulder conglomerates (mainly derived from the Menderes Massif) with sandstone intercalations of alluvial fan origin. The unit has well-preserved outcrops at the eastern and western margin of Demirci basin. The İnay Group unconformably overlies the Menderes Massif along an erosional surface in both sectors of Demirci basin (Figure 7b). Towards the centre of the basin, the conglomerates pass laterally into grey to green colored semi-lithified sandstone-claystone alterations of the Köprübaşı Formation that also includes locally developed marl and limestone lenses. The Köprübaşı Formation is conformably overlain by the Asitepe Volcanics in the eastern margin of Demirci basin (Ersoy et al., 2011).

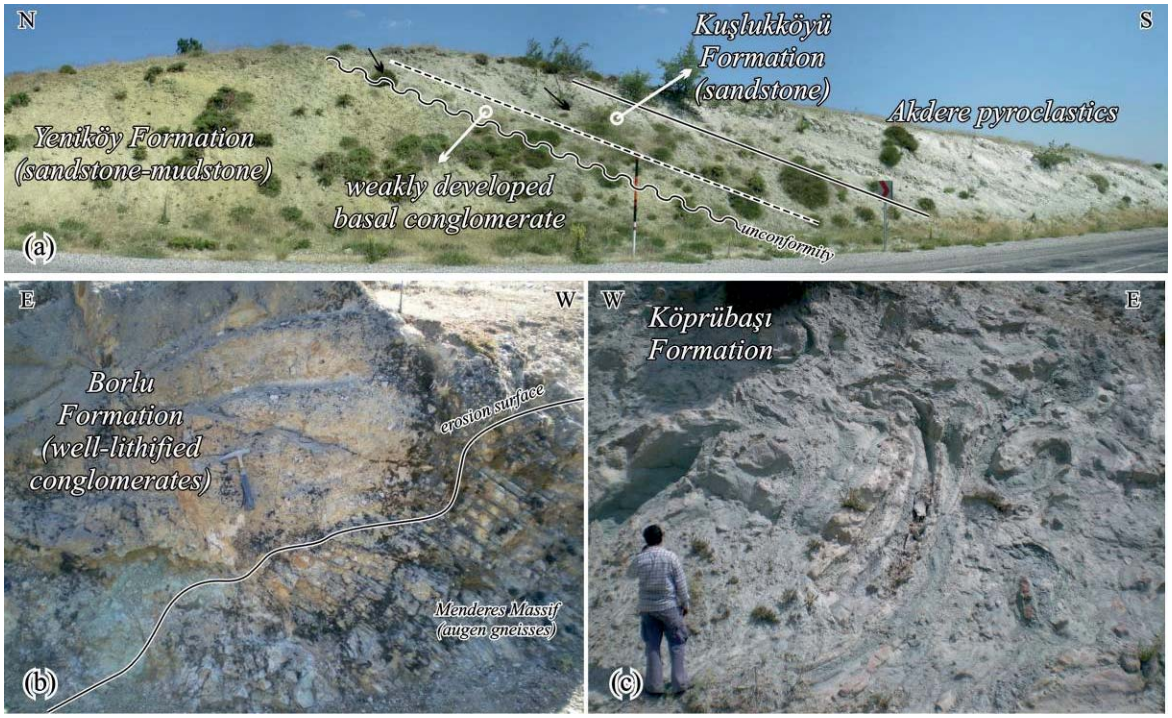

Figure 14. Field photographs from Demirci basin: (a) unconformity between the Yeniköy Formation and the İnay Group, (b) unconformity between the well-lithified conglomerates of the Borlu Formation and the metamorphic rocks of the Menderes Massif, and (c) syn-depositional deformation structures (slumps) in the Köprübaşı Formation, which were developed close to the basin-bounding faults (from Ersoy et al., 2011)

Figure 15. Field photograph of the Demirci Formation with partly silicified limestones, marls and claystones.

In Demirci basin, the Köprübaşı Formation passes transitionally into the marls, bituminous shales and limestones (with claystone and sandstone intercalations) of the Demirci Formation (Figure 15; İnci, 1984), which can be correlated with the Ulubey Formation in Selendi basin (Seyitoğlu, 1997a, Ersoy et al., 2010). Small basaltic outcrops on the eastern margin of Demirci basin, the Taşokçular basalt, are also described (Ersoy et al., 2011).

3.1.3. Selendi Basin

The Selendi basin is located between the Gediz graben to the south, the Simav graben to the north, the Demirci basin to the west, and the Uşak-Güre basins to the east (Figures 8, 10 and 16). The Neogene stratigraphy of the Selendi basin is characterized by two main volcano-sedimentary successions, namely the Hacıbekir and İnay groups. These rock units are unconformably overlain by the Kocakuz formation, the Kabaklar basalt, Plio−Quaternary sediments and the Kula volcanics (Ercan et al., 1983; Seyitoğlu, 1997a; Ersoy et al., 2010; Figure 16).

The early Miocene Hacıbekir group is divided into the interfingering Kürtköyü and Yeniköy formations, where the latter is intercalated with the Eğreltidağ volcanics and the Kuzayır lamproite (Figure 9; Ersoy and Helvacı, 2007). The early Miocene Kürtköyü formation is exposed southeast of Selendi town, and is composed of grey, reddish brown and yellow conglomerates with sandstone and local mudstone and limestone intercalations. The conglomerates at the bottom of the formation are unsorted and composed mainly of subrounded metamorphic clasts of variable sizes. In the Selendi basin, ophiolitic and cherty limestone bodies occur as local olistolites in the Kürtköyü formation. The clastic matrix of the Kürtköyü formation intruded into the cracks of the olistoliths, indicating that the olistolites were transported into the basin during the deposition of Kürtköyü formation (Figure 17). The early Miocene Yeniköy formation widely crops out in the north of the Selendi basin (Figures 16 and 18). It is mainly composed of brownish-yellowish sandstones with local mudstone, claystone and limestone lenses and coal occurrences. The sandstones are turbiditic and represent Bouma sequences with an ungraded coarse-sandy part at the bottom [Ta], parallel laminations [Tb], and cross-laminations at the top [Tc]. The sandstone beds also contain sedimentary structures such as ripple-marks, mud-cracks, flute casts, and normal- and reverse-gradations. The contact between the Yeniköy formation and the Menderes metamorphic rocks is a low-angle normal fault (N40–50°E/20−35°NW) that can easily be traced in the Eskin-Çakırlar-Tepeköy area. The beds of the Yeniköy formation are cut and displaced along the fault. The Yeniköy formation is intercalated with the early Miocene Eğreltidağ volcanics and the Kuzayır lamproite (Ersoy and Helvacı, 2007). The early Miocene Eğreltidağ volcanics widely crops out in the northern part of the Selendi basin. They are represented by dacitic-rhyolitic domes and lava flows and associated wide-spread pyroclastic rocks. The early Miocene Kuzayır lamproite is represented by a small-volume lava flow that covers an area of about 1 km^2. The lavas interfinger with the Yeniköy formation and this relationship is well exposed in the vicinity of Kuzayır village and Orhanlar-Kuşuköy area to the north of the Selendi (Ersoy and Helvacı, 2007).

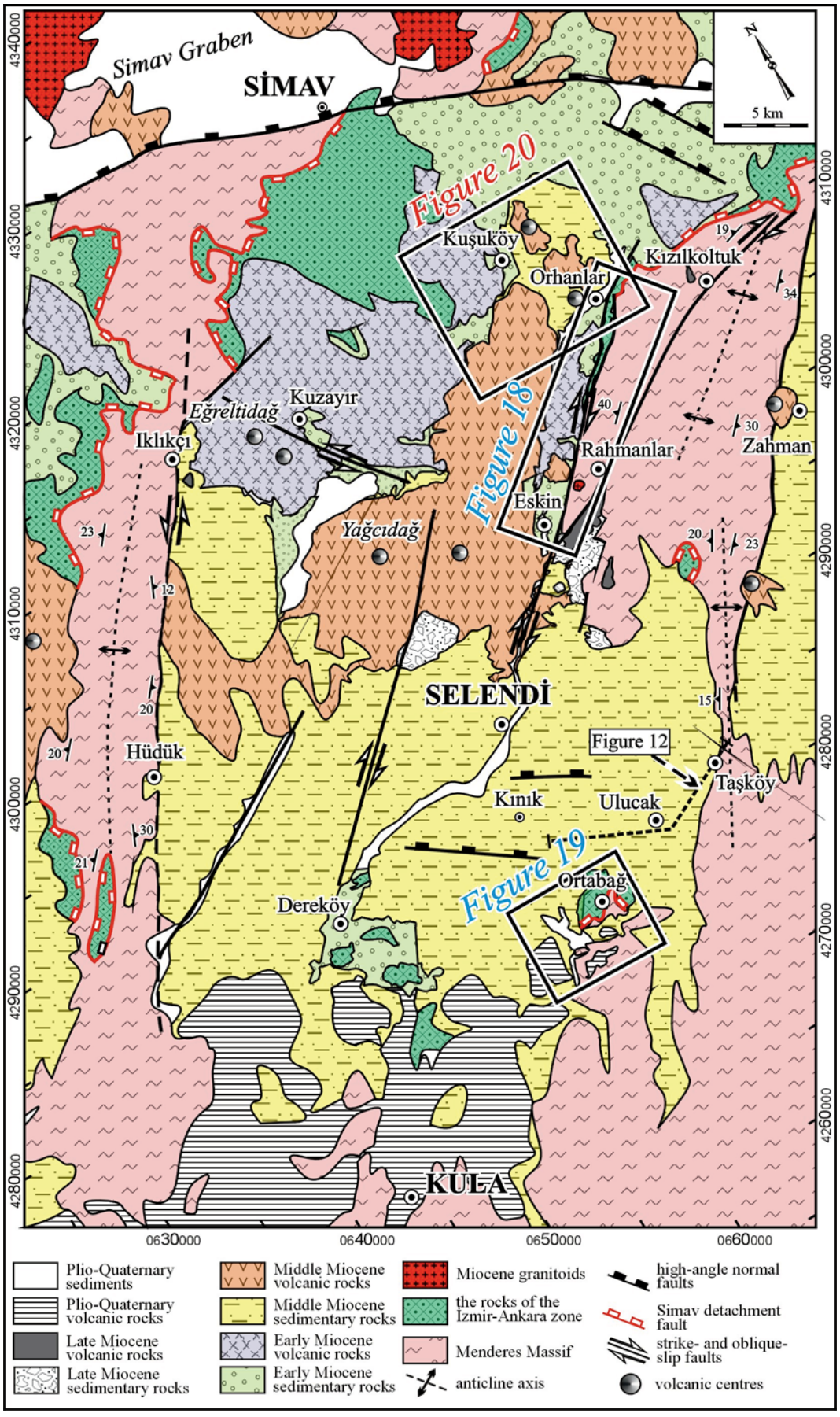

Figure 16. Generalized geological map of the Selendi Basin (from Ersoy et al., 2010).

Figure 17. (c and d) Limestone blocks from the ophiolitic mélange rocks of the İzmir-Ankara zone (İAZ) embedded in the clastic matrix of the Kürtköyü formation of the Hacıbekir group (Kf). The block contacts are characterized by injections of clastic matrix of the Kf (from Ersoy et al., 2010).

The middle Miocene İnay group is well-exposed in the south of the Selendi basin but small outcrops can be followed throughout the northern parts as well. The İnay group unconformably overlies the older units. The İnay group can easily be recognized by its white or pale green colour and its nearly horizontal bedding (where it has not been affected from the late Miocene or younger faults). It is represented by a fining-upward sequence with two sedimentary packages (middle Miocene Ahmetler and Ulubey formations) and intercalated with two volcanic rock units (middle Miocene Yağcıdağ volcanics and Orhanlar basalt). The Ahmetler formation is made up of basal conglomerates, fluvial sandstones and siltstones (Ercan et al., 1983; Seyitoğlu, 1997a). The green claystone horizons also include altered borate occurrences within pale white tuffaceous levels (compacted ash-fall deposits) in some parts of the Ahmetler formation, similar to those of the Emet and Bigadiç basins (Helvacı, 1984; 1995; Helvacı and Alonso, 2000). The formation grades into the Ulubey formation and the Yağcıdağ volcanics. The Ulubey formation (Ercan et al., 1983; Seyitoğlu, 1997a) is composed mainly of nearly horizontal carbonate-dominated lacustrine sediments. In the Orhanlar-Kuşuköy area, the formation interfingers with basaltic lava flows of the middle Miocene Orhanlar basalt.

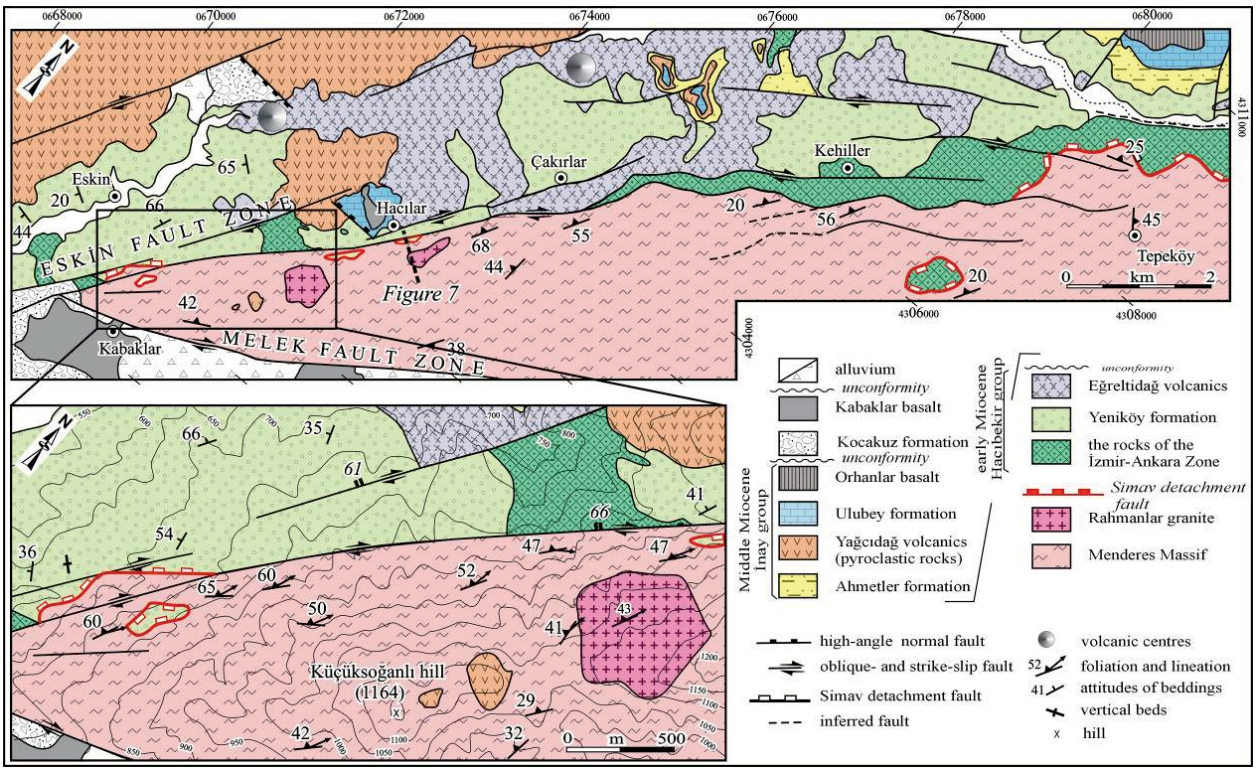

Figure 18. Detailed geological map of the Eskin-Çakırlar-Tepeköy area (the eastern margin of the Selendi Basin; from Ersoy et al., 2010).

The middle Miocene Yağcıdağ volcanics cover an area of 350 km^2 and are represented by dacitic lava flows, dykes and volcanic necks and associated pyroclastic rocks. The volcanic rocks occur around Yağcıdağ volcanic centre located in the centre of the Selendi basin (Figure 16). The ignimbrites of the Yağcıdağ volcanics wedge out between the Ahmetler and the Ulubey formations. The middle Miocene Orhanlar basalt is represented by basaltic lava flows in the Orhanlar-Kuşuköy area in the northeastern part of the Selendi basin. Well-exposed volcanic centres aligned in a NE–SW-direction have been mapped to the north of Orhanlar village. The unit is composed of 10–20-m-thick greyish black massive basaltic lava flows. The lavas flowed onto the carbonate rocks of the Ulubey formation. They also show local interfingering relationships. Peperitic textures are characteristic features of the contact between the middle Miocene Ulubey formation and the middle Miocene Orhanlar basalt.

The Kocakuz formation is composed of reddish boulder conglomerates, and minor sandstone intercalations with locally laminated limestone lenses that unconformably overlie the İnay group. The conglomerates are composed mainly of metamorphic clasts with minor limestone and volcanic clasts. This unit is well-exposed in the Kabaklar-Kocakuz area, cropping out in the hanging wall of the NE–SW-trending dextral oblique- to strike-slip and NW–SE-trending normal fault (Melek fault zone; Figure 17). The continental deposits have been mapped previously as the Quaternary Asartepe formation by Ercan et al. (1983), Seyitoğlu (1997a) and Westaway et al. (2004), assuming that the overlying basaltic lava flows are Quaternary in age. However, these basalts are late Miocene in age (Ercan et al., 1996; Innocenti et al., 2005).

The Kula volcanics crop out in an area of ~300 km^2 located along the northern shoulder of the active Gediz graben. They belong to the late Pliocene to late Quaternary alkaline volcanic activity (Ercan and Öztunalı, 1983; Ercan et al., 1983, Richardson, 1996; Innocenti et al., 2005; Alıcı et al., 2002; Aldanmaz, 2002; Westaway et al., 2004). The Kula volcanics are represented by cinder or spatter cones, maars, lava flows and tephra deposits of basanite, phonolitic tephrite and trachybasalt in

composition. The eruption centres follow a WNW−ESE trend on the northern shoulder of the Gediz graben. The Kula basaltic volcanism developed in three different phases from the late Pliocene to historical times. Richardson (1996) reported 1.94±0.16 and 0.13±0.05 Ma 40Ar/39Ar ages from the Kula lavas. Recently, Westaway et al. (2004) have obtained 1264 ka and ~60 ka ages from the late stage Kula volcanics.

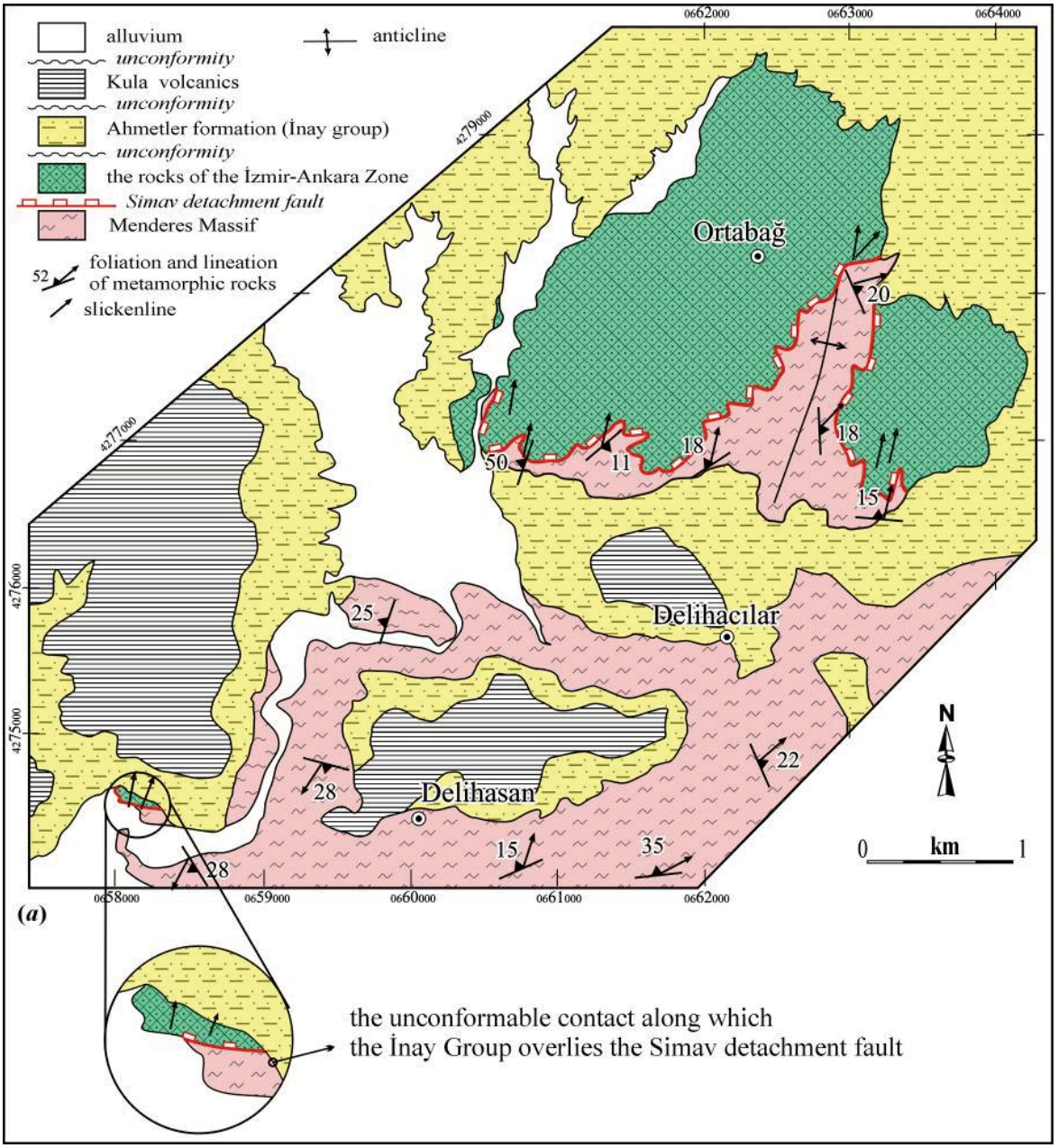

Figure 19. Detailed geological map of the Ortabağ area (to the south of the Selendi Basin; from Ersoy et al., 2010).

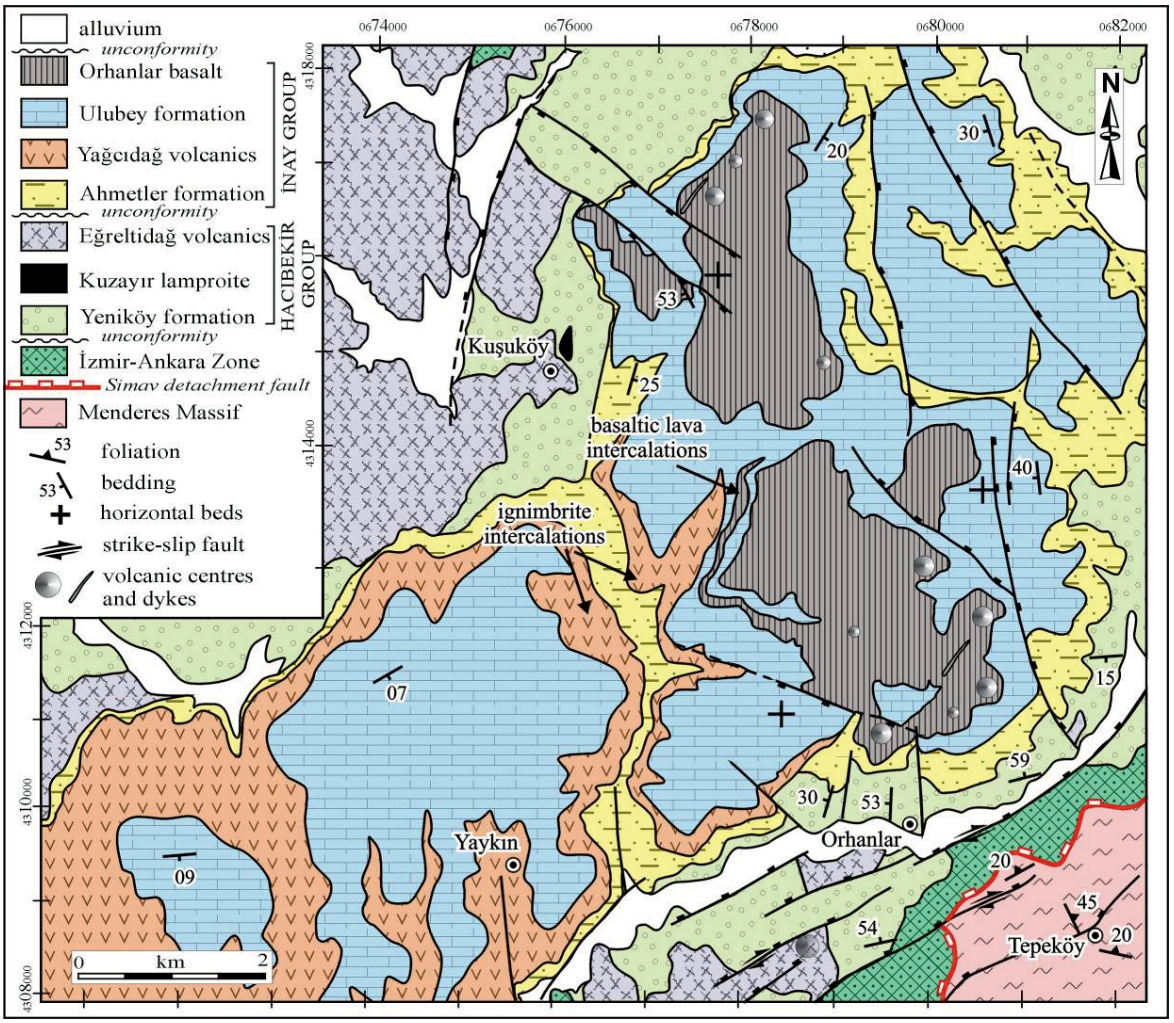

Figure 20. Detailed geological map of the Orhanlar-Kuşuköy area (to the north of the Selendi Basin; from Ersoy et al., 2010).

3.1.4. Uşak-Güre Basins

The Uşak-Güre basin is a 65 km by 55 km NE–SW-trending basin located on the eastern margin of the NE–SW-trending Neogene volcano-sedimentary basins in the western Anatolia (Ercan et al., 1978; Seyitoğlu et al., 1997; Çemen et al., 2006; Karaoğlu et al., 2010; Karaoğlu and Helvacı, 2012a,b; Figure 21). The basement units are made up of the Menderes Massif, represented by metagranite, schist and marble, and the structurally overlying upper Cretaceous ophiolitic mélange rocks of the İzmir-Ankara zone. Dominant foliation trending of the schist and gneiss is in NE–SW direction (017°-054°), nevertheless dip direction of the rocks vary rest on NE–SW-trending antiform and synform geometries of the metamorphic rocks. Large-scale asymmetric folds and associated crenulations, and cleavage commonly described in Menderes Metamorphic rocks. These large antiforms and synforms are first identified by Ercan et al. (1978), and after that are detailed by Çemen et al. (2006) which have NE-SW oriented axes. The mélange is mainly made up of unmetamorphosed ultramafic rocks, radiolarites and highly altered silicic rocks.

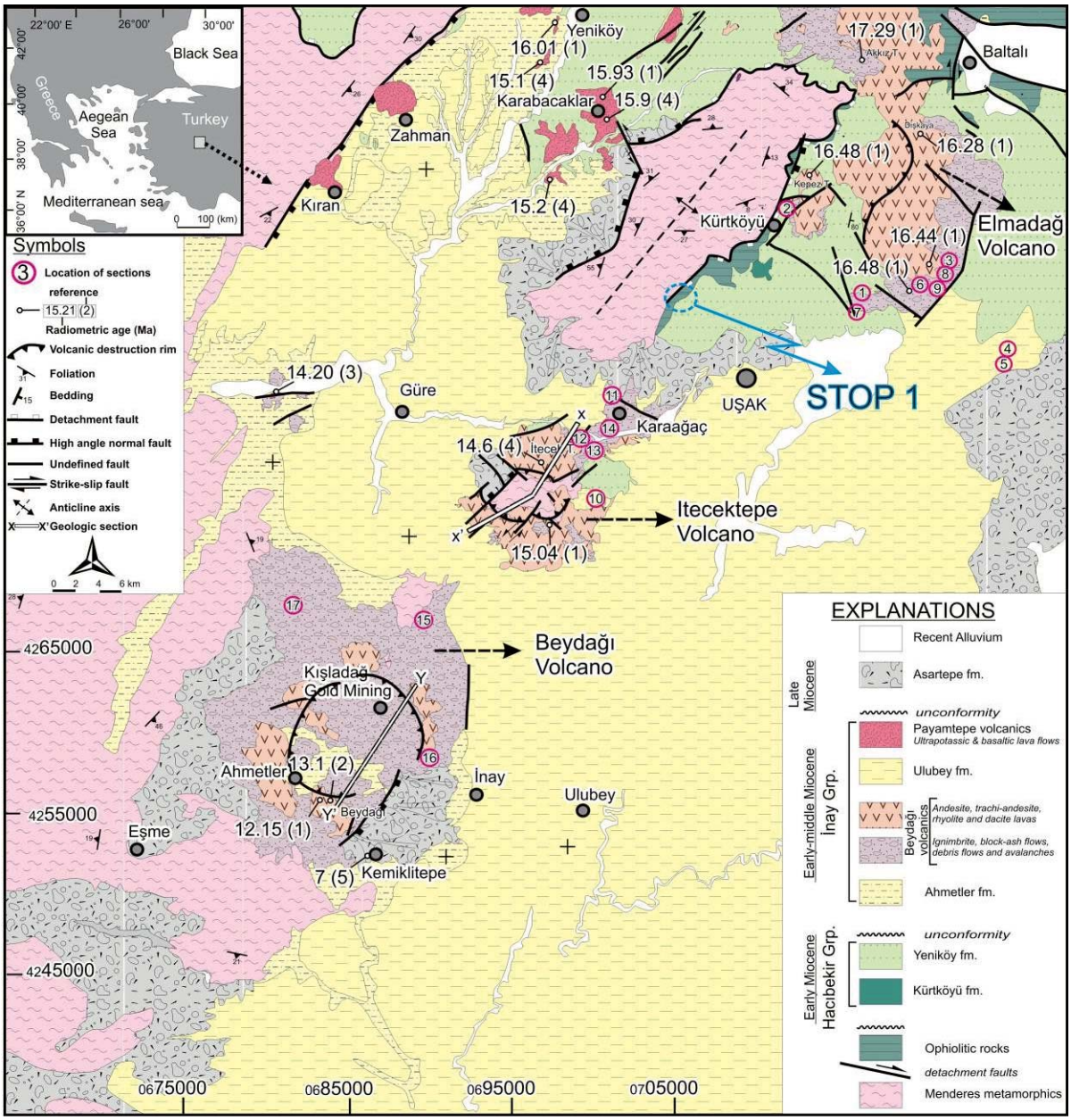

Figure 21. Geological map of the Uşak–Gure basin including radiometric age data from the volcanic rocks and a mammalian age from the Asartepe Formation (modified from Karaoğlu et al. 2010. References: (1) Karaoğlu et al. (2010); (2) Ercan et al. (1996); (3) Innocenti et al. (2005); (4) Seyitoğlu (1997a); (5) Seyitoğlu et al. (2009).

The Uşak-Güre basin contains a detailed record of early to late Miocene syn-extensional sedimentation and volcanism that accompanied exhumation of the metamorphic core complex (Menderes Massif). The basin is filled by fluvio-lacustrine deposits assigned to three unconformity-bounded sequences: (1) Hacıbekir Group; (2) İnay Group; and (3) Asartepe Formation. The Hacıbekir Group is exposed north of the Güre-Uşak-Banaz trend in respectively and laterally variable, subdivided into interfingered Kürtköyü and Yeniköy formation (Ercan et al., 1978; Seyitoğlu et al., 1997; Çemen et al., 2006; Karaoğlu et al., 2010; Karaoğlu and Helvacı, 2012a,b).

The Lower Miocene Hacıbekir Group is composed of Kürtköyü and Yenitköy Formations. The thickness of the Hacıbekir Group in the study area also is not well constrained. Measured sections up to ~800 m thick have been mapped within fault blocks of the northern side of the Uşak-Güre basin

(e.g. Ercan et al., 1978), but the whole formation is probably considerably thicker than that and may be more than 1000 m thick. The type locality of the formation is in the vicinity of Kürtköyü village. There the formation structurally overlies the rocks of the ophiolitic mélange along a sheared contact (see below). The Kürtköyü formation mostly crops out in the vicinity of Kürtköyü (the type locality), Baltalı and Çukurağıl villages (Figure 21) and consists of monolithic grey, reddish brown boulder conglomerates. The boulder conglomerates are composed of moderately to poorly sorted and coarse clast size. The Kürtköyü formation also consists of thin-bedded massive conglomerate with moderately to well-rounded clasts of ultramafic (harzburgites and pyroxenites) ranging from pebble to boulder grade and minor unmetamorphic clasts of the Lycian rocks. The Kürtköyü formation passes laterally and vertically into the Yeniköy formation in the Uşak-Güre basin.

The Yeniköy formation contains sedimentary structures such as tabular cross-beddings, channel structures, ball and pillow, ripple, flaser beddings (Figure 22). The early Miocene Yeniköy formation is composed of three fabric and architecture sequences: 1) parallel laminated bedsets; 2) tabular cross-stratified bedsets; 3) architecture of parallel-laminated and cross-stratified sandstone and conglomerate. All of the sequences are dominantly made up sandstone, claystone, mudstone, limestone and coal lenses. Medium-grained, yellow-brown sandstone with occasional pebble lenses dominate much of the section; thin, lenticular grey mudstones and siltstone are also common. Coal lenses are especially observed in the transition zone of Kürtköyü formation to Yeniköy formation.

The unconformably overlying İnay group is composed of conglomerate, sandstone, tuff, mudstone marl and limestone of fluvio-lacustrine setting, and is accompanied by volcanic rocks (Figure 23). According to Seyitoğlu (1997a), the volcano-sedimentary succession of the İnay group was deposited during the early–middle Miocene. The İnay group was deposited under the control of NE–SW-trending strike- to oblique-slip faults (Seyitoğlu, 1997a; Ersoy et al., 2010). Seyitoğlu (1997a) proposed that the volcanic rocks of the Uşak-Güre basin are intercalated with the İnay group based on their stratigraphic position and the radiometric age of the volcanic rocks (dated as 15.5±0.4 to 14.9±0.6 Ma, K/Ar ages). Bingöl (1977) also noted that the K-Ar dates of the Muratdağı volcanic rocks which are located in the NE edge of the basin, lie between 16.9±0.2 and 20.9±0.5 Ma. Karaoğlu et al. (2010) presented new $^{40}Ar/^{39}Ar$ ages from the Beydağ and Payamtepe volcanic units and proposed that Cenozoic volcanism in the Uşak–Gure basin started (at 17.29 Ma) with the Beydağı volcanic unit, which is located in the northern part of the basin. The data indicate that volcanism has been active since the late early Miocene (Burdigalian). The youngest radiometric age from the Beydağı volcanic unit is from the Beydağı stratovolcano (12.15±0.15 Ma) in the south. Also, the $^{40}Ar/^{39}Ar$ dates of the Payamtepe volcanic unit restrict it to a period between 16.01±0.08 and 15.93±0.08 Ma. The internal characteristics of the Inay Group have much in common with alluvial fans dominated by sediment gravity flow (e.g., debris flow, rock avalanche, rock slide facies, Merdivenlikuyu member); fluvial and lacustrine deposits (Balçıklıdere member) and fluvial deposits (Gedikler member), also are interstratified with volcanic rocks of Uşak-Güre basin.

.

Figure 22. Field photographs of Yeniköy formation. (a) Planar cross bedding in pebbly sandstones of Yeniköy Formation near Yeniköy town. (b) Channel slightly incised fill conglomerate (c) Ball and pillow structures. (d) Plan view of oscillation (wave generated) ripples on the upper surface of a fine grained sandstone bed, north of Uşak. Individual lamination sets exceed 7-8 cm in thickness. (e) Flaser bedding in sandstone, near Aşağıkaracahisar village. (f) Coal bearing sandstone, near Kürtköyü village.

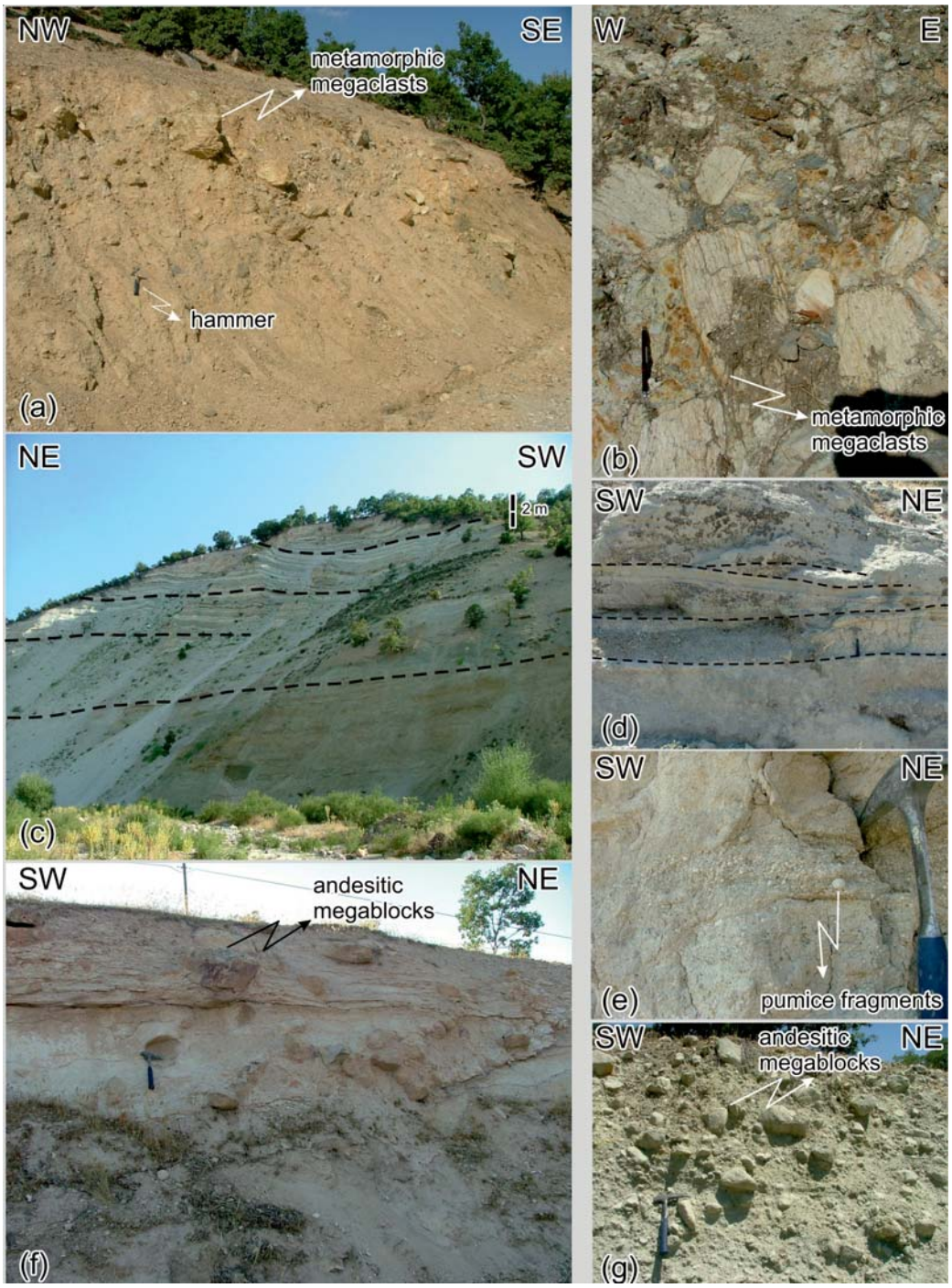

Figure 23. Three distinct members of the Ahmetler formation. (a) Photograph showing matrix-supported Merdivenlikuyu member in the western margin of the Güre basin. (b) Close-up view of Merdivenlikuyu member showing subordinate matrix-supported metamorphic breccias and blocks, near the western margin. (c) Balçıklıdere member with siltstone and mudstone horizontal bedding, near Kıran village-western side of the basins. (d) Close-up view of Balçıklıdere member, western side of the Beydağı volcano, showing fine-grained sandstone within horizontal bedding and small scale channel structures. (e) Pumice bearing sandstone demonstrating syndeposition of Balçıklıdere member-İnay Group with explosive eruptions within Uşak-Güre basin. (f) Gedikler member is characterised with matrix-supported volcanic conglemarate bearing mainly andesitic blocks which most probably originated from Beydağı volcanic unit. (g) Volcanic blocks from Gedikler member.

The Asartepe Formation is mainly characterized by volcanic successions with minor metamorphic rocks on the Beydağı stratovolcano, and metamorphic and volcanic clasts are observed on the İtecektepe stratovolcano. The Asartepe Formation displays rapid lateral fining away from the Uşak margin faults in the north and the NW–SE-trending fault at Beydağı in the south of the basin (Fig. 2). The thickness of the red-beds sequence is estimated from map relationships and crosssections as c. 300–350 m. Şen et al. (1994) and Seyitoğlu et al. (2009) documented a biostratigraphic and magnetostratigraphic age of 7.38 ± 0.1 Ma for the Asartepe Formation in the Uşak–Gure basin.The Asartepe Formation in the Uşak–Gure basin is well correlated with the Upper Miocene Kocakuz Formation, which is overlain by the 8.37–8.5 Ma Kabaklar basalt in the adjacent Selendi basin (Ercan et al., 1996; Innocenti et al., 2005; Ersoy & Helvacı, 2007).

The Beydağı volcanic unit occurs in three different NE–SW-trending volcanic centers (Karaoğlu et al., 2010). These are the high-K calc-alkaline to shoshonitic Beydağı, İtecektepe, and Elmadağ calderas from southwest to northeast respectively. The Beydağı caldera is approximately 16×9 km in diameter and is represented by voluminous, block and ash flows, ignimbrites which are associated with onset of the caldera collapse, debris flows and overlying lava flows. The İtecektepe caldera is ~ 5x6 km in diameter and extensive dacitic ignimbrites were associated with the collapse of the İtecektepe caldera. Subsequent uplift of the caldera floor led to the exposure of metamorphic basement in the middle of the caldera. The eastern half of the Elmadağ caldera is preserved and the half-deformed caldera size is ~ 5x9 km in diameter. Dacitic ignimbrites were formed during the collapse of the Elmadağ caldera. The oldest radiometric ages from the Beydağı volcanic unit were obtained from the Elmadağ volcanic centre in the north, and range between 17 and 16 Ma. The data indicate that volcanism was active since the late early Miocene (Burdigalian). The youngest radiometric age from the Beydağı volcanic unit was obtained from the Beydağı caldera (12.15±0.15 Ma) in the south. These data indicate that Beydağı volcanism was active until the late middle Miocene, and that activity migrated from north to the south with time. The volcanic products of the Beydağ volcanic unit interfinger with the fluvio-lacustrine sediments of the İnay Group.

The Payamtepe volcanic unit consists of several lava flows and dikes. These are the shoshonitic Kıran rocks, Yeniköy latite dikes, ultrapotassic Güre lavas and Karabacaklar lava flows. The lava flows and locally developed dykes of the Payamtepe volcanic unit were emplaced along NE–SW-trending oblique-slip faults and are most abundant in the northeastern part of the Güre region. The Payamtepe volcanic unit also interfingers with the fluvio-lacustrine sedimentary rocks of the İnay group. The Karaağaç latite/andesite dikes were emplaced along a NE–SW- direction and cut the late Miocene Asartepe formation (Karaoğlu et al., 2010).

3.2. Tectonic Evolution

Both the western and eastern margins of Gördes basin are bounded by NNE–SSW-trending right-lateral strike-slip faults, along which the early Miocene sedimentary rocks (the Kızıldam Formation) were deposited (Ersoy et al., 2011; Figure 10). In the eastern margin of Gördes basin several fault planes of the Kızıldam fault zone have been measured with a strike of 18–35°, a dip of 62–70° to the NW, and a rake of 17–27°N (Figure 24). The boulder conglomerates of the Kızıldam Formation was also deposited on an E–W-trending dip-slip normal fault zone (Börez fault Zone) in the Börez-Salur districts where a fault plane strikes nearly E–W and dips ~85–89°S with a rake of ~90°. In the western margin of Gördes basin, N–S- to NE–SW-trending right-lateral strike-slip faults (the Göcek fault zone,) controlled the deposition of the Kızıldam Formation (Figure 25). Here, a right-lateral strike-slip fault plane of the Göcek fault zone is defined by strikes between 05–20° and dips ~85°SE with a rake of ~0°. **These data indicate that Gördes basin formed under the control of NE–SW-**

trending strike-slip faults and E–W-trending dip-slip normal faults where the N–S extension is slightly oblique to the margins that bounded the basin during the early Miocene (see also Ersoy et al., 2011). Reactivation of these faults may be responsible for deposition of the middle Miocene(?) Gökçeler Formation to the western margin of the basin.

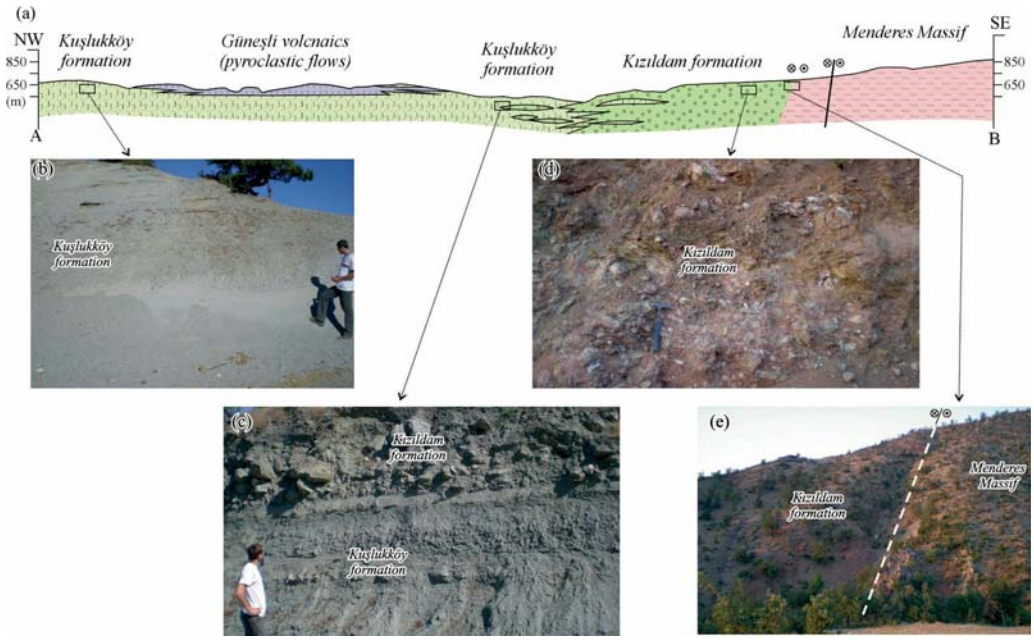

Figure 24. (a) A-B geological cross-section on the eastern margin of the Gördes basin and (b-e) related field photos from the key locations (see Figure 4 for location). The fine grained tuffaceous sediments of the Kuşlukköy formation in the centre of the basin (b) are wedged by conglomerates of the Kızıldam formation to the east (b). The reddish conglomerates of the Kızıldam formation (c) were deposited along the NE–SW-trending right-lateral strike-slip fault zone in the eastern margin of the basin (e) (from Ersoy et al., 2011).

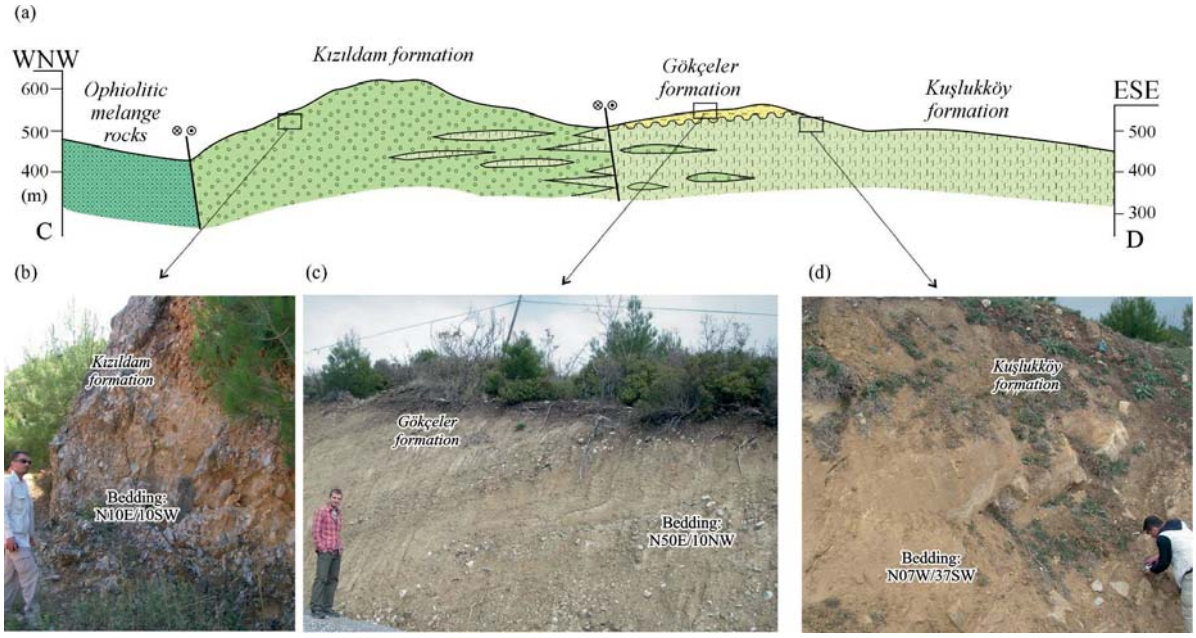

Figure 25. (a) C-D geological cross-section on the western margin of the Gördes basin and (b-d) related field photos from the key locations (see Figure 6 for location). The well-lithified reddish brown conglomerates of the Kızıldam formation (b) occur along the nearly N–S-trending right-lateral strike-slip fault zone in the western part of the basin. Pale yellow to greenish grey colored conglomerate-sandstone alternation of the Gökçeler formation (c) ubconformably overly the yellowish brown sandstone-mudstone alternation of the Kuşlukköy formation (d) (from Ersoy et al., 2011).

In the northeastern part of Demirci basin, to the southeast of Sevinçler village, the contact relationship between the Lower Miocene Hacıbekir Group (the Kürtköyü and Yeniköy formations) and the tectonically underlying Menderes Massif is well-exposed (Ersoy et al., 2011; Figures 26 and 27). The reddish conglomerates of the Kürtköyü Formation are underlain by metamorphic rocks and separated by a low-angle fault, along which the metamorphic rocks were progressively deformed in a ~70 m shear zone which is characterized by ductile deformation overprinted by cataclasites (Figure 27). The transition from ductile to brittle deformation, with top to the N-NE sense of shear, indicates that the low-angle fault is normal in character. The low-angle normal-faulted contact relationship between the Kürtköyü Formation and the metamorphic basement is also observed in the northwestern part of Demirci basin, where conglomerates of the Kürtköyü Formation are separated from the augen gneisses of the Menderes Massif by a low-angle (~30°) fault plane (Figure 28). Mylonitic augen gneisses show progressive deformational features towards the fault plane, as they become cataclastized. The fault surface is marked by brownish and reddish fine-grained cataclastics. The ductile deformed mylonitic rocks were also overprinted by a brittle deformation that is characterized by micro-scale faults and fragmented crystals of quartz and feldspar. The deformational textures also indicate a top to N-NE sense of shear.

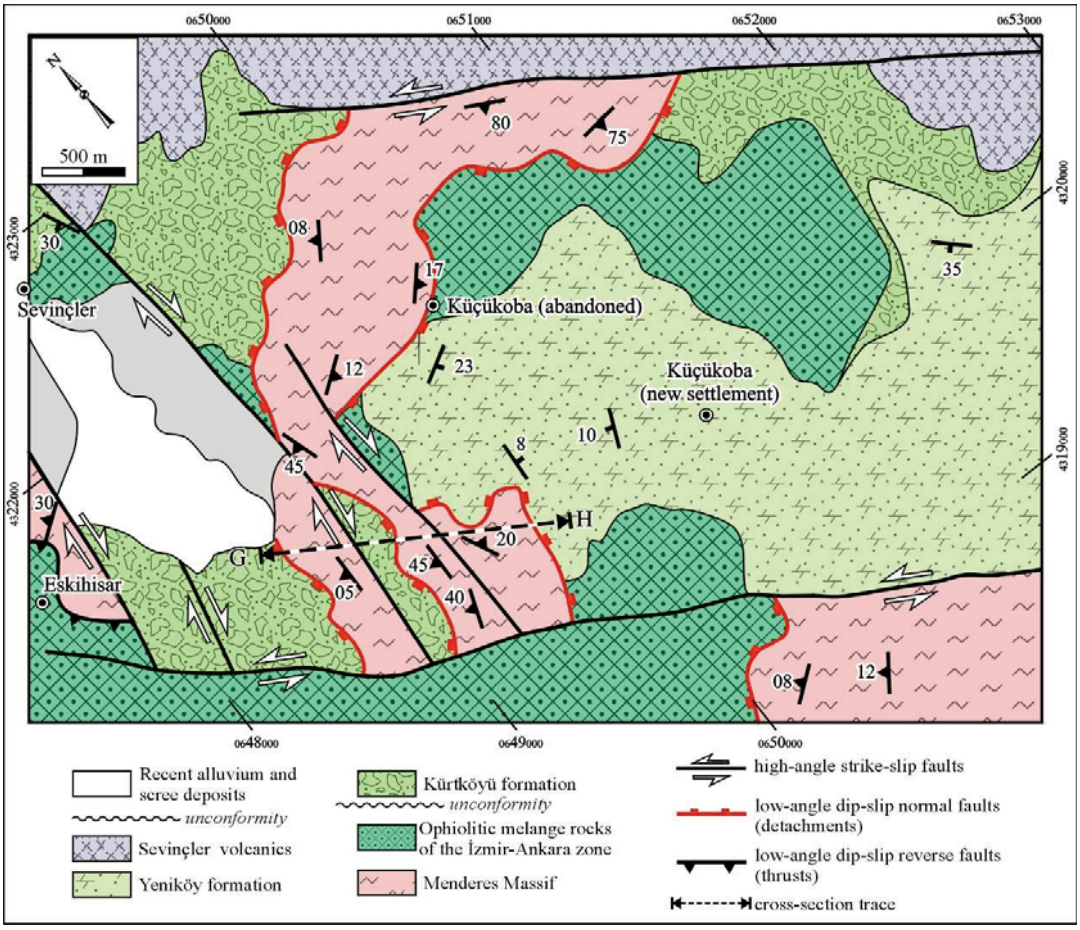

Figure 26. Detailed geological map of the northeastern part of the Demirci basin, where the older detachment surface are cut and displaced by (a) nearly N–S-trending right-lateral, and (b) NW–SE-trending left-lateral oblique- to strike-slip faults.

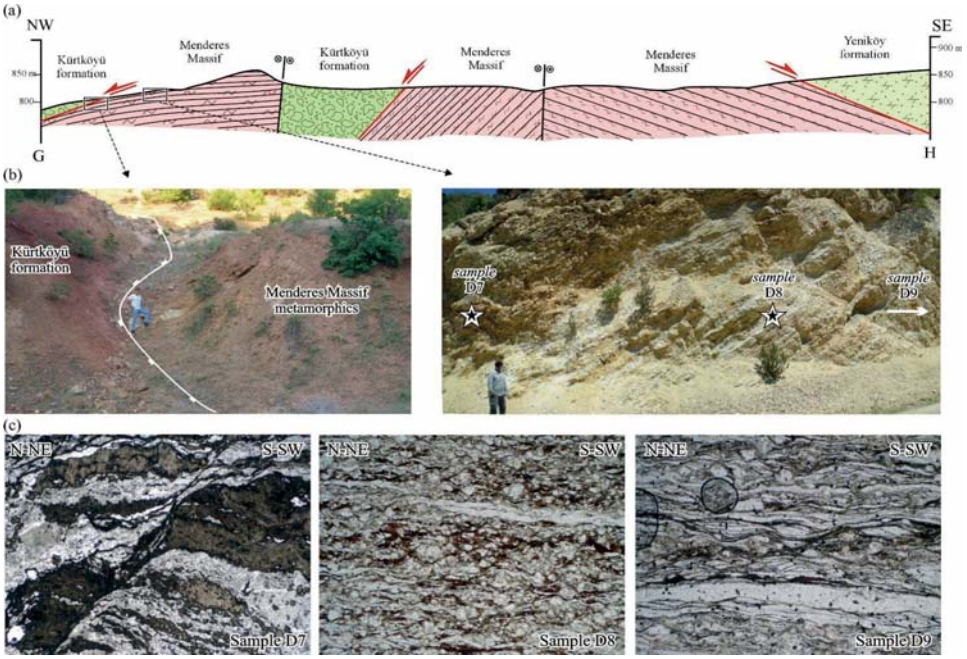

Figure 27. (b) G-F geological ross section, (b) related field photos, and (c) thin sections of the metamorphic rocks along the cross-section that marked on the Figure 19.

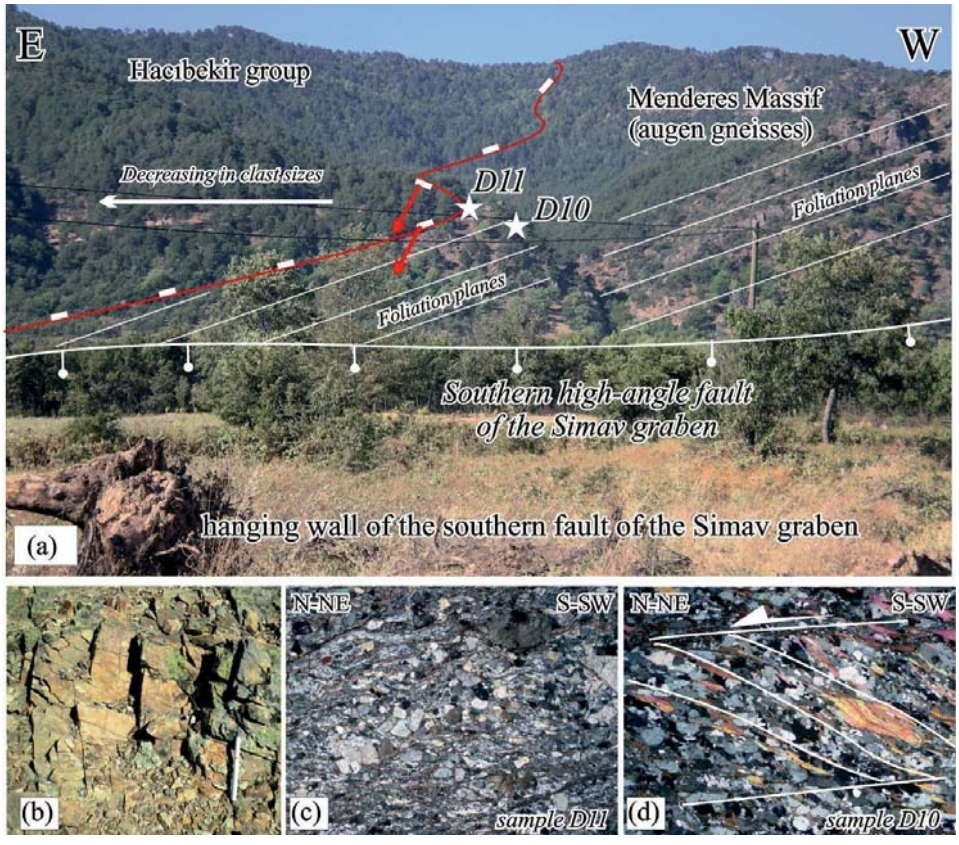

Figure 28. (a) Field photo from the northwestern margin of the Demirci basin, looking from the graben-floor of the Simav graben to the south. Note that the metamorphic rocks of the Menderes massif underlie the early Miocene Hacıbekir group along a low angle normal fault. The red arrows indicate the slickenlines on the fault surface. (b) Field and (c) microscope view of cataclatised gneisses (sample D11) just below the low-angle normal fault. (d) Microscope view of the ductilely deformed gneisses (sample D10).

In the Selendi Basin, low angle detachment fault juxtaposes the Yeniköy formation (Hacıbekir group) and the mélange rocks of the İzmir-Ankara zone in the hanging wall against the metamorphic rocks of the Menderes metamorphic rocks in the footwall during the early Miocene (Ersoy et al., 2010; Figures 18 and 29). The detachment fault can be traced in the Ortabağ (~ 5–6 km) and the Eskin-Çakırlar-Tepeköy (~ 500 to 2000 m) areas (Figures 18, 19 and 30). This fault has only limited outcrops in the Eskin-Çakırlar-Tepeköy area, mainly because of younger NE–SW-trending high-angle faults cutting and displacing the older structural elements in the region (Figure 18 inset map and Figure 30). The footwall rocks of the detachment fault were intruded by the Rahmanlar granite in the Eskin-Çakırlar-Tepeköy area. In the Ortabağ area, the detachment fault seems to be folded with a NE–SW-trending fold-axis as well as the underlying regional gneissic foliations and is unconformably overlain by the horizontal beds of the middle Miocene İnay group (Figure 19). Hence, the detachment faulting in the region occurred by the early Miocene at the latest, as the detachment fault cuts the beds of the early Miocene Yeniköy Formation. Moreover, the fault is unconformably overlain by the middle Miocene İnay Group in the vicinity of the Kula, and hence, the detachment faulting must have ceased by the middle Miocene (Ersoy et al., 2010).

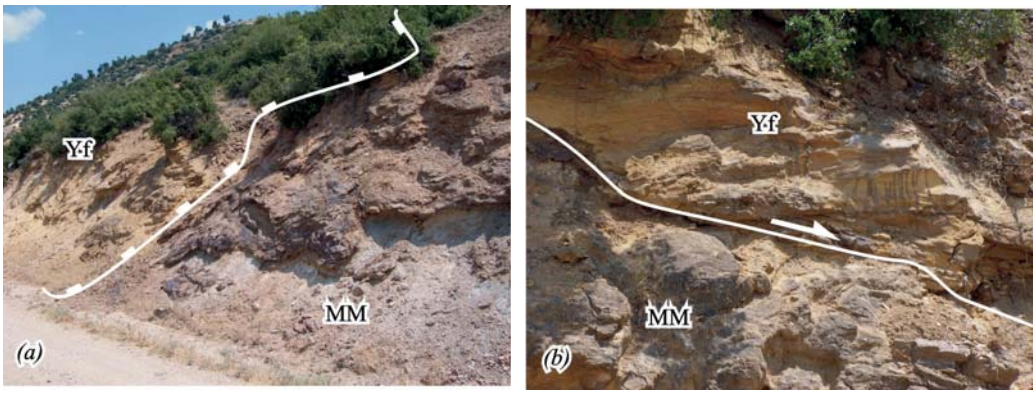

Figure 29. (a and b) Field photo of the Simav detachment fault between the Yeniköy Formation (Yf) and the Menderes Massif metamorphics (MM) (from the eastern margin of the Selendi basin) (from Ersoy et al., 2010).

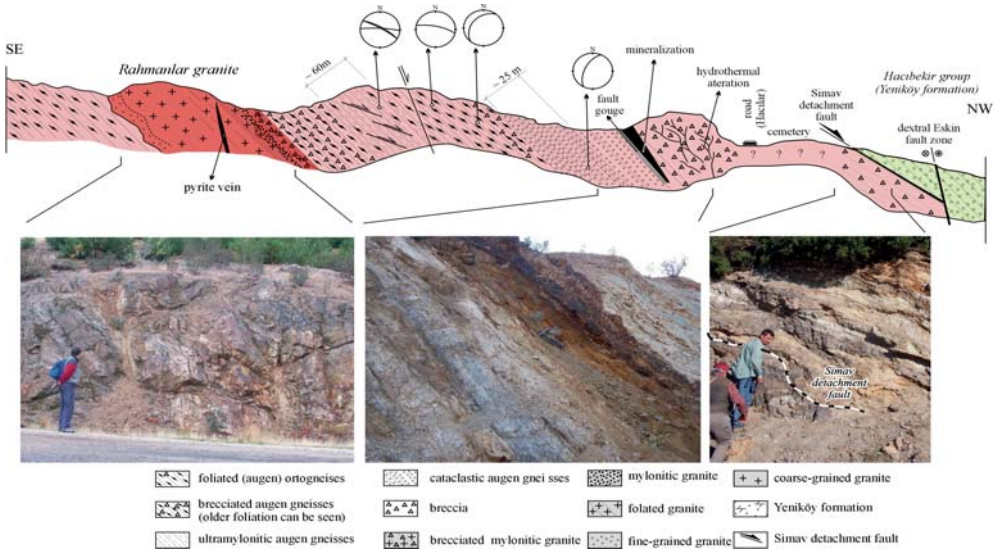

Figure 30. Cross-section throughout the Simav detachment fault showing the contact relationship between the Rahmanlar granite and the hosting gneisses of the Menderes Massif (from Ersoy et al., 2010).

Along the detachment fault, two deformational fabrics can be observed. The older S1 regional gneissic foliation in the Menderes metamorphic rocks is cut by a mylonitic foliation S2 (C' shear bands; Figures 31), which is associated with a slickenslide lineation (L2). The mylonitic foliation S2, which affected the Menderes metamorphic rocks, commonly strikes NE–SW with dips towards the NW (Ersoy et al., 2010). It is characterized by preferred alignment of micas and recrystallized and elongated quartz. Asymmetrical porphyroclasts are predominantly composed of K-feldspar, plagioclase, garnets and polymineralic aggregates of feldspar, quartz, muscovite and biotite, and are common in the mylonitic gneisses and schists. These are similar to the σ-type porphyroclasts having narrow mantles and elongated tails composed of quartz, feldspar and micas. Mica fishes are inclined with a narrow angle to the mylonitic foliation (Figure 31c). These micro-tectonic features, as a whole, indicate a top-to-the-NE sense of shear. Well-developed C'-type shear band cleavages in mylonitic gneisses also indicate top-to-NE sense of shear. The L2 mylonitic stretching lineation trends N10–57° E and is oriented oblique to the strike of the foliation, with plunges mainly towards the NE. Both S2 and L2 resulted from a deformation phase D2. Hence, the D2 deformation is represented by a top-to-the-NE ductile deformation in the Menderes metamorphic rocks, forming the S2 mylonitic foliation cutting and displacing the older S1 gneissic foliation (Ersoy et al., 2010).

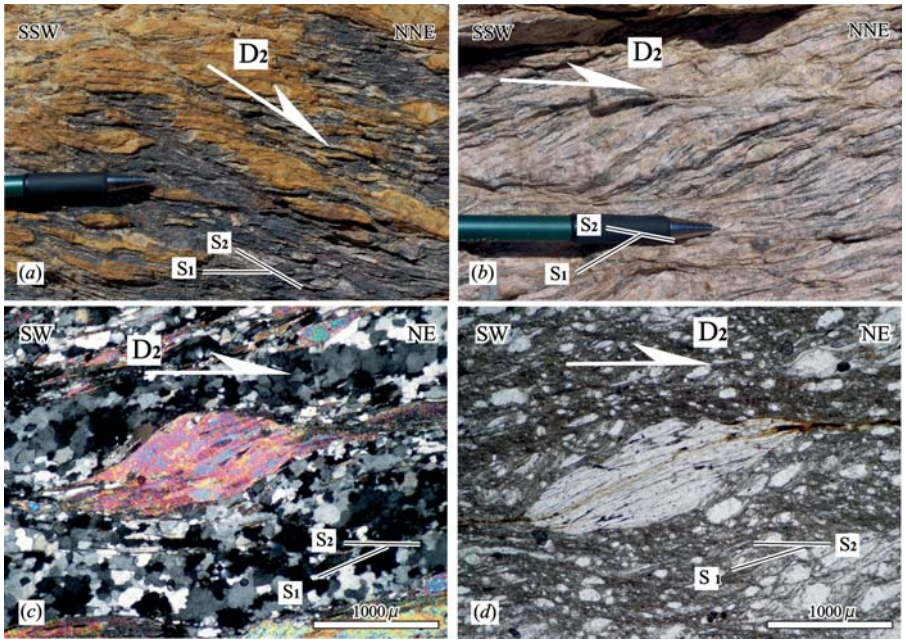

Figure 31. (a and b) Field photographs of the metamorphic rocks of the Menderes Massif displaying S-C' fabrics from the mylonitic gneisses in the eastern margin of Selendi basin. S (S1 foliation) and C' (S2 foliation) planes are defined by feldspar porphyroclasts and aligned micas respectively. (c) thin section view showing asymmetrical microstructures in the garnet mica schists (mica "fish" structure); (d) thin section view showing older asymmetrical microstructures from the cataclastic gneisses in the eastern margin of the Selendi basin indicating that the ductile textures are overprinted by brittle deformation. All photographs are parallel to the stretching lineation and normal to the foliation. The fabrics are consistent with top-to-the-NE (dextral) shearing (from Ersoy et al., 2010).

During the deformation phase D2, the Menderes metamorphic rocks also deformed under brittle conditions, overprinting the early mylonitic fabrics in the vicinity of the detachment fault (Figure 31d). The brittle deformation under decreasing P-T conditions resulted in the formation of cataclastic

fabrics in a zone of ca. 100 m (Ersoy et al., 2010; Figure 31d). The deformation along the detachment fault in the Selendi basin is therefore characterized by a ductile-to-brittle transition. The orientations of the mylonitic foliation S2 and associated mylonitic stretching lineation L2 are also concordant with the kinematic indicators on the fault surface. These observations show that the D2 deformation phase is related to an extensional event with a top to the NE sense of shear. This is evidenced by: (1) displaced broken grains of feldspar in a ductile matrix, (2) obliquely elongate recrystallized grains and subgrains of quartz with respect to the main foliation, (3) asymmetric mica "fish" structures, and (4) ductile to brittle transition in the deformation towards the low-angle fault; all of which indicate a top-to-the-NE normal sense of shear (Ersoy et al., 2010).

Similar to Demirci and Selendi basins, in the Uşak-Güre Basins the low-angle detachment fault between the Hacıbekir Group and the Menderes Metamorphic rocks, as well as between the İzmir-Ankara Zone ophiolitic mélange units and the Menderes Metamorphic rocks is well observed (Çemen et al. 2006; Ersoy et al., 2010; Karaoğlu and Helvacı 2012a). In the northwestern margin of the Güre basin, the sandstones of the Yeniköy Formation are tectonically underlain by the cataclatised metamorphic rocks of the Menderes Massif (Figure 32). In the vicinity of the Kürtköyü village, the conglomerates of the Kürtköyü Formation unconformably overlie the ophiolitic rocks of the İzmir-Ankara Zone. There, the basal parts of the Kürtköyü Formation include near-horizontal shear zones indicating a top-to-NE movement (Figure 33).

Figure 32. Field photograph of the low-angle detachment fault between the Yeniköy Formation and the Menderes Metamorphic rocks in the northwestern margin of the Güre basin.

Taking into account the data from the Demirci, Selendi and Uşak-Güre basins presented above, it is concluded that (1) ophiolitic mélange units of the İzmir-Ankara Zone (İAZ) overlie the Menderes Massif along a low-angle top-to-NE detachment fault (the Simav detachment fault, SDF); (2) early Miocene Hacıbekir Group also juxtaposed with the metamorphic rocks along the SDF; (3) the Hacıbekir group include olitolites from the İAZ in the Selendi basin. **These data indicate that the Hacıbekir Group was deposited in a supra-detachment basin comprising Demirci, Selendi and Uşak-Güre basins, under the control od the Simav Detachment Fault during the early Miocene**

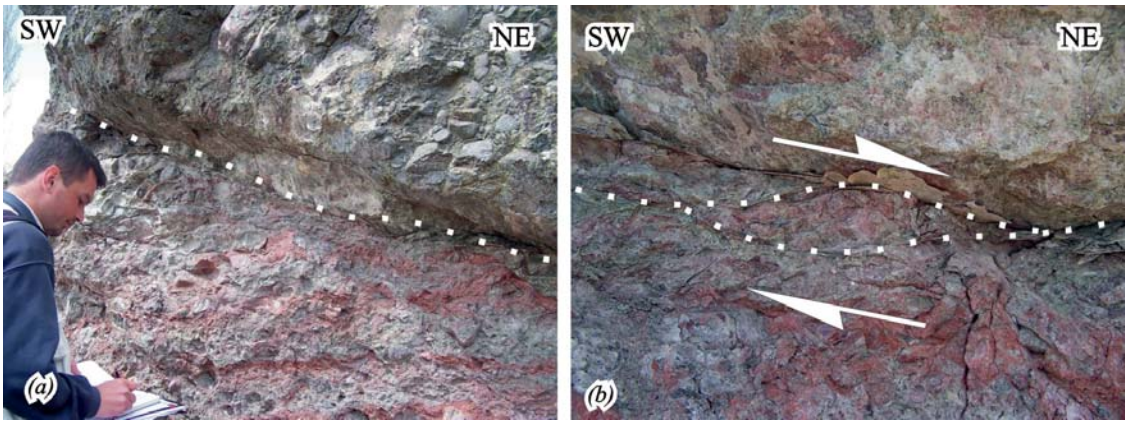

Figure 33. Field photograph of the low-angle shear zones in the Kürtköyü Formation observed at the basal parts of the unit (from the western margin of the Uşak Basin, near Kürtköyü village).

The eastern margins of Demirci basin were deformed by nearly NE–SW-trending right-lateral strike- to oblique-slip faults with a normal component (Figure 34). The middle Miocene volcano-sediments, the İnay Group, partially overlap onto these faults. The Middle Miocene Asitepe Volcanics and the Naşa basalt are also located on these NE–SW-trending faults. In contrast, the western margin of these basins was deformed by left-lateral strike- to oblique-slip faults with a normal component. The sedimentary facies of the İnay Group show a gradual change from coarse- to fine-grained the clasts, from the margins of the basin to the centre, as well as from bottom to top. In the eastern margin of Demirci basin, a NE–SW-trending fault zone is interpreted to have controlled the deposition of the Middle Miocene Borlu Formation, because the coarser-grained sediments of the unit are located on the hanging-wall of this fault and the sediment becomes finer-grained further away from the fault. Several planes have been measured, which strike 16–55° and dip 48–90°NW, with two distinct rakes of 45–72°S and 70–86°N. In the western margin of Demirci basin, a dextral fault plane is recognized striking at 25° and dipping at 55°SE, with a rake of 14–22°NE. These faults juxtapose the Borlu Formation on the hanging wall with the Menderes Massif on the footwall (Ersoy et al., 2011).

In some locations along the western margin of the Selendi basin, the deposition of the middle Miocene İnay Group seems to have been controlled by NE–SW-trending sinistral faults (in the vicinity of Hüdük village see also Seyitoğlu, 1997a). The alluvial fan deposits with boulder conglomerates pass laterally into the fine-grained sedimentary rocks of the İnay Group, as well as in the eastern margin of the Selendi basin. The relative amounts of the conglomerate intercalations and their clast sizes systematically increase toward the eastern margin of the basin. Long-axis alignment of the clasts suggests derivation from the eastern margin of the basin. Syn-sedimentary faults were also developed within the İnay group throughout the Selendi basin. Several planes have been measured, which strike N70°–85°W and N65°–87°E, and dip ~77°–81°W. These faults may be indicative of the middle Miocene tectonics in the region, as they formed synchronously with deposition of the İnay group. Such a relation is best observed along the western margin of the Güre basin (Ersoy et al., 2010; Karaoğlu et al., 2012a), where alluvial fans of the Ahmetler formation were fed by this margin. Two basaltic extrusions (Kıran and Zahman basalts of the Payamtepe volcanics) of Middle Miocene were also located along this tectonic line (Figures 16 and 21). **All these data indicate that the Middle Miocene İnay Group was deposited in the Demirci, Selendi and Uşak-Güre basins which was bounded by NE–SW-trending strike- to oblique-slip high-angle faults with a normal component in the middle Miocene**.

Figure 34. Field view of an oblique fault controlled the İnay Group in the western margin of the Demirci basin. (from Ersoy et al., 2011)

In Demirci basin, the NW-SE-trending left-lateral fault zone cuts the Middle Miocene Asitepe Volcanics and the Köprübaşı Formation and the basement rocks (Güneşli fault zone; Figures 10, 13 and 35). Well-exposed fault planes show a dominant strike-slip component. The fault zone can be traced outside Demirci basin, where it also cuts the metamorphic highs between the Demirci and Gördes basins, and into the Güneşli district in the northern part of Gördes basin. NW–SE-trending left-lateral faulting is also seen in the Ören fault zone (Figure 13), which cuts the metamorphic high between the Demirci and Selendi basins, and the early Miocene volcano-sedimentary units in both basins. These data indicate that the basin was deformed under the control of NW–SE-trending left-lateral and NE–SW-trending right-lateral strike-slip faults during the late Miocene.

The NE–SW-trending sinistral Ören fault and the NW–SE-trending dextral strike-slip faults and associated oblique- to dip-slip normal faults along the Eskin fault zones are formed during late Miocene (Figure 10). The Eskin fault zone can be best followed along the eastern margin of the Selendi basin where the pre- and middle Miocene units are cut and displaced along them. Dextral slickenside striations occur on the NW–SE-trending normal faults of the fault zone which strike N24°–33°E, and dip 54°–77°SW, and rake 60°–65°NW (in the vicinity of Melek village). Near Kabaklar town, the beds of the late Miocene Kocakuz formation are also inclined as high as 65° and are juxtaposed with volcaniclastic rocks of the middle Miocene Yağcıdağ volcanics along the NE–SW-trending right-lateral strike-slip Eskin fault zone. The NE–SW-trending fault planes of the Eskin fault system strike N65°–80°E and dip 80°–87°SE with a rake of 10o–15oNW near the Kabaklar village. It strikes N30°–37°E and dips 66°–75°SE with a rake of 10°–12°NW ~1 km west of the Eskin. The Eskin fault zone forms the present-day border of the Selendi basin. **These data indicate that the region was deformed by NW–SE-trending left lateral and NE–SW-trending right lateral strike-slip faults during the late Miocene, which controlled the deposition of the late Miocene Kocakuz Formation and the emplacement of the late Miocene basalts**.

Figure 35. Field view of a segment of the Güneşli fault zone (cutting the volcanic rocks of the Asitepe volcanics) (from Ersoy et al., 2011).

During the Plio-Quaternary, all the Miocene sedimentary units and tectonic elements of the NE–SW-trending basins were cut by ~E–W-trending normal faults of the Simav half-graben and the Gediz graben. The reader is referred to Cohen et al., (1995); Emre (1996), Seyitoğlu (1997b), Çiftçi and Bozkurt (2009) for further information on the E–W-trending grabens. ~2 km south of Yeniköy village a fault plane from the southern fault zone of the Simav half-graben strikes 80–85° and dips ~65–84°NE, with a rake of 43–65°E, indicating that the fault has right-lateral strike-slip component. The southern faults of the Simav half-graben (Figure 36) cut and displaced Demirci basin (Figure 10), with its northern part termed as the Akdere basin (Seyitoğlu, 1997b). From this perspective, Ersoy et al (2011) also suggest that Emet basin is the northward continuation of Selendi basin (Figure 10).

3.2.1. Summary

As a summary, the Demirci, Selendi, Uşak-Güre basins have similar tectono-stratigraphic evolution differing from the Gördes basin. Comparative Stratigraphic evolutions of the basins are summarized in the Figure 37. In the Demirci, Selendi, Uşak-Güre basins, the early Miocene volcano-sedimentary succession, the Hacıbekir Group, was deposited on a regionally corrugated low-angle normal (detachment fault) which can be correlated with the Simav Detachment Fault (SDF). On the other hand, the Gördes basin has separated from the Menderes Core Complex by NE–SW-trending strike-

slip Kızıldam Fault which controlled the deposition of the early Miocene Kızıldam Formation. In these respects, Ersoy et al. (2011) suggested that exhumation of the northern flank of the Menderes Massif (controlling the deposition of the Hacıbekir group) was accommodated by strike-slip faulting on its western margin, along which Gördes basin is formed. They proposed that exhumation of the Menderes Massif occurred by; (a) low-angle normal detachment faults to the northeast, on which Neogene volcano sedimentary basins (Demirci, Selendi and Uşak-Güre basins) developed, and (b) dextral strike-slip shear zones to the west, along which Gördes basin was developed (Figure 38a). Similarly, Çemen et al. (2006) suggested that the first exhumation of the massif along the low-angle normal detachment faults may have been accommodated by steeply dipping oblique- to strike-slip faults in the eastern margin of the massif. This zone is named as Uşak-Muğla Transfer Zone by Karaoğlu and Helvacı (2012a). During the Middle Miocene strike- to oblique-slip faults deformed the basins and controlled the deposition of the middle Miocene volcano-sedimentary units (İnay Group). These faults remain in the hanging-wall of the Gediz Detachment Fault and can be explained by a model proposed by Şengör (1987) (differential stretching in the hanging-wall of a low-angle normal fault; Figures 37 and 38b). In the late Miocene, NW–SE-trending left-lateral (Güneşli and Ören fault zones) and NE–SW-trending right-lateral (e.g., Eskin fault zone) strike-slip faults deformed the NE–SW-trending basins (Figures 10, 37 and 38c). These faults cut the older units and structures in all basins. The pattern of the late Miocene faults indicates that the region was deformed under N–S-directed extension and E–W-directed compression under pure shear during late Miocene, and the N–S-directed extension in the region was continuous. All basins are deformed and cut by E–W-trending high angle normal faults in Plio-Quaternary (Figures 10 and 38d).

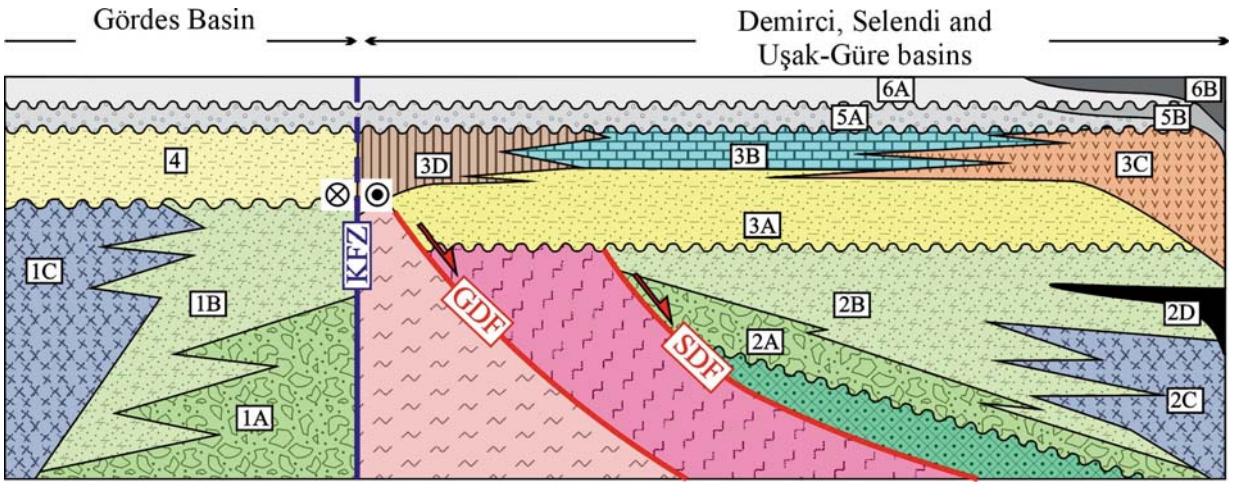

Figure 37. Comparative tectono-stratigraphic sections of the NE–SW-trending basins. The Gördes basin. 1A-Kızıldam Fm.; 1B-Köprübaşı Fm.; 1C-Güneşli and Kayacık volcanics; 2A and 2B-Kürtköyü and Yeniköy Fm.; 2C and 2D-early Miocene felsic and mafic volcanics; 3A and 3B-Ahmetler and Ulubey Fm. 3C and 3D-middle Miocene felsic and mafic volcanics; 4-Gökçeler Fm. 5A-late Miocene sediments; 5B-late Miocene basalts; 6A and 6b-plio-Quaternary volcanic and sediments

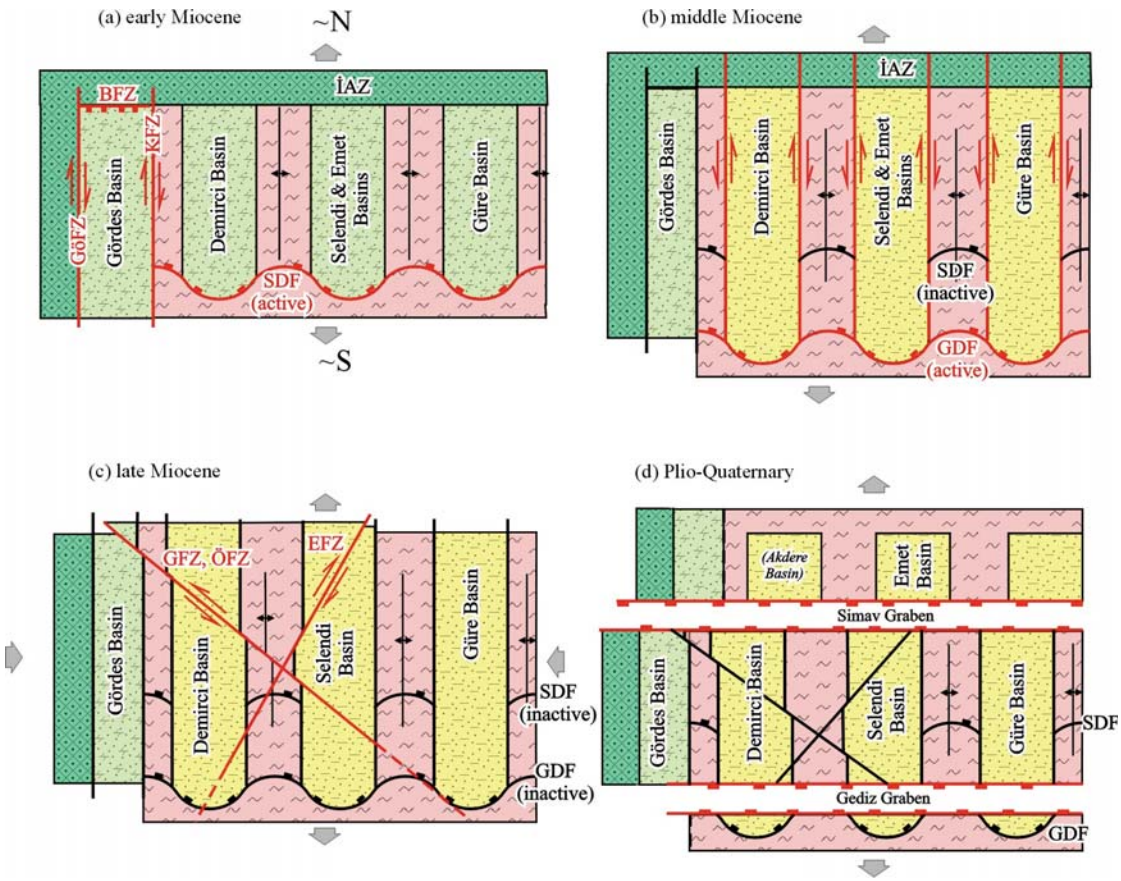

Figure 38. Cartoon showing the evolution of the NE–SW-trending Gördes, Demirci, Selendi, Emet and Güre basins from the early Miocene to Recent: (a) the early Miocene exhumation of the Menderes Massif along the Simav detachment fault (SDF) caused formation of synclines on the SDF in which early Miocene sedimentary units were deposited. (b) Second-stage collapse and formation of the Gediz detachment fault (GDF) during the middle Miocene. (c) Differential stretching in the hanging wall of the corrugated GDF formed a number of NE–SW-trending oblique-slip accommodation faults that controlled deposition of the middle Miocene İnay group. (d) Formation of late Miocene NE–SW-trending right-lateral (Eskin fault zone, EFZ) and NW–SE-trending left-lateral (Güneşli and Ören fault zones, GFZ and ÖFZ) strike-slip faults that locally deposited the late Miocene volcano-sedimentary units. (e) Last phase of the N–S extension (rift-mode) was responsible for formation of the E–W-trending grabens (from Ersoy et al., 2011).

3.3. Volcanic Evolution

3.3.1. Gördes Basin

In the Gördes basin two felsic units are described which early Miocene are in age (Ersoy et al., 2011): Güneşli and Kayacık volcanics (Figure 39a). The Güneşli Volcanics cover a large area to the north of the basin. This unit is composed of rhyolitic dykes and lava flows and associated rhyolitic pyroclastic rocks to the north of the Gördes basin. The volcanic products are best observed around Güneşli (Figure 11). The pyroclastic rocks of the unit interfinger with the fine-grained sedimentary rocks of the Kuşlukköy Formation. The thickness of the tuff intercalations increases towards the northern part of the basin (1-2 m in the south and ~30m to the north of the Gördes town) where rhyolitic volcanic rocks crop out, suggesting that the pyroclastic flows in the basin fill deposits originated from the rhyolitic volcanic centers to the north of the basin (Figure 11). These acidic volcanic rocks are correlated with the dacitic to rhyolitic volcanic rocks of the Kayacık Volcanics in the centre of Gördes basin and the Sevinçler and Eğreltidağ volcanics in the Demirci and Selendi basins,

respectively (Figure 39). Purvis et al. (2005) obtained 19.16±0.09 to 17.04±0.35 Ma biotite and feldspar Ar/Ar ages from the pyroclastic rocks of the Güneşli Volcanics. Similarly, Ersoy et al. (2012a) obtained 18.906±0.026 Ma (MSWD =1.90) and 18.763±0.890 Ma (MSWD =9.50) sanidine Ar/Ar ages from the Güneşli volcanics (Table 3). The Güneşli volcanics are classified geochemically as high-K calc-alkaline rhyolites (Ersoy et al., 2012a) (Figure 35).

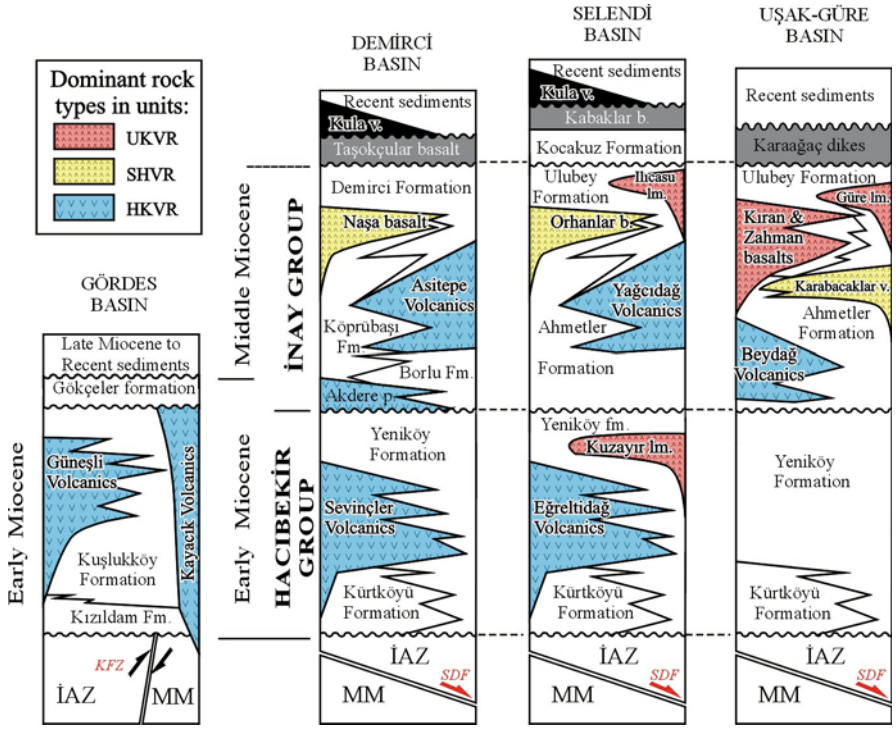

Figure 39. Stratigraphic correlation of the volcanic units in the NE–SW-trrending basins (from Ersoy et al., 2012a).

Table 3. Radiometric age data from the volcanic rocks in the NE–SW-trending basins.

Basin and Unit	*Sample*	*Rock Type*	*Radiometric age (Ma), material and reference*
Gördes Basin			
Kayacık volcanics	S1/36	Rhyodacite	17.60±0.10 (biotite, Ar/Ar) (Purvis et al., 2005)
	S1/38	Rhyodacite	17.62±0.07 (biotite, Ar/Ar) (Purvis et al., 2005)
	S2/5	Rhyodacite	20.86±0.08 (feldspar, Ar/Ar) (Purvis et al., 2005)
	S2/5	Rhyodacite	20.45±0.38 (feldspar, Ar/Ar) (Purvis et al., 2005)
	S2/11	Acidic tuff	21.71±0.04 (biotite, Ar/Ar) (Purvis et al., 2005)
	S2/11	Acidic tuff	20.49±0.09 (biotite, Ar/Ar) (Purvis et al., 2005)
	S2/4	Acidic tuff	19.16±0.09 (biotite, Ar/Ar) (Purvis et al., 2005)
Güneşli volcanics	S2/68	Acidic tuff	17.04±0.35 (biotite, Ar/Ar) (Purvis et al., 2005)
	S2/68	Acidic tuff	18.78±0.30 (biotite, Ar/Ar) (Purvis et al., 2005)
	861	Rhyolite	18.91±0.03 (sanidine, Ar/Ar) (Ersoy et al., 2012a)
	861	Rhyolite	18.76±0.09 (sanidine, Ar/Ar) (Ersoy et al., 2012a)

International Earth Science Colloquium on the Aegean Region, IESCA-2012
1-5 October 2012, Izmir, Turkey

Demirci Basin			
Sevinçler volcanics	721	Dacite	19.06±0.05 (plagioclase, Ar/Ar) (Ersoy et al., 2012a)
	721	Dacite	19.75±0.07 (biotite, Ar/Ar) (Ersoy et al., 2012a)
	721	Dacite	19.75±0.05 (biotite, Ar/Ar) (Ersoy et al., 2012a)
	721	Dacite	19.56±0.04 (biotite, Ar/Ar) (Ersoy et al., 2012a)
Naşa basalt	ÖD-50	Shoshonite	15.80±0.30(K-Ar) (Ercan et al., 1996)
	ÖD-52	Latite	15.20±0.30 (K-Ar) (Ercan et al., 1996)
Asitepe volcanics	717	Andesite	17.58±0.09 (plagioclase, Ar/Ar) (Ersoy et al., 2012a)
Taşokçular basalt	727	Shoshonite	10.46±0.03 (whole rock, Ar/Ar) (Ersoy et al., 2012a)
Selendi Basin			
Eğreltidağ volcanics	SE-1	Rhyolite	18.90±0.60 (biotite, K-Ar) (Seyitoğu et al., 1997)
	521	Dacite	18.90±0.10 (plagioclase, Ar/Ar) (Ersoy et al., 2008)
	521	Acidic tuff	20.00±0.20 (amphibole, Ar/Ar) (Ersoy et al., 2008)
Kuzayır lamproite	518	Lamproite	17.90±0.20 (groundmass, Ar/Ar) (Ersoy et al., 2008)
	518	Lamproite	18.60±0.20 (phlogopite, Ar/Ar) (Ersoy et al., 2008)
Yağcıdağ volcanics	SE-3	Trachydacite	14.90±0.60 (biotite, K-Ar) (Seyitoğlu et al., 1997)
	S1/3	Acidic tuff	16.42±0.99 (feldspar, Ar/Ar) (Purvis et al., 2005)
	S1/3	Acidic tuff	16.61±0.14 (biotite, Ar/Ar) (Purvis et al., 2005)
	YF-2	Dacite	16.43±0.32 (plagioclase, Ar/Ar age) (Ersoy et al., 2012a)
Orhanlar basalt			*Middle Miocene (Stratigraphic relations)*
Kabaklar basalt	S-1	K-trachybasalt	8.50±0.20 (K-Ar) (Ercan et al., 1996)
	IZ-67	K-trachybasalt	8.37±0.07 (Ar/Ar) (Innocenti et al., 2005)
Ilıcasu lamproite	IZ-41	Lamproite	15.87±0.13 (phlogopite, Ar/Ar) (Innocenti et al., 2005)
	IZ-41	Lamproite	15.83±0.13 (groundmass, Ar/Ar) (Innocenti et al., 2005)
	05IS01	Lamproite	15.54±0.06 (phlogopite, Ar/Ar) (Prelevic et al., 2012)
	05IS03	Lamproite	15.77±0.09 (phlogopite, Ar/Ar) (Prelevic et al., 2012)
Uşak-Güre Basin			
Elmadağ volc. centre	U-31	Trachydacite	16.28±0.05 (biotite, Ar/Ar) (Karaoğlu et al., 2010)
	U-68	Pyroclastic	16.48±0.08 (biotite, Ar/Ar) (Karaoğlu et al., 2010)
	U-70	Latite	16.44±0.07 (groundmass, Ar/Ar) (Karaoğlu et al., 2010)
	U-132	N/A	16.48±0.33 (biotite, Ar/Ar) (Karaoğlu et al., 2010)
	U-164	Trachytic dome	17.29±0.13 (amphibole, Ar/Ar) (Karaoğlu et al., 2010)
İtecektepe volcanic centre	UG-63	Dacite	14.60±0.30 (whole rock, K-Ar) (Seyitoğlu et al., 1997)
	U-159	Dacite dike	15.04±0.10 (biotite, Ar/Ar) (Karaoğlu et al., 2010)

International Earth Science Colloquium on the Aegean Region, IESCA-2012
1-5 October 2012, Izmir, Turkey

Beydağ volcanic centre	U-2 U-161	dacite Dacitic dome	13.10±0.20 (K-Ar) (Ercan et al., 1996) 12.15±0.15 (biotite, Ar/Ar) (Karaoğlu et al., 2010)
Yeniköy dikes	UG-58 U-153	Trachydacite Trachyte	15.10±0.40 (whole rock, K-Ar) (Seyitoğlu et al., 1997) 16.01±0.08 (sanidine, Ar/Ar) (Karaoğlu et al., 2010)
Karabacaklar volcanics	UG-75 UG-142 U-144	Trachyte Trachyte Trachyte	15.90±0.40 (whole rock, K-Ar) (Seyitoğlu et al., 1997) 15.20±0.60 (whole rock, K-Ar) (Seyitoğlu et al., 1997) 15.93±0.08 (groundmass, Ar/Ar) (Karaoğlu et al., 2010)
Kıran-Zahman basalt	UG-145	Latite	15.50±0.40 (whole rock, K-Ar) (Seyitoğlu et al., 1997)
Güre lamproite	IZ-38 05GÜ02 05GÜ02 05GÜ02	Lamproite Lamproite Lamproite Lamproite	14.20±0.12 (groundmass, Ar/Ar) (Innocenti et al., 2005) 15.54±0.33 (groundmass, Ar/Ar) (Prelevic et al., 2012) 15.67±0.29 (groundmass, Ar/Ar) (Prelevic et al., 2012) 15.32±0.25 (groundmass, Ar/Ar) (Prelevic et al., 2012)
Karaağaç dikes			*Late Miocene (Stratigraphic relations)*

The Kayacık Volcanics crop out in the centre of Gördes basin (Figure 11). They are composed of mainly green colored dacitic to rhyolitic volcanic necks (Figures 40 and 41) and associated lava flows and minor pyroclastic rocks interfingering with the Kuşlukköy Formation. The volcanic necks cut and deform the sandstones of the Kuşlukköy Formation. These volcanic rocks have previously been described as central volcanics (Seyitoğlu and Scott, 1994a). The volcanic products of the unit yielded 18.4±0.6 to 16.3±0.5 Ma K-Ar (Seyitoğlu and Scott, 1994b) and 21.71±0.04 to 17.6±0.1 Ma Ar/Ar ages (Purvis et al., 2005) (Table 3). The geochemical data from the Kayacık volcanics indicate that they are classified as medium- to high-K calc-alkaline dacite and rhyolite (Figure 42).

Figure 40. Field view of the rhyolitic necks of the Kayacık volcanics located in the centre of the Gördes Basin.

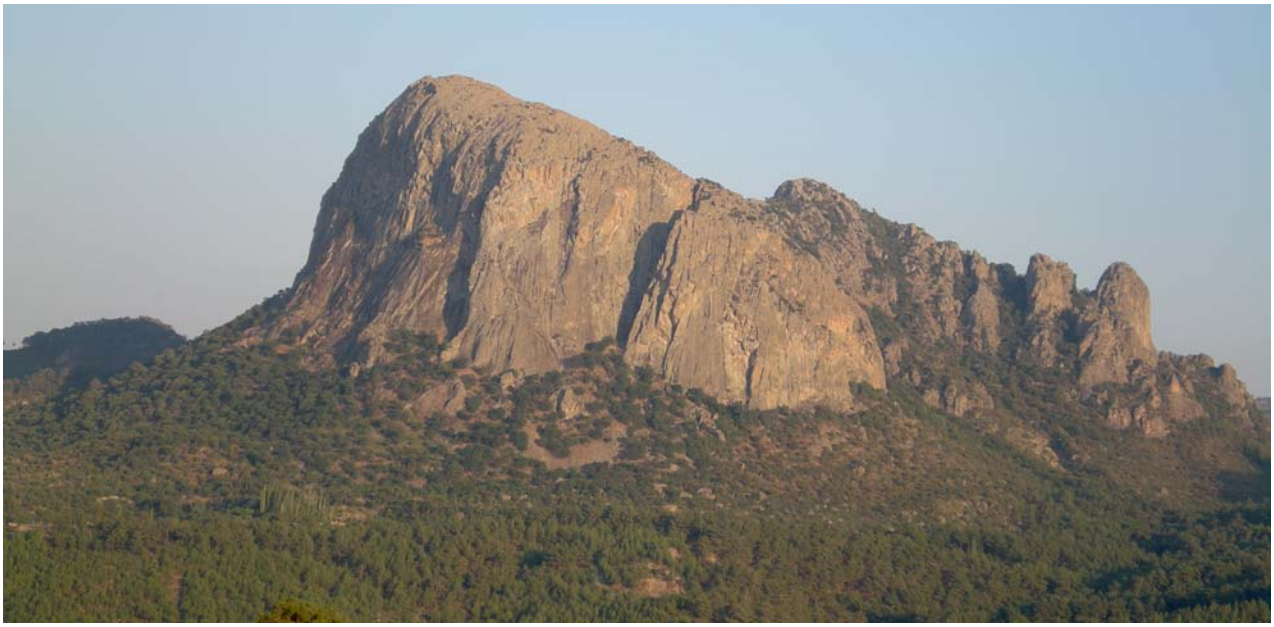

Figure 41. Field view of the rhyolitic necks of the Kayacık volcanics located in the centre of the Gördes Basin.

3.3.2. Demirci Basin

Neogene volcanic units in the Demirci basin are: (1) early Miocene Sevinçler volcanics, (2) middle Miocene(?) Akdere pyroclastics, (3) latest early Miocene - earliest Asitepe volcanics, (4) middle Miocene Naşa basalt, (5) late Miocene Taşokçular basalt. The Plio-Quaternary Kula volcanics may also be added into the Demirci basin (Figures 9, 13 and 39b).

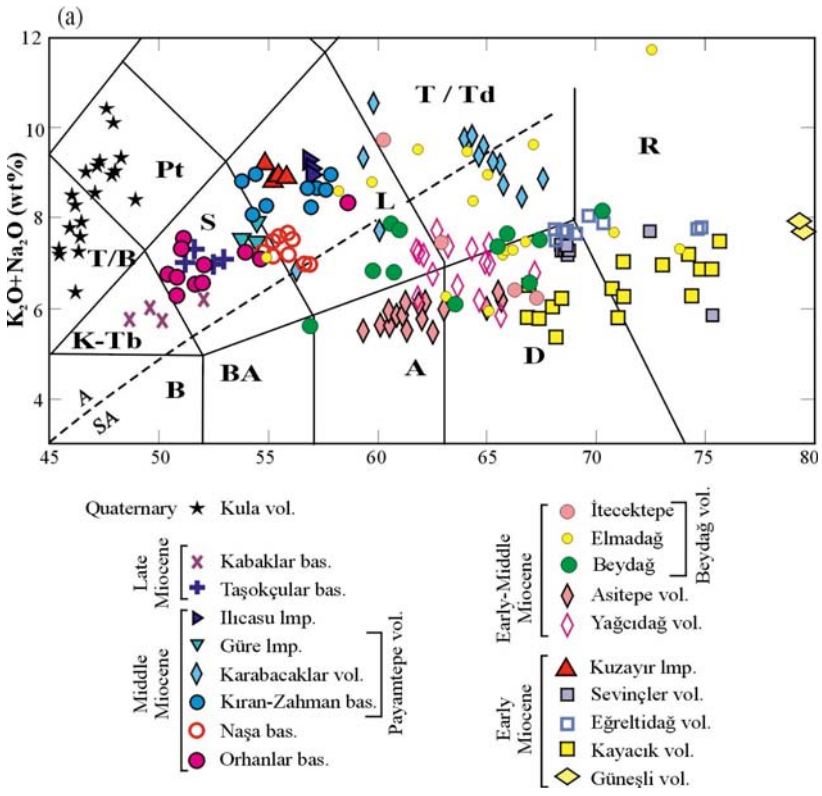

Figure 42. Total alkalis–silica (TAS) classification (Le-Maitre, 2002) of the Neogene volcanic rocks in the NE–SW-trending Gördes, Demirci, Selendi and Uşak-Güre basins. T/B-tephrite/basanite, Pt-phonotephrite, K-Tb-K-trachybasalt, S-shoshonite, L-latite, T/Td-trachyte/trachydacite, B-basalt, BA-basaltic andesite, D-dacite, R-rhyolite.

The Sevinçler Volcanics, located to the northeastern part of the Demirci basin (Figure 13), is composed dacitic-rhyolitic dykes, volcanic necks, rhyolitic pyroclastics and lava flows. Ersoy et al. (2012a) obtained 19.057±0.045 Ma (MSWD =1.80) plagioclase and 19.748±0.047 Ma (MSWD =2.10) biotite Ar/Ar ages (Table 3). Geochemical data from the Sevinçler volcanics show that they are composed of high-K calc-alkaline dacite and rhyolites (Figure 42). Stratigraphic and geochemical data from the dacitic-rhyolitic lavas of the Sevinçler Volcanics indicate that they are correlated with the Lower Miocene Eğreltidağ Volcanics that crops out in the northern part of the Selendi basin (Ersoy and Helvacı, 2007; Ersoy et al., 2010).

The Akdere pyroclastics occur along the base of the İnay Group and cover the Hacıbekir group along an unconformity. They are seen especially to the north of the basin (Figure 13). The Akdere pyroclastics are a key marker horizon linking the stratigraphy of the Demirci basin either side of the Simav half-graben. The thickness of the Akdere pyroclastics decreases from the north (~50 m) to the south (~1 m) within the Demirci basin, implying that they originated from a volcanic centre located further north. However, this proposed centre is obscured by the normal to oblique slip faults of the Plio-Quaternary Simav half-graben which cut and displaced the infill of Demirci basin. There is no age and geochemical data from these rocks, but Stratigraphic relationships indicate that they are probably latest early Miocene or earliest middle Miocene. The Akdere pyroclastics are conformably overlain by the fine grained sediments of the Köprübaşı Formation (Figure 43).

Figure 43. Field view of the volcanic centers of the Asitepe and Yağcıdağ volcanics (The photo has taken from a point to the western margin of the Demirci basin towards southeast). The Akdere pyroclastics are also seen with near-horizontal white colors to the centre of the picture.

The Asitepe volcanics are located on the eastern margin of the Demirci basin (Figure 13). These volcanics are composed of pyroclastic rocks and andesitic lava flows, with field observations showing that the pyroclastic rock intercalations (ignimbrites) flowed southward. The ignimbrites are overlain by block-and-ash fall and finally andesitic-dacitic pink-colored plagioclase-phyric lavas. The early lavas of the Asitepe volcanics contain plagicolas and orthopyroxene minerals while the late-stage lavas composed of plagicoalse, amphibole and/or biotite with minor quartz. On a geochemical base, the Asitepe volcanics are classified as high-K andesite and dacite. Ersoy et al. (2012a) obtained 17.580±0.094 Ma (MSWD =0.52) Ar/Ar plagioclase age from the andesitic lavas of the unit. The Asitepe Volcanics can be correlated with the Yağcıdağ Volcanics in the Selendi basin (Ersoy et al., 2008; 2012a) on the basis of their stratigraphic positions, lithology and geochemistry.

The Naşa basalts are located in the northern part of the Demirci basin (so-called Akdere basin) along the northern edge of the Simav half-graben. The Naşa basalt (15.8±0.3 and 15.2±0.3 Ma K-Ar

ages of Ercan et al., 1996; Table 3) is composed mainly of syn-sedimentary basaltic lava flows that flowed over the sedimentary rocks of the Borlu Formation. On the basis of their geochemical features, the Naşa basalt is classified as shoshonite and latite with high-MgO shoshonitic character (Figure 42).

The Taşokçular basalt probably emplaced along the NW-SE trending Güneşli fault zone, in the eastern margin of the Demirci basin (Figure 13). Taşokçular basalt is classified as shoshonite with higg-K or shoshonitic character (Ersoy et al., 2012a). The unit has similar geochemical features to the late Miocene basalts in Selendi basin. The youngest unit in Demirci basin is the basaltic lavas and pyroclastics with cinder cones of the Kula volcanics that crop out to the south of the basin, on the northern shoulder of the Pliocene-Quaternary Gediz graben.

3.3.3. Selendi Basin

Neogene volcanic units in the Demirci basin are: (1) early Miocene Eğreltidağ volcanics, (2) early Miocene Kuzayır lamproite, (3) Yağcıdağ volcanics, (4) Orhanlar basalt and (5) Kabaklar volcanics (Figures 9, 16 and 39c). The Ilıcasu lamproite, located along the Simav half-graben in the present day configuration of the basins can also be included into the Selendi basin, as the basin has been cut by Plio-Quaternary Simav half-graben.

The Eğreltidağ volcanics, located to the northern part of the Selendi basin (Figure 16) are composed of dacitic-rhyolitic lava flows, domes and wide-spread pyroclastic rocks. The pyroclastic rocks of the unit interfinger with the sandstones of the Yeniköy Formation (Figure 44). The lava and pyroclastic rock samples of this unit yielded Ar/Ar and K-Ar ages between 20.00±0.20 and 18.90±0.10 (Seyitoğlu 1997a; Ersoy et al., 2008; Ersoy et al. 2012a; Table 3). Geochemical data from the unit indicate that the Eğreltidağ volcanic unit is composed of high-K calc-alkaline dacite and rhyolite. The Eğreltidağ volcanic unit is correlated with Sevinçler volcanics in the Demirci basin (Figure 42).

Figure 44. The conformable contact between Yeniköy Formation (Yf) and Eğreltidağ volcanic unit (Ev) (from Ersoy and Helvacı, 2007).

The Kuzayır lamproite (Ersoy and Helvacı, 2007) has small outcrops to the northern part of the Selendi basin (Figure 16). The lava flows of the unit are up to 5 m thick and cover an area up to 1 km. In hand specimen, they are characterized by dark brown phlogopite minerals within a dark grey to black matrix. The lower contact of the lava flows with the underlying sedimentary rocks display

chilled and glassy margins with minor in-situ fragmentation and irregular columnar joints (Figure 45a). The sedimentary rocks, just below the lower contact of the lava flows were deformed during the emplacement. On the other hand, the upper contact is very sharp and the Yeniköy Formation, just above the lava flow, is undeformed (Figure 45b). The lava flows were sharply covered by the mudstones and siltstones. The Kuzayır lamproite is especially important as it represents the first lamproitic product in western Anatolia (Ersoy and Helvacı, 2007). The Kuzayır lamproite is classified as ultrapotassic latite according to major element contents. Moreover, geochemical and mineralogical data indicate that the unit is composed of lamproitic lava flows. The lava samples of the unit yielded Ar/Ar ages between 17.18±0.23 and 18.60±0.20 (Ersoy et al., 2008; Ersoy et al. 2012a; Table 3).

The Yağcıdağ volcanic unit is located to the centre of the Selendi Basin (Figure 16). The Yağcıdağ volcanic unit is composed of, from bottom to top, pyroclastic fall deposits, ignimbrites, block-and-ash flow deposits and lava flows with dykes and domes. The Yağcıdağ volcanic unit interfingers with, and conformably overlies, the Ahmetler Formation which is overlain by the Ulubey Formation. The wide-spread pyroclastic flows can be traced from the Yağcıdağ volcanic centre towards northeast (e.g., around the Eynehan village; Figure 46). The geochemical analyses from the fresh lavas of the unit indicate that they are composed of high-K calc-alkaline andesite, dacite, latite and trachydacite. Seyitoğlu et al. (1997a) obtained 14.90±0.60 Ma K-Ar age from the Yağcıdağ volcanic unit. Purvis et al. (2005) presented Ar/Ar age of 16.42±0.09 Ma. Similarly, Ersoy et al. (2012a) have obtained 16.43±0.32 Ma (MSWD=5.10) Ar/Ar plagioclase age from the andesitic lavas of the unit (Table 3).

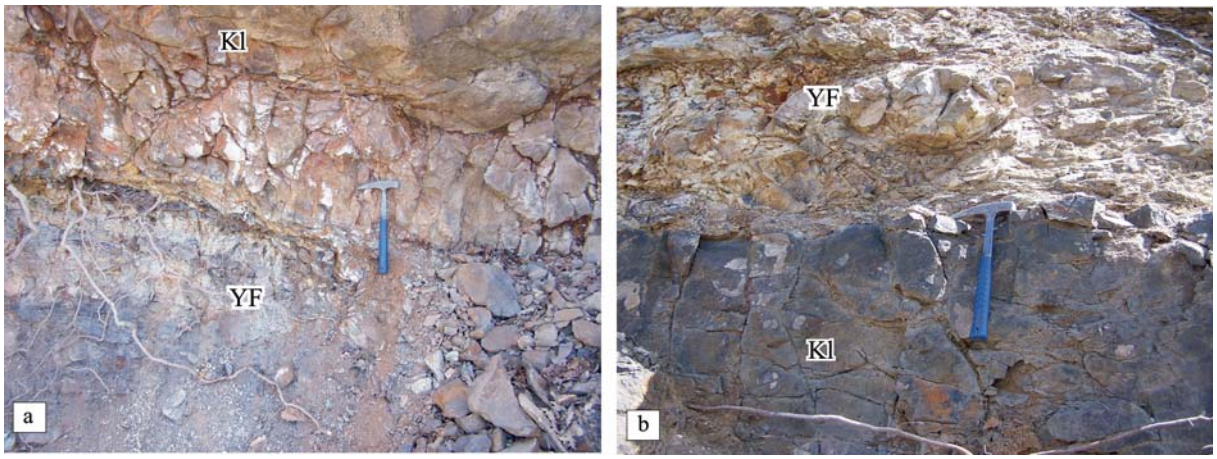

Figure 45. (a) The upper and (b) the lower contact between the Yeniköy Formation (Yf) and the overlying Kuzayır lamproite (Kl) (from Ersoy and Helvacı, 2007).

Figure 46. The pyroclastic rocks of the Yağcıdağ volcanics around Eynehan village

The Orhanlar basalt croups out to the northeast of the Yağcıdağ volcanic centre (Figure 9). The basaltic flows of the unit ingterfinger with the uppermost parts of the İnay Group. The Orhanlar basalt is geochemically composed of shoshonite and latite with a clear shoshonitic to ultrapotassic affinity (Figure 42).

The Kabaklar basalt emplaced along the NE–SW-trending zone of strike-slip deformation along the eastern border of the Selendi Basin (Ercan et al., 1996; Ersoy and Helvacı 2007; Figures 16 and 47). The basaltic lava flows of the unit are geochemically classified as K-trachybasalt and shoshonite with high-K affinity.

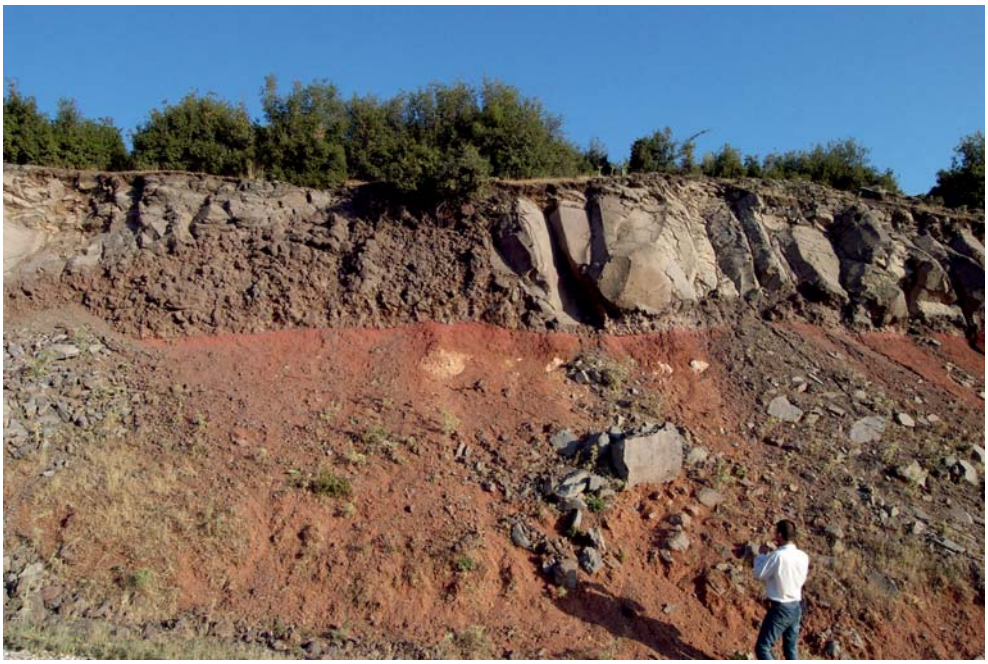

Figure 47. Field view of the contact between the Kabaklar basalt and underlying Kocakuz Formation.

3.3.4. Uşak-Güre Basin

The Beydağ volcanics emplaced along 3 volcanic centres: Beydağ, İtecektepe and Elmadağ volcanic centres. The Elmadağ volcanic center lies 12 km NE of the city of Uşak and covers approximately 210 km^2 (Figure 48). It is interpreted as a typical stratovolcano comprising a >700 m-thick succession of predominantly subaerial calc-alkaline lavas. More than 15 lava flows show low paleo-slope gradients (15o-23o) with the styles of blocky, columnar-jointed and a'a lava flows (Karaoğlu et al., 2010; Karaoğlu and Helvacı 2012b). Central parts contain moderate-level trachytic and lamproitic intrusions that have 35 and 30 meter depths respectively, and were affected by locally pervasive hydrothermal alteration, particularly the potassic and argillic stages. Some marginal parts interfinger with lacustrine sediments

.

Figure 48. Field photographs from characteristic and well-exposed intrusions around the Elmadağ volcano: (a) ultrapotassic dikes cutting lacustrine sediments of the İnay group in the Güre basin; (b) columnar-jointed trachytic intrusions at Davulkayası; (c) lamproitic dike within the Elmadağ eroded structure; (d) micro-diorite intrusion, northern Elmadağ volcano; (e) trachytic dike west of Kartaltepe; (f) rhyolitic dome structures in the Eğlence sector, northern part of Elmadağ; (g) uppermost rhyolitic rocks with "hydraulic breccias" (from Karaoğlu and Helvacı 2012b).

The İtecektepe volcanic centre is located 11 km SW of the city of Uşak, is a NE–SW-oriented 6x7 km elliptical shape and has a 3x4 km diameter deformed-ring plain area (Figure 49). The volcano was mainly constructed of andesite with minor latite and trachytes, with explosive products dominated by pyroclastic flows (ignimbrites) (Karaoğlu and Helvacı 2012b). The volcano has experienced intense internal tectonic deformation and erosion related to tectonic uplift of basement rocks of the Menderes Massif and İzmir-Ankara Zone, which crop out in the center of the volcano along reverse faults that offset the volcano/basement contact. Radiometric dating yields ages of 14.6 Ma (K–Ar) from the andesitic lavas, summit of İtecektepe (Seyitoğlu, 1997a), and 15.04 Ma (^{39}Ar–^{40}Ar) from an andesitic dike cutting the main cone lavas within the inferred vent area (Karaoğlu et al., 2010).

Andesitic volcanic sequences dominate the İtecektepe volcanic center, with minor dacite, latite, rhyolite and trachyte. Two phases have been identified: (1) lava flows and lava domes, including the 3.2 km-diameter lava dome from which the whole edifice takes its name; and (2) dike structures and intrusive bodies piercing the effusive phase of the volcano (Karaoğlu and Helvacı 2012b). The İtecektepe dome (1249 m) show flow-banded lavas, thickness is ca. 250 m. Andesitic lava flow sequences, some of which flowed up to 1.5 km radially, drape the flanks of the dome structure.

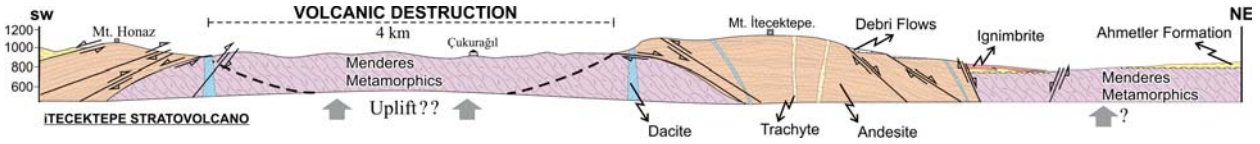

Figure 49. Geological cross-sections across the İtecektepe volcanic center. See Figure 2 for localities (from Karaoğlu and Helvacı 2012b).

The Beydağı volcanic edifice covers an area of 16.5x9 km, and contains a central, 12.5x5.5 km area of subsidence that displays a ~300 m elevation difference between the base and the top at c. 1170 m (Figure 50) (Karaoğlu and Helvacı 2012b). The northern and western outer flanks of the volcano preserve its original cone shape (Fig. 56). Two different radiometric age data are available from the southern summit area of the volcano: 12.15 Ma ($^{40}Ar/^{39}Ar$ method by Karaoğlu et al., 2010) and 13.1 Ma (K/Ar method by Seyitoğlu, 1997a). Intense deformation since the middle Miocene has resulted in dissection of the southern flank of the volcano by a NE–SW-striking oblique fault, causing accumulation of the late Miocene Asartepe Formation that is made up of weakly cemented coarse-grained conglomerates (Seyitoğlu et al. 2009). Metamorphic basement was uplifted by several oblique-slip normal faults within the subsidence area (Karaoğlu and Helvacı, 2012b), resulting in its exposure. Lacustrine sediments (Ahmetler Formation of İnay Group) occur within the subsidence area, suggesting that the lake was present during the volcano's post-destructive phase. Multi-stage intense hydrothermal alteration occurring at the margin of collapse structure are related to intrusive bodies and dike swarms, and affect a range of volcanic rocks and pyroclastic deposits both inside and outside of the subsidence zone.

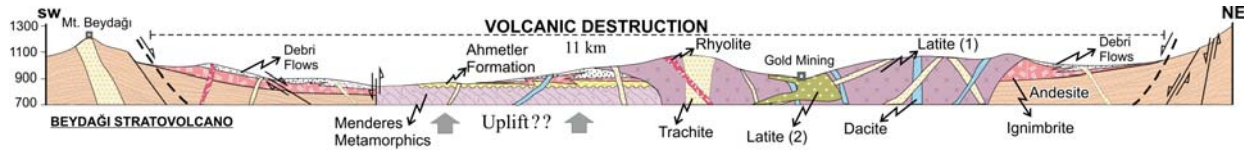

Figure 50. Geological cross-sections across the Beydağı volcanic center (from Karaoğlu and Helvacı 2012b).

4. E–W-Trending Alaşehir (Gediz) Graben

4.1. Stratigraphy

The Alasehir basin is a ~E-W-trending, 5-to-30-km wide, ~140 km long, Neogene depocenter developed above low-angle Alasehir detachment fault during Late Cenozoic extensional deformation in western Turkey (Figures 2 and 51). Two main sets of fault systems, WNW-ESE-striking high-angle normal faults and NNE-SSW-striking high-angle oblique-slip hinge faults control its internal structure and deposition (Figure 52). Occurrence of these main fault systems result in segmented basin structure and variations in sedimentary thicknesses and sedimentary facies along the basin (Öner and Dilek, 2011; Çiftçi et al., 2011). Its structural and sedimentological features indicate that the Alasehir basin can be defined as a supradetachment basin according to main features of extensional basins described by Friedmann and Burbank (1995). Recent geophysical studies show that the total sedimentary thickness in the Alasehir supradetachment basin ranges from 2000 to ~3000 meters in different segments from west to east (Sarı and Şalk, 2002; Çiftçi and Bozkurt, 2009; Çiftçi et al, 2011; Öner and Dilek, 2011). Local unconformities are most likely formed as a result of rotational deformation within the basinal strata and disappearance of some sedimentary units may be related to primary sedimentological processes or fault-controlled deposition in the basin.

The oldest sedimentary rocks of the Alasehir basin strata overlie the Alasehir detachment fault around Alasehir and consist of red-color, lacustrine shale alternating with conglomerate, sandstone,

mudstone at the bottom of the sequence (Gerentaş formation, Ağırbaş, 2004; Öner and Dilek, 2011). Relatively younger, upper levels includes lacustrine limestone alternating with clastic rocks (Kaypaktepe formation, Ağırbaş, 2004; Öner and Dilek, 2011) conformably overlain by red-colored, medium-to-thick bedded, poorly sorted conglomerate of Acidere formation (Emre, 1995; Öner and Dilek, 2011). An early-middle Miocene age is assigned to these lacustrine rocks according to palynological age from the lowermost part of the Alasehir basinal strata suggested by Ediger et al. (1996). In some localities, volcanic intercalations within these units revealed an isotopic age of 20-14 Ma (Benda et al., 1974; Seyitoğlu and Benda, 1998).

Poorly-sorted, polygenic conglomerate layers of the Acıdere formation includes angular-to-subangular, pebble-to-boulder-size clasts of metamorphic and igneous rocks exposed in the footwall of the Alaşehir detachment fault. The lowermost part of the Acıdere formation is observed as directly deposited on the low-angle detachment surface in western section of the basin, whereas it overlies the older lacustrine formations in the eastern part. Polygenic conglomerate layers alternate with fine-to-medium grain-sized, well-sorted, sandstone layers. Pebble imbrications in conglomerate layers, and cross-bedding, graded-bedding, lamination in sandstone layers are primary sedimentary structures in the Acıdere formation. Erosional and undulatory contacts between coarse-grained and fine-grained layers can be observed locally. The majority of bedding planes dip south-southwestward into the detachment surface. Seyitoğlu and Scott (1996) yielded middle-to-late Miocene palynological age from Eskihisar sporomorph association in the lowermost part of the Acidere formation. Ediger et al. (1996) also reported middle Miocene ages (14-11 Ma) from the upper section of the formation.

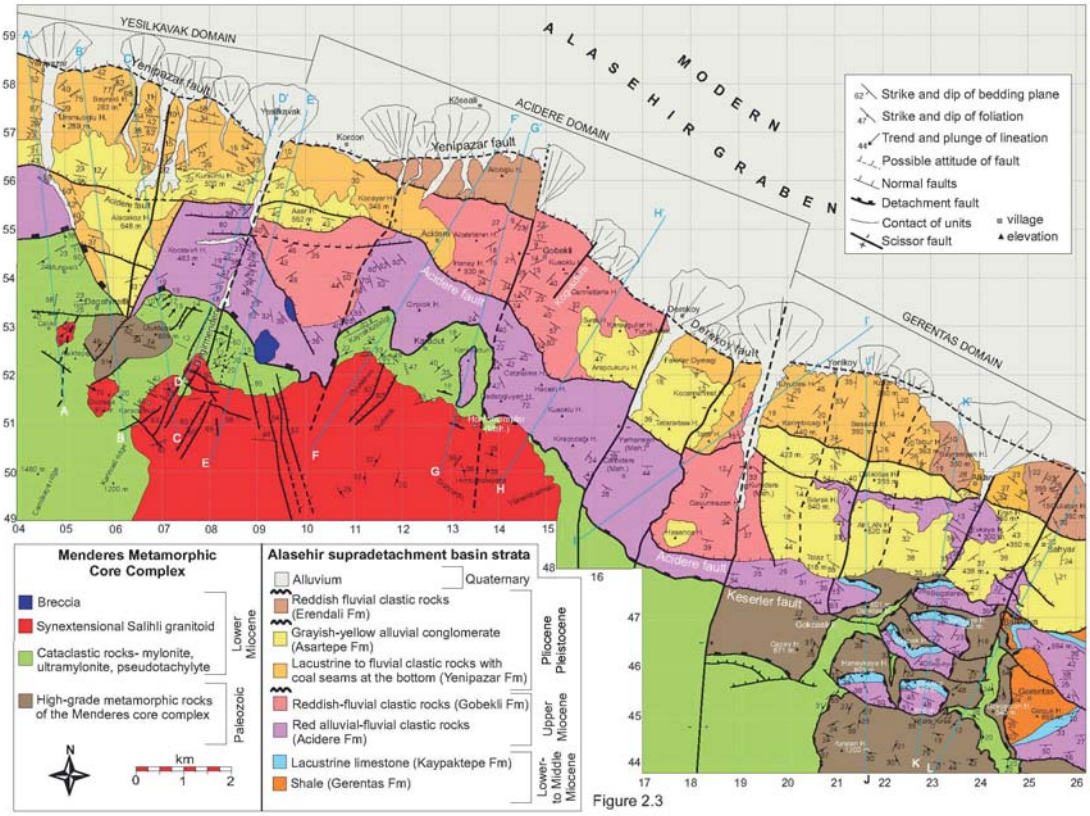

Figure 51: Geological map of the southern margin of the Alasehir supradetachment basin (from Öner and Dilek, 2011).

The relatively younger Göbekli formation conformably overlies the Acıdere formation (Emre, 1996). It consists of light-red-colored and gray-colored, conglomerate and sandstone layers alternating with laminated mudstone, siltstone layers. As a result of different resistance of alternating conglomerate and sandstone-mudstone layers to erosion, cone-like erosional structures are one of the characteristics of the Göbekli formation (Öner and Dilek, 2011). Normal- and reverse-graded bedding, pebble imbrications can be observed in the lower polygenic conglomerate layers and cross-bedding, graded-bedding, lamination are common primary structures in poorly-consolidated sandstone layers. Sedimentary layers of the Göbekli formation mainly dip to the S,SW and SE, whereas some layers locally dip northward as a result of rotational deformation (Öner and Dilek, 2011). Since the Gobekli formation is usually observed in faulted contacts with other formations, and its outcrop and map pattern may indicate fault-controlled deposition of the formation. Emre (1996) reported late Miocene age based on the fresh-water gastropoda fauna discovered in the Gobekli formation. These lower to upper Miocene lacustrine formations and red-colored alluvial-fluvial formations are unconformably overlain by buff-colored, moderately-to-poorly consolidated conglomerate, sandstone, mudstone layers of the Yenipazar formation.

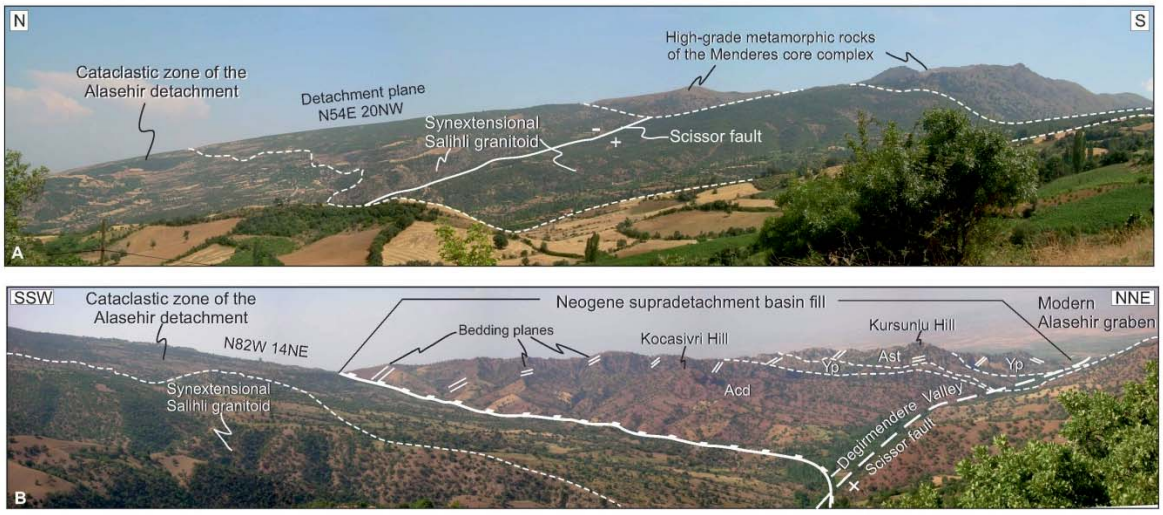

Figure 52: Field photos showing the spatial relationship of N-dipping Alasehir detachment fault, ~E-W-striking major high-angle normal faults and extension-parallel scissor faults (from Öner and Dilek, 2011).

The Yenipazar formation consists of relatively coarse-grained sandstone-siltstone-mudstone layers at the bottom and fine-grained clastic rocks alternating with lignite and bituminous coal layers. It coarsens upward into sandstone and conglomerate in the upper section. The main primary sedimentary structures observed in the Yenipazar formation include cross bedding, graded bedding, lamination, sandstone-siltstone lenses and wedges. Clast lithologies similarly include gneiss, schist, quartz, granite, cataclasites; however the amount of cataclastic rock clasts is less than those in the older formations, and layers dip both to the NE and to the SW. The plant fossils, fresh water gastropoda fauna, and rare mammalian fossils from fine-grained sections of the formation indicate late Pliocene and younger ages. The Yenipazar formation conformably overlain by the buff-colored, massive to poorly-sorted, poorly-consolidated, debris flow deposits of the Asartepe formation. Similary, the layers of the Asartepe formation dip northward and southward and observed as affected by rotational deformation. The younger, light red-colored, unlitified Erendali formation unconformably overlie Plio-Quaternary formations and form terraces cut by seismically-active Yenipazar-Derekoy fault at the further north of the southern section of the Alasehir basin. Cross

bedding, graded bedding and lamination can be observed in these alluvial fan deposits and thin-to-medium-bedded layers of the Erendali formation display subhorizontal orientation, even though they are relatively much younger in the basin. The youngest alluvial fan deposits are fed by N-S-trending, N-flowing streams and unconformably overlie the Asartepe and Yenipazar formations.

4.2. Depositional Characterization And Paleocurrent Directions

The Alaşehir basin strata starts with shale and limestone layers alternating with clastic sedimentary rocks indicating a lacustrine-fan delta depositional environment in the late-middle Miocene times. Since the deposition of these formations appears to be limited mostly in the eastern section, it indicates that the oldest formations deposited in short-lived, fault-bounded, playa lakes in the initial stages of extensional deformation. Cross bedding, pebble imbrications measurements in the alternating conglomerate and sandstone layers of lower-middle Miocene formations show that fluvial systems with SW-NE paleocurrent direction developed as a result of further footwall uplift during this stage.

Similarly, Acıdere formation deposited in an alluvial-fluvial depositional environment. Alternating coarse-grained layers of Acidere formation include unsorted, couble to boulder size clasts and indicate debris flows originated from major fault activities during the deposition of alluvial-fluvial sedimentary rocks. Maturity of clasts in the Acidere formation indicate long-distance transportation of footwall-derived sediments along the N-S-directed, transverse fluvial systems in the Miocene times. Pebble imbrications and cross beddings show SW-NE and SE-NW paleocurrent directions in this formation (Öner and Dilek, 2011).

The overlying Gobekli formation display main characteristics of fluvial-alluvial depositional environment. Normal to reverse graded bedding and cross bedding measurements show SW to NE paleocurrent directions. Organic-matter enriched clay horizons and coal layers in the Yenipazar formation indicate fluviolacustrine deposition in limited-size paleolakes during Early Pliocene-Pleistocene. Occurrence of coal layers within clayey layers might be evidence for burial alteration due to rapid upload of relatively younger sediments of the Asartepe formation during syndepositional tectonic activities.

The grain size coarsens upward in the Yenipazar formation as a result of transition from lacustrine to fluvial depositional environment during this stage. The Asartepe formation shows characteristics of alluvial-fan deposits and clast size coarsens upward and clast lithologies relatively differ from those in the other formations. Pebble imbrications measurements show SW-NE paleocurrent directions in Plio-Quaternary times.

The younger, Erendali formation with subhorizontal layers represent axial alluvial-fan deposits and fluvial deposits and indicate more westward paleocurrent directions in recent geological time. In general, paleocurrent measurements from lower-to-upper Miocene formations show SSW-NNE-directed flow, whereas paleocurrent directions shit to WNW due to development of WNW-ESE-oriented high-angle normal fault systems in the late Pliocene. Establishment of the main drainage systems in the Alaşehir basin has been highly controlled by extensional faulting, which had a significant role on deposition, accommodation, and overall intrabasinal structure.

4.3. Suprdetachment Basin Evolution of The Alasehir Graben

Late Cenozoic extensional deformation and exhumation of the central Menderes massif was still an ongoing process by the end of early Miocene according to the reported monazite ages of 17±5 Ma (Catlos and Cemen, 2005) and U-Pb ages of 16.1±0.2 Ma - 15±0.3 Ma (Glodny and Hetzel, 2007) yielded from synextensional intrusions in the footwall of the Alasehir detachment fault. The Alasehir detachment separates high-grade metamorphic rocks of the central Menderes submassif and

syn-extensional Miocene intrusions from Neogene sedimentary rocks. In the hanging wall of the N-dipping, low-angle detachment fault, the Alasehir basin developed as a curvilinear depocenter and recorded important information about the uplift and exhumation history of the Menderes massif. Crustal extension and exhumation in the northern and southern submassifs initiated approximately 10 my before the exhumation of syn-extensional intrusions in the central submassif in the latest Early Miocene-late Miocene. In addition to that, the occurrence of the Burdigalian to middle Serravalian Eskisehir sporomorph assemblage (Ediger et al., 1996; Seyitoglu et al., 2002) in the lower portion of the basinal strata indicate an early Miocene age for the initiation of the basin formation.

The oldest, lacustrine sedimentary rocks (Gerentas and Kaypaktepe Formations) were deposited in locally developed, short-lived lakes that were located further away from the breakaway fault of the detachment system (Öner and Dilek, 2011). Extensive dispersal of high-grade metamorphic rock clasts into the depocenter in the hanging wall during the early stages of the Alasehir basin was mainly controlled by NNE-directed (in general), transverse stream systems. Alternation of fine-grained and coarse-grained sedimentary rocks indicates a transition from a low-energy, lacustrine, fan-delta depocenter to a higher-energy, alluvial depositional environment. As a result of seismic activities along major normal faults, local debris flows interrupted the low-energy deposition system. The continued uplift and exhumation of the massif facilitated the formation of alluvial-fan deposits in the early Miocene. Pebble- to cobble-sized channel deposits deposited in a fan-delta depositional environment in the middle Miocene and braided stream networks and distal alluvial fans formed and dominated the basin in the late Miocene. Prograding fan deposits, the Acidere formation deposited in the distal parts of the Alasehir depocenter.

Further crustal extension in the central submassif produced high-angle, oblique slip, hinge faults as a major component of the differential uplift and exhumation of the core complex (Öner and Dilek, 2011). These extensional faults strongly controlled the deposition, facies changes, and accommodation in the basin. This interplay between scissor faulting and synextensional deposition resulted in basin segmentation. The spatial and kinematic interaction between extension-parallel hinge faults and ~E-W-striking high-angle normal faults strongly controlled the deposition of the Upper Miocene–Lower Pliocene Gobekli formation. These two fault systems also resulted in the rotation of the older Neogene sedimentary layers and caused the formation of intrabasinal angular unconformities. With the onset of block faulting in the late Pliocene, the WNW-ESE–striking normal faults created additional accommodation space in their hanging walls and their footwall blocks became a secondary provenance for the alluvial-fan and debris flow deposits of the Plio-Quaternary Yenipazar and Asartepe formations. Rigid block faulting and block rotation resulted in the development of half-graben systems in this phase, and E-W-oriented, axial stream systems formed and facilitated sediment dispersal in the basin. The youngest sedimentary formation deposited in an E-W-trending half graben and exhibits westerly paleoflow directions.

Back-tilting and rotation in the basinal strata changed the primary orientation of sedimentary layers and other structures and resulted in a pseudo-appearance of folding around W-NW–trending fold axes (Öner and Dilek, 2011). These orientation changes in dip directions have been interpreted as an artifact of folding associated with a short-termed contractional event in the latest Pliocene by Koçyigit et al. (1999), Gessner et al. (2001b), Bozkurt and Sözbilir (2004), Bozkurt and Rojay (2005). However, our field observations demonstrate that there is no evidence for contractional deformation as implied. Orientation changes within the basin strata are associated with block rotation and tilting occurred during the late-stage extensional deformation (Figure 53).

The modern Gediz-Alasehir graben represents the main depocenter in present time and is filled with more than 3 km of sedimentary rocks (Gürer et al., 2001; Sarı and Şalk, 2006; Çiftçi and Bozkurt, 2010). The modern graben is bounded to the south by WNW-oriented, north-dipping, seismically active (1969 Alasehir earthquake, M =6.9; Eyidogan and Jackson, 1985) Yenipazar-Derekoy fault.

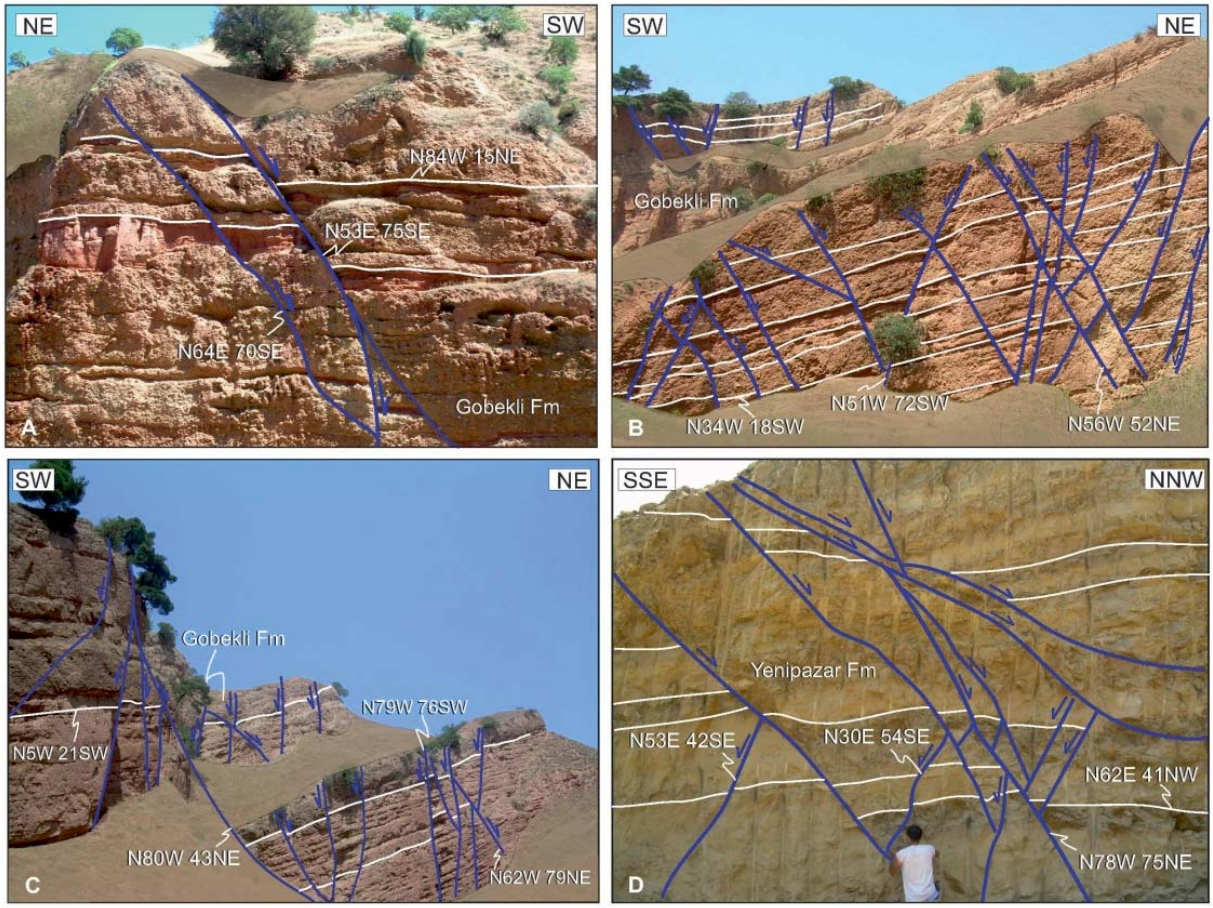

Figure 53. Field photos showing high-angle normal faults resulted in orientation changes and the formation of graben-horst structures in the Gobekli and Yenipazar formations (Öner and Dilek, 2011).

4.4. Proposed Model Of Post Collisional Cenozoic Extension In Western Turkey

Çemen et al. (2006) suggests a testable model for the Cenozoic extensional tectonics evolution of the western Anatolian extensional terrain (WAET) (Figure 54). The regional Alpine contraction, which produced the Izmir-Ankara suture zone in West Anatolia, may have ceased in the Eocene (Şengör et al., 1984; Okay, 2001). They suggest that the Cenozoic extension in WAET is the product of a continuous north-directed extension. The extension has not been interrupted since its initiation and still continues today as is evidenced by GPS measurements (McClusky et al., 2000) and earthquake activity in the region with normal fault first motion studies (e.g., Taymaz et al., 1991). However, the extensional deformation in the region can be divided into three phases and each phase may have been triggered by different mechanisms.

The first phase occurred in the Late Oligocene when extension was probably initiated along an extensional simple shear zone, the southwestern Anatolian shear zone (SWASZ), in the southern part of the WAET (Figure 54) as evidenced by the presence of the Oren, Yatagan and Kale-Tavas extensional sedimentary basins containing Late Oligocene conglomerate. Seyitoglu and Scott (1996) suggested that the Late Oligocene extension may have initiated by an orogenic collapse of thermally weakened crust of the Izmir-Ankara suture zone. Some researchers suggest also that the extension might have initiated in a similar manner to the simple shear-rolling hinge models (e.g. Wernicke, 1985, 1998; Axen and Bartley, 1997).

According to the model suggested by Çemen et al. (2006), the SWASZ extends from the south side of the Gökova Gulf to the southeastern margin of the Denizli basin. The seismic reflection profiles in the Gulf of Gokova (Kurt et al., 1999) clearly show a listric normal fault and an associated roll over structure The Ören basin formed on the hanging wall of this simple shear zone as an extensional basin (Özerdem et al., 2002). The basin contains an Oligocene conglomerate unit called Gokceoren Formation (Yılmaz et al., 2000; Gürer and Özerdem, 2002), suggesting that the shear zone formed in the Late Oligocene.

The Kale-Tavas basins are also extensional basins located adjacent to the SWASZ which has a substantial strike-slip component as it progrades east-northeastward and controls the southwestern margins of these basins. Extension across the SWASZ and associated erosion and tectonic unroofing caused the high-grade metamorphic rocks of the Menderes Massif to be brought to the surface by the Late Miocene (Figure 54).

Three lines of evidence for the existence of erosion and tectonic unroofing due to the extension in the Late Oligocene are: (1) fission track ages that indicate that metamorphic rocks of the Menderes Massif were close to the surface ~20 Ma (Gessner et al., 2001b); (2) pervasive top to the north extensional shear sense indicators are well exposed throughout high grade metamorphic rocks of the Menderes Massif (Figures 2, 6 and 7); and (3) the sedimentary basins that were formed in the Early Miocene (i.e., the north trending basins of the Northern Menderes Massif, the Alaşehir and Büyük Menderes Graben) contain only high grade metamorphic rocks of the Menderes Massif in their Lower Miocene conglomerate units. However, the Oligocene Gökçeören conglomerate of the Ören and Yatağan Basins is made up of Mesozoic recrystallized platform carbonate and underlying phyllitic low grade metamorphic rocks (Yılmaz et al., 2000; Özerdem et al., 2002).

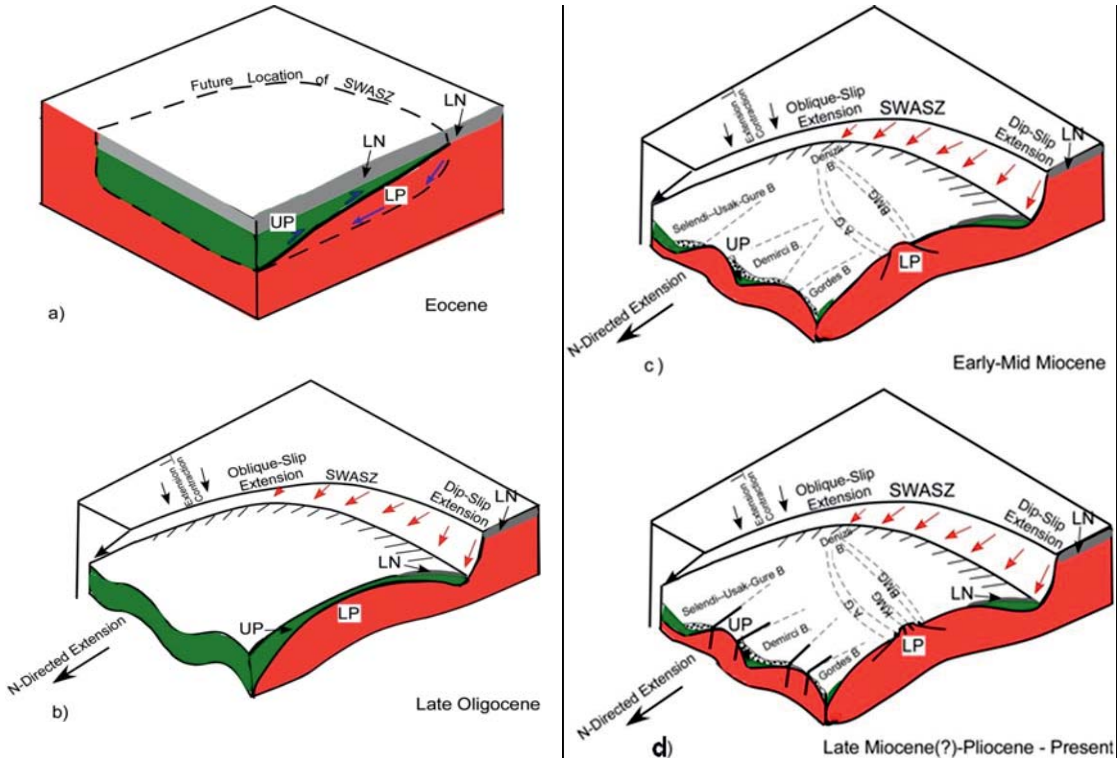

Figure 54: Three dimensional cartons emphasizing the role of the SWASZ in the structural evolution of the WAET a) in Eocene; b) Late Oligocene and C) Early Miocene. They do not include the Simav Detachment area. The cross-sections and the 3-D cartons are not drawn to scale and do not indicate the amount of extension in each stage. Abbreviations: AG= Alaşehir Graben; BMG= Büyük Menderes Graben; OB/KTB= Oren and Kale-Tavas Basins; LN= Lycian Nappes; KMG= Kucuk Menderes Graben; SG= Simav Graben; SWASZ= Southwest Anatolian Shear Zone (from Çemen et al., 2006).

The Oligocene conglomerates of the Kale-Tavas basin contain predominantly ophiolitic material derived from the uppermost tectonic slice in the Lycian Nappe pile (Yılmaz et al., 2000), which was overlying the Menderes Massif in the Eocene (Şengör et al., 1984). The Miocene sedimentary succession in Oren, Yatagan and Kale-Tavas basins, however, contain high-grade metamorphic rock fragments of the Menderes Massif (Sözbilir et al., 2000). This sedimentary record indicates that extension in WAET started in the Oligocene when the Lycian Nappes were covering the Menderes Massif. The rocks in the upper structural levels of the nappe pile (i.e., ophiolitic, recrystallized carbonates and low-grade phyllitic metamorphic rocks) provided clasts in the Oligocene. However, the high-grade metamorphic rocks were at the surface in the Miocene and provided clasts for the conglomerates in the sedimentary basins.

Continued extension produced a secondary breakaway in the Early Miocene along the Alaşehir Detachment surface. The original dip angle of the Alaşehir Detachment surface is controversial. One group suggest that the Alaşehir Detachment surface may have formed with a steep dip in the Early Miocene and rotated to its present low angle as the extension continued (Seyitoğlu et al., 2000 and 2002). Alternatively, the Alaşehir Detachment may have originally initiated as a low-angle detachment fault (Purvis and Robertson, 2004).

Presently, The Simav Detachment appears to be in the hanging wall of the Alaşehir Detachment. The south-dipping high-angle normal faults along the northern margin the Alaşehir basin brought the footwall of the Simav Detachment to the surface that contains extension-perpendicular antiforms and synforms with a wide range of scale. The axial traces of all folds are parallel to the N10°E to N30°E mylonitic stretching lineations. Considering that mylonitic lineations form parallel to the direction of extension, these folds suggest compression perpendicular to extension. Large-scale antiforms and synforms are also observable along the unpublished TPAO east-west seismic reflection profiles in sedimentary succession of the Alaşehir Graben.

Çemen et al. (2006) also suggest that the large antiforms and synforms that formed in the lower plate of the SWASZ provided initial configuration in Early Miocene for the North trending sedimentary basins of the northern Menderes Basin (i.e., Demirci, Gordes and Usak- Selendi Basins). However, the northeast trending faults that control the eastern and western margins of these basins may have been formed as accommodation faults due to differential stretching since they have substantial strike-slip component (Şengör, 1987; Cemen et al., 2006; Öner and Dilek, 2011).

Purvis and Robertson, (2004) proposed that the Early Miocene extension is related to subduction roll back of the Aegean subduction zone. The roll back may still be an effective mechanism of extension in western Anatolia.

The third stage of extension in Western Anatolia is started in Late Miocene about 5 Ma ago (Purvis and Robertson, 2004; Catlos and Çemen, 2005) which coincides with the formation of the North Anatolian Fault Zone as a major strike-slip fault zone (Barka, 1997). The third stage produced continuous extension along the Simav, Alaşehir, Büyük Menderes Detachments and oblique-slip movement along the SWASZ (Figure 54). This extension is probably also responsible for the formation of the Kucuk Menderes Graben and the second and third order of the normal faults (Seyitoğlu et al., 2000) along the Alaşehir Graben.

The North Anatolian fault zone influenced the structural development of western Anatolia within the last 5 Ma and accommodated tectonic escape (Şengör, 1979) or lateral extrusion of the Turkish Plate westward (Çemen et al., 1993, 1999), which was proposed as a possible mechanism for the north-directed extension in western Anatolia, Turkey (Şengör and Yılmaz, 1981, Şengör et al., 1985).

REFERENCES

Ağırbaş, H., 2006. Alkan koyu (Alaşehir) ve yakin cevresinde Gediz grabeni' nin stratigrafisi ve yapisal ozellikleri [B.Sc. thesis]: İstanbul, İstanbul University, (in Turkish), 115 p.

Akgun, F. Sözbilir, H., 2001. A palynostratigraphic approach to the SW Anatolian molasse basin: Kale-Tavas molasse and Denizli molasses. Geodynamica Acta 14, 71-93.

Akkök, R., 1983. Structural and metamorphic evolution of the Menderes Massif: new data from the Derbent area and their implication for the tectonics of the massif. Journal of Geology 91, 342–350.

Aldanmaz, E., 2002. Mantle source characteristics of alkali basalts and basanites in an extensional intracontinental plate setting, Western Anatolia, Turkey: Implications for multi-stage melting. International Geology Review 44, 440–457.

Alıcı, P., Temel, A., Gourgaud, A., 2002. Pb-Nd-Sr isotope and trace element geochemistry of Quaternary extension-related alkaline volcanism: a case study of Kula region (western Anatolia, Turkey). Journal of Volcanology and Geothermal Research 115, 487–510.

Ashworth, J.R., Evirgen, M.M., 1984. Garnet and associated minerals in the southern margin of the Menderes Massif, southwest Turkey: Mineralogical Magazine 121, 323–337.

Ashworth, J.R., Evirgen, M.M., 1985. Plagioclase relations in pelites, central Menderes, Massif, Turkey; II, Perturbation of garnet-plagioclase geobarometers. Journal of Metamorphic Geology 3, 219–229.

Axen, G. J., Bartley, J., 1997. Field tests of rolling hinges: Existence, mechanical types and implications for extensional tectonics. Journal of Geophysical Research 102, 20515–20537.

Barka, A., 1997. Neotectonics of the Marmara region: in Schindler, C., and Pfister, M., (eds) Active Tectonics of Northwestern Anatolia - The MARMARA Ploy-Project; A multidisciplinary Approach by Space-Geodesy, Geology, Hydrogeology, Gethermic and Seismology. Vdf Hochschulerlag AG an der ETH Zurich, 55–87.

Benda, L., Innocenti, F., Mazzuoli, R., Radicati, F., Steffens, P., 1974. Stratigraphic and radiometric data of the Neogene in Northwest Turkey: Zeitschrift der Deutschen Geologischen Gesellschaft 125, 183–193.

Benda, L., Meulenkamp, J.E., 1979, Biostratigraphic correlations in the Eastern Mediterranean Neogene; 5. Calibration of sporomorph associations, marine microfossils and mammal zones, marine and continental stages and the radiometric scale: Annales Geologiques Des Pays Helleniques, v. Tome hors ser, 61–70.

Bingöl, E., Delaloye, M., Ataman, G., 1982. Granitic intrusions in Western Anatolia: a contribution to the geodynamic study of this area. Eclogae Geoogica. Helvatica 75, 437–446.

Bozkurt, E., 2007. Extensional v. contractional origin for the southern Menderes shear zone, SW Turkey: tectonic and metamorphic implications. Geological Magazine 144, 191–210.

Bozkurt, E., Oberhansli R. 2001. Menderes Massif (Western Turkey): structural, metamorphic and magmatic evolution – a synthesis. International Journal of Earth Sciences 89(4), 679–708.

Bozkurt, E., Park, R.G., 1994. Southern Menderes Massif-an Incipient Metamorphic Core Complex in Western Anatolia, Turkey. Journal of Geological Society of London 151, 213–216.

Bozkurt, E., Sözbilir, H., 2004. Tectonic evolution of the Gediz graben: field evidence for an episodic, two-stage extension in Western Turkey. Geological Magazine 141, 63–79.

Bozkurt, E., Satir, M., 2000, The southern Mendres Massif (western Turkey): Geochronology and exhumation history. Geological Journal 35, 285–296.

Buck, W.R., 1988. Flexural rotation of normal faults: Tectonics 7, 959–973.

Candan, O., Dora, O.O., Oberhansli, R., Centinkaplan, M., Partzsch, J.H., Warkus, F.C., Durr, S., 2001, Pan-African high-pressure metamorphism in the Precambrian basement of the Menderes Massif, western Anatolia, Turkey. International Journal of Earth Sciences 89, 793–811.

Candan, O., Dora, O.O., Oberhansli, R., Koralay, E., Centinkaplan, M., Akal, C., Satır, M., Chen, F., Kaya, O., 2011. Menderes Masifi'nin Pan-Afrikan Temelin Stratigrafisi Ve Gondvana'nin Geç Neoproterozoyik / Kambriyen Evrimi ile İlişkisi. MTA Dergisi 142, 25-68.

Candan, O., Dora, O.O., Oberhansli, R., Oelsner, F., Durr, S., 1997. Bluseschist relics in the Mesozoic cover series of the Menderes Massif and correlations with Samos Island, Cyclades. Schweizerische Mineralogische und Petrographische Mitteilungen 77, 95–99.

Catlos, E.J., Baker, C.B., Sorensen, S.S., Çemen, İ., Hançer, M., 2008. Monazite geochronology, magmatism, and extensional dynamics within the Menderes Massif, Western Turkey. IOP Conference Series: Earth and Environmental Sci. 2, 012013.

Catlos, E.J., Çemen, I., 2005. Monazite ages and the evolution of the Menderes Massif, western Turkey: Journal of International Journal of Earth Sciences 94, 204–217.

Çemen, İ., Catlos, E.J., Göğüş, O., Özerdem, C., 2006. Postcollisional extensional tectonics and exhumation of the Menderes Massif in Western Anatolia extended terrane, Turkey. Geological Society of America Special Publication 409, 353–379.

Çemen, İ., Göncuoğlu, C., Dirik, K., 1999. Structural Evolution of the Tuzgolu Basin in Central Anatolia, Turkey. Journal of Geology 107, 693–706.

Çemen, İ., Goncüoğlu, M. C., Erler, A., Kozlu, H., Perinçek, D., 1993. Indentation tectonics and associated lateral extrusion in east, southeast and central Anatolia. Geological Society of America Abstracts with Programs 25(7), A116.

Çemen, İ., Tekeli, O., Seyitoğlu, G., 2005. Are Turtleback Fault Surfaces common tectono-morphologic features of highly extended Terranes, Earth-Science Reviews, v. 72, p.

Çiftçi, B., Bozkurt, E., 2009a. Evolution of the Miocene sedimentary fill of the Gediz Graben, SW Turkey. Sedimentary Geology 216, 49–79.

Çiftçi, G., Pamukçu, O., Çoruh, C., Çopur, S., Sözbilir, H., 2011. Shallow and deep structure of a supradetach ment basin based on geological, conventional deep seismic refl ection sections and gravity data in the Buyuk Menderes graben, western Anatolia: Surveys in Geophysics 32, 271–290.

Çiftçi, N.B., Bozkurt, E., 2009b. Pattern of normal faulting in the Gediz graben, SW Turkey. Tectonophysics 473, 234–260.

Çiftçi, N.B., Bozkurt, E., 2010. Structural evolution of the Gediz graben, SW Turkey: Temporal and spatial variation of the graben basin. Basin Research 22, 846–873.

Cohen, H.A., Dart, C.J., Akyüz, H.S., Barka, A., 1995. Syn-Rift Sedimentation and Structural Development of the Gediz and Büyük-Menderes Graben, Western Turkey. Journal of Geological Society of London 152, 629–638.

Davis, H. G., 1980, Structural characteristics of metamorphic core complexes, in Crittenden, M.D., Jr., and Coney, P. J., and Davis, G. H., (eds.) Cordilleran metamorphic core complexes. Geological Society of America Memoir 153, 543–569.

Dewey, J. F., 1986. Shortening of continental lithosphere, the neotectonics of eastern Anatolia, a young collision zone: Geological Society Special Publications 19, 3–36.

Dewey, J. F., 1988. Extensional collapse of orogens. Tectonics 7, 1123–39.

Dewey, J. F., Şengor, A.M.C., 1979. Aegean and surrounding regions: Complex multiplate and continuum tectonics in a convergent zone. Geological Society of America Bulletin, 90, 84-92.

Dilek, Y., Thy, P., Hacker, B., Grundving, S., 1999 Structure and Petrology of Tauride Ophiolites and mafic dike intrusions (Turkey); Implications for the NeoTethyan ocean. Geological Society of America Bulletin 3, 1192-1216.

Dilek, Y., Whitney, D.L., 2000. Cenozoic crustal evolution in central Anatolia: extension, magmatism, and landscape development. In: Panayides, I., Xenophontos, C., and Malpas, J. (eds). Proceedings of the Third International Conference on the Geology of the Eastern Mediterranean. Geological Survey Department, Nicosia, Cyprus, 183-192.

Ediger, V., Batı, Z., Yazman, M., 1996. Palynology of possible hydrocarbon source rocks of the Alasehir-Turgutlu area in the Gediz graben (western Anatolia). Turkish Association of Petroleum Geologists Bulletin 8, 94–112.

Emre, T., 1996. Gediz grabeninin jeolojisi ve tektoniği [Geology and tectonics of the Gediz graben]. Turkish Journal of Earth Science 5, 171–185.

Emre, T., Sözbilir, H., 1997. Field evidence for metamorphic core complex, detachment faulting and accommodation faults in the Gediz and Büyük Menderes grabens (Western Turkey). International Earth Science Colloquium on the Aegean

Ercan, E., Dinçel, A., Metin, S., Türkecan, A., Günay, A., 1978. Uşak yöresindeki Neojen havzalarının jeolojisi [Geology of the Neogene basins in Uşak region]. Bulletin of the Geological Society of Turkey 21, 97–106.

Ercan, E., Satır, M., Sevin, D., Türkecan, A., 1996. Batı Anadolu'daki Tersiyer ve Kuvaterner yaşlı volkanik kayaçlarda yeni yapılan radyometrik yaş ölçümlerinin yorumu [Some new radiometric ages from Tertiary and Quaternary volcanic rocks from West Anatolia]. Mineral Research and Exploration Bulletin (Turkey) 119, 103–112.

Ercan, E., Türkecan, A., Dinçel, A., Günay, A., 1983. Kula-Selendi (Manisa) dolaylarının jeolojisi [Geology of Kula-Selendi (Manisa) area]. Geological Engineering 17, 3–28.

Ercan, T. Öztunalı, Ö., 1983. Demirci-Selendi çevresinde Senozoyik yaşlı volkanitlerin petrolojisi ve kökensel yorumu [Petrology and source interpretation of Cenozoic volcanites around the Demirci-Selendi]. Geoscience 10, 1–15.

Erinc, S., 1955. Uber die Entstehung und morphologishe Bedeutung des Tmolusschutts. Rev. Univ. Istanbul geogr. Inst. 2, 57-72.

Erkül, F., Helvacı, C., Sözbilir, H., 2005a. Stratigraphy and Geochronology of the Early Miocene Volcanic Units in the Bigadiç Borate Basin, Western Turkey. Turkish Journal of Earth Science 14, 227–253.

Erkül, F., Helvacı, C., Sözbilir, H., 2005b. Evidence for two episodes of volcanism in the Bigadic borate basin and tectonic implications for Western Turkey. Geological Journal 40, 545–570.

Ersoy, E.Y., Dindi, F., Karaoğlu, Ö. Helvacı, C. 2012b. Soma Havzası ve Çevresindeki Miyosen Volkanizmasının Petrografik ve Jeokimyasal Özellikleri. Yerbilimleri 33, 59-80.

Ersoy, E.Y., Helvacı, C., 2007. Stratigraphy and Geochemical Features of the Early Miocene Bimodal (Ultrapotassic and Calc-alkaline) Volcanic Activity within the NE-trending Selendi basin, Western Anatolia, Turkey. Turkish Journal of Earth Science 16, 117–139.

Ersoy, E.Y., Helvacı, C., Palmer, M.R. 2011. Stratigraphic, structural and geochemical features of the NE-SW trending Neogene volcano-sedimentary basins in western Anatolia: implications for associations of supradetachment and transtensional strike-slip basin formation in extensional tectonic setting. Journal of Asian Earth Science 41, 159–183.

Ersoy, E.Y., Helvacı, C., Palmer, M.R. 2012a. Petrogenesis of the Neogene volcanic units in the NE-SW-trending basins in western Anatolia, Turkey. Contributions to Mineralogy and Petrology 163, 379–401.

Ersoy, E.Y., Helvacı, C., Sözbilir, H., 2010. Tectono-stratigraphic evolution of the NE-SW-trending superimposed Selendi basin: implications for Late Cenozoic crustal extension in western Anatolia, Turkey. Tectonophysics 488, 210–232.

Ersoy, E.Y., Helvacı, C., Sözbilir, H., Erkül, F., Bozkurt, E., 2008. A geochemical approach to Neogene–Quaternary volcanic activity of Western Anatolia: An example of episodic bimodal volcanism within the Selendi Basin, Turkey. Chemical Geology 255, 265–282.

Eyidogan, H., Jackson, J., 1985. A seismological study of normal faulting in the Demirci, Alasehir and Gediz earthquakes of 1969–70 in western Turkey: Implication for the nature and geometry of deformation in the continental crust. Geophysical Journal of the Royal Astronomical Society 81, 569–607.

Friedmann, S.J., Burbank, D.W., 1995. Rift basins and supra detachment basins: Intracontinental extensional end-members. Basin Research 7, 109–127

Geological Map of Turkey–İzmir (1:500000), 2002. Publication of Mineral Research and Exploration Institute of Turkey.

Gessner, K., Collins, A.S., Ring, U., Güngör, T., 2004. Structural and thermal history of poly-orogenic basement: U-Pb geochronology of granitoid rocks in the southern Menderes Massif, western Turkey. Journal of the Geological Society of London 161, 93-101.

Gessner, K., Piazolo, S., Güngör, T., Ring, U., Kroner, A., Passchier, C.W., 2001a. Tectonic significance of deformation patterns in granitoid rocks of the Menderes nappes, Anatolide belt, southwest Turkey. International Journal of Earth Science 89, 766–780.

Gessner, K., Ring, U., Johnson, C., Hetzel, R., Passchier, C.W., Güngör, T., 2001b. An active bivergent rolling-hinge detachment system; central Menderes metamorphic core complex in Western Turkey. Geology (Boulder) 29, 611–614.

Glodny, J., Hetzel, R., 2007. Precise U-Pb ages of syn-extensional Miocene intrusions in the central Menderes Massif, Western Turkey. Geological Magazine 144, 235–246.

Göğüş, O., 2004. Geometry and Tectonic Significance of the Buyuk Menderes Detachment in the Bascayir area, Buyuk Menderes Graben, Western Turkey, Unpublished M.S. Thesis, Oklahoma State University.

Göğüş, O., Çemen, İ., Catlos, E. J., Işık, V., Seyitoğlu, G., 2003. Geometry and Tectonic Significance of the Bascayir Detachment, Büyük Menderes Graben, Western Turkey, Geological Society of America, Annual Meeting 35(6), 27.

Gürer, A., Gurer, O.F., Pince, A., Ilkisik, O.M., 2001. Conductivity structure along the Gediz graben, west Anatolia, Turkey. Tectonic implications: International Geology Review 43, 1129–1144.

Gürer, F. Yılmaz, Y., 2002. Geology of the Oren and surrounding areas, SW Anatolia. Turkish Journal of Earth Sciences 11, 1-13.

Hakyemez, H.Y., Erkal, T., Göktaş, F., 1999. Late Quaternary evolution of the Gediz and Büyük Menderes grabens, Western Anatolia, Turkey. Quaternary Science Review 18, 549–554.

Hamilton, W. B., 1988. Detachment faulting in the Death Valley region, California and Nevada: United States Geologic Survey Bulletin 11790, 51-85.

Helvacı, C., 1984. Occurrence of rare borate minerals: Veatchite-A, tunellite, teruggite and cahnite in the Emet borate deposit, Turkey. Mineral Deposita, 19, 217–226.

Helvacı, C., 1986, Stratigraphic and structural evolution of the Emet borate deposits, Western Anatolia. Dokuz Eylül University, Faculty of Engineering and Architecture, Research Papers, No: MM/JEO-86 AR 008.

Helvacı, C., 1995. Stratigraphy, mineralogy, and genesis of the Bigadiç borate deposits, Western Turkey. Economic Geology 90, 1237–1260.

Helvacı, C., Alonso, R.N., 2000. Borate deposits of Turkey and Argentina; a summary and geological comparison. Turkish Journal of Earth Science 24, 1–27.

Helvacı, C., Yağmurlu, F., 1995, Geological setting and economic potential of the lignite and evaporite-bearing Neogene basins of Western Anatolia, Turkey. Israel Journal of Earth Science 44, 91–105.

Hetzel, R., Passchier, C.W., Ring, U., Doram, O.Ö., 1995b. Bivergent extension in orogenic belts; the Menderes Massif (southwestern Turkey). Geology 23, 455-458.

Hetzel, R., Reischmann, T., 1996. Intrusion age of Pan-African augen gneisses in the southern Menderes Massif and the age of cooling after Alpine ductile extensional deformation: Geological Magazine 133, 565-572.

Hetzel, R., Ring, U., Akal, C., Troesch, M., 1995a. Miocene NNE-directed extensional unroofing in the Menderes Massif, southwestern Turkey. Journal of Geological Society of London 152, 639–654.

Hetzel, R., Romer, R.L., Candan, O., Passchier, C.W., 1998. Geology of the Bozdag area, central Menderes Massif, SW Turkey: Pan-African basement and Alpine deformation: Geologische Rundschau 87, 394-406.

Holm, D.K., Snow, J.K., Lux, D.R., 1992. Thermal and barometric constraints on the intrusive and unroofing history of the Black Mountains: Implications for timing, initial dip, and kinematics of detachment faulting in the Death Valley region, California. Tectonics 11, 507-522.

Holm, D.K., Wernicke B.P., 1992. Black Mountains crustal section, Death Valley extended Terrane, California. Geology 18, 520-523.

İnci, U. 1998. Miocene synvolcanic alluvial sedimentation in lignite-bearing Soma Basin, Western Turkey. Turkish Journal of Earth Science 7, 63–78.

İnci, U., 1984. Neogene oil shale deposits of Demirci and Burhaniye regions. 27th International Geological Congress, Abs. Vol. VII, 13–16, 57.

Innocenti, F., Agostini, S., Di Vincenzo, G., Doglioni, C., Manetti, P., Savaşçın, M.Y., Tonarini, S., 2005. Neogene and Quaternary volcanism in Western Anatolia: magma sources and geodynamic evolution. Marine Geology 221, 397-421.

Işık, V., Seyitoğlu , G., and Çemen, İ., 2003a. Ductile-brittle transition along the Alaşehir shear zone and its structural relationship with the Simav Detachment, Menderes Massif, western Turkey. Tectonophysics 374, 1-18.

Işık, V., Seyitoğlu , G., and Çemen, İ., 2003b, Extensional Structures of the Menderes Core Complex, Western Turkey: Geological Society of America Abstracts with Programs 35(6), 27-28 .

Işık, V., Tekeli, O., 2001. Late orogenic crustal extension in the northern Menderes Massif (Western Turkey); evidence for metamorphic core complex formation. In: Bozkurt, E., Oberhänsli, R. (Eds.), Menderes Massif (Western Turkey); structural, metamorphic and magmatic evolution. Springer Int. Berlin (Germany).

Işık, V., Tekeli, O., Çemen, İ., 1997. Mylonitic fabric development along a detachment surface in northern Menderes massif, western Anatolia, Turkey: Geological Society of America Abstracts with Programs 29(6) A-220.

Işık, V., Tekeli, O., Seyitoğlu, G., 2004. The Ar-40/Ar-39 age of extensional ductile deformation and granitoid intrusion in the northern Menderes core complex: implications for the initiation of extensional tectonics in Western Turkey. Journal of Asian Earth Science 23, 555–566.

İztan, H., Yazman, M., 1990. Geology and hydrocarbon potential of the Alaflehir (Manisa) area, western Turkey, in Proceedings, International Earth Sciences Congress. Aegean regions, İzmir, 327-338.

Karaoğlu, Ö., Helvacı, C., 2012a. Structural evolution of the Uşak-Güre-supra-detachment basin during Miocene extensional denudation in western Turkey. Journal of the Geololgical Society, London (in press). doi: 10.1144/0016-76492011-014.

Karaoğlu, Ö., Helvacı, C., 2012b. Growth, destruction and volcanic facies architecture of three volcanic centres in the Miocene Uşak–Güre basin, western Turkey: Subaqueous–subaerial volcanism in a lacustrine setting. Journal of Volcanology and Geothermal Research 245–246, 1–20.

Karaoğlu, Ö., Helvacı, C., Ersoy, E.Y., 2010. Petrogenesis and 40Ar/39Ar Geochronology of the Volcanic Rocks of the Uşak-Güre basin, western Türkiye. Lithos 119, 193–210.

Koçyiğit, A., Yusufoğlu, H., Bozkurt, E., 1999. Evidence from the Gediz graben for episodic two-stage extension in Western Turkey. Journal of Geological Society of London 156, 605–616.

Koralay, O. E., Satır, M.., Dora, O.O., 2001. Geochemical and geochronological evidence for early Triassic calc-alkaline magmatism in the Menderes Massif, western Turkey. International Journal of Earth Sciences 89, 822-835.

Kurt, H., Demirbag, E., Kuscu, I., 1999. Investigation of submarine active tectonism in the Gulf of Gokova, southwest Anatolia- southeast Aegean sea, by multi-channel seismic reflection data. Tectonophysics 305, 477-496.

Le Pichon and Angelier, J., 1979. The Hellenic arc and trench system: A key to the neotectonic evolution of the Eastern Mediterranean area: Tectonophysics, v. 60, p. 1-42.

Le Pichon and Angelier, J., 1981. The Aegean Sea: Philosophical Transactions of the Royal Society of London A 300, 357-72.

LeMaitre, R.W., 2002. Igneous rocks: a classification and glossary of terms: recommendations of the International Union of Geological Sciences, Subcommission on the Systematics of Igneous Rocks, Cambridge University Press.

Lips, A.L.W., Cassard, D., Sözbilir, H., Yılmaz, H., Wijbrans, J.R., 2001. Multistage exhumation of the Menderes Massif, Western Anatolia (Turkey). International Journal of Earth Science 89, 781–792.

Loos, S., Reischmann, T., 1999. The evolution of the southern Menderes Massif in SW Turkey as revealed by zircon dating. Journal of the Geological Society of London 156, 1021-1030.

Mancktelow, N.S. Pavlis, T.I., 1994. Fold-fault relationships in low-angle detachment systems. Tectonics 13, 668-685.

McClusky, S., Balassanian, S., Barka, A., Demir, C., Ergintav, S., Georgiev, I., Gurkan, O., Hamburger, M., Hurst, K., Kahle, H.G., Kastens, K., Kekelidze, G., King, R., Kotzev, V., Lenk, O., Mahmoud, S., Mishin, A., Nadaria, M., Ouzounis, A., Paradissis, D., Peter, Y., Prilepin, M., Reilenger, R.E., Sanli, I., Seeger, H., Tealeb, A., Toksoz, M.N., Veis, G., 2000. Global Positioning system constraints on plate kinematics and dynamics in the Eastern Mediterranean and Caucasus. Journal Geophysical Research 105, 5695-720

McKenzie, D., 1978. Active tectonics of the Alpine-Himalayan belt: The Aegean Sea and surrounding regions. Geophysical Journal of Royal Astronomical Society 55, 217-254.

Meulenkamp, J.E., 1988. One the Hellenic subduction zone and the geodynamic evolution of Crete since the late middle Miocene. Tectonophysics 146, 203-215.

Nebert, K., 1961. Gördes (Batı Anadolu) bölgesindeki Neojen volkanizması hakkında bazı bilgiler [Some information on Neogene volcanism in Gördes (Western Anatolia) region]. Mineral Research and Exploration Bulletin (Turkey) 57, 50–54.

Oberhansli, R., Candan, O., Dora, O.O., Durr, S., 1997. Eclogites within the Menderes Massif, western Turkey. Lithos 41, 135-150.

Oberhansli, R., Candan, O., Warkus, F.C., Partzsch, J.H., Dora, O.O., 1998. The age of blueschist metamorphism in the Mesozoic cover series of the Menderes Massif: Schweizerische Mineralogische and Petrographische Mitteilungen 78, 309-316.

Okay A.İ., Tansel, İ., Tüysüz, O., 2001. Obduction, subduction and collision as reflected in the Upper Cretaceous-Lower Eocene sedimentary record of Western Turkey. Geological Magazine 138, 117–142.

Okay, A.I., 2001. Stratigraphic and metamorphic inversions in the central Menderes Massif: A new structural model. International Journal of Earth Sciences 89, 709-727.

Okay, A.I., Harris, N., Kelley, S.P., 1998. Exhumation of blueschists along a Tethyan suture in northwest Turkey. Tectonophysics 285, 275-299.

Okay, A.İ., Tüysüz, O., 1999. Tethyan Sutures of northern Turkey. In: Durand, B., Jolivet, L., Hovarth, F., and Séranne, M. (Eds.), The Mediterranean Basins: Tertiary Extension within the Alpine Orogen. Journal of Geological Society of London, 156, 475–515.

Öner, Z., Dilek, Y., 2011. Supra-detachment basin evolution during continental extension: The Aegean province of western Anatolia. The Geological Society of America Bulletin 123, 2115-2141.

Özerdem, Çemen, İ., Işık, V., 2002. The Conglomerate member of the Gokceoren Formation, Oren Basin, western Turkey: Its age, sedimentology and tectonic significance: Geological Society of America Abstracts with Programs 34(6), 250.

Phillipson, A.,1910-1915. Reisen und Forshungen im westlichen Kleinasien. Erganzunghefte 167, 172, 177, 180, 183 der Petermanns Mitteilungen Gotha, Justus Perthes.

Prelević, D., Akal, C., Foley, F., Romer, R.L., Stracke, A., Bogaard, P. van den, Bogaard, 2012. Ultrapotassic mafic rocks as geochemical proxies for post-collisional dynamics of orogenic lithospheric mantle: the case of southwestern Anatolia, Turkey. J. Petrol. 53, 1019–1055.

Purvis, M., Robertson, A., 2004. A pulsed extension model for the Neogene-Recent E-W-trending Alaşehir Graben and the NE-SW-trending Selendi and Gördes Basins, Western Turkey. Tectonophysics, 391, 171–201.

Purvis, M., Robertson, A., 2005. Sedimentation of the Neogene-Recent Alasehir (Gediz) continental graben system used to test alternative tectonic models for Western (Aegean) Turkey. Sedimentary Geology 173, 373–408.

Purvis, M., Robertson, A., Pringle, M., 2005. Ar-40-Ar-39 dating of biotite and sanidine in tuffaceous sediments and related intrusive rocks: Implications for the Early Miocene evolution of the Gördes and Selendi basins, W Turkey. Geodinamica Acta 18, 239–253.

Régnier, J.I., Ring, U., Passchier, C.W., Gessner, K., Güngör, T., 2003. Contrasting Metamorphic Evolution of Metasedimentary Rocks From The Çine and Selimiye Nappes In The Anatolide Belt, Western Turkey. Journal of Metamorphic Geology 21, 699–721.

Régnier, J.L., Mezger, J.E., Passchier, C.W., 2007. Metamorphism of Precambrian–Palaeozoic schists of the Menderes core series and contact relationships with Proterozoic orthogneisses of the Western Çine Massif, Anatolide belt, Western Turkey. Geological Magazine 144, 67–104.

Richardson, B.J.M., 1996. The Kula volcanic field, Western Turkey; the development of a Holocene alkali basalt province and the adjacent normal-faulting graben. Geological Magazine 133, 275–283.

Rimmele, G., Oberhansli, R., Goffe, B., Jolivet, L., Candan, O., Cetinkaplan, M., 2003. First evidence of high-pressure metamorphism in the “Cover series” of the southern Menderes Massif. Tectonic implications and metamorphic implications for the evolution of SW Turkey. Lithos 71, 19-46.

Ring, U., 1999. Structural analysis of a complex nappe sequence and late-orogenic basins from the Aegean island of Samos, Greece. Journal of Structural Geology 21, 1575-1601.

Ring, U., Collins, A.S., 2005. U-Pb SIMS dating of synkinematic granites: timing of core-complex formation in the northern Anatolide belt of Western Turkey. Journal of Geological Society of London 162, 289–298.

Ring, U., Gessner, K., Güngör, T., Passchier, C.W., 1999a. The Menderes Massif of Western Turkey and the Cycladic Massif in the Aegean - do they really correlate? Journal of Geological Society of London 156, 3–6.

Ring, U., Johnson, C., Hetzel, R., Gessner, K., 2003. Tectonic Denudation of a Late Cretaceous-Tertiary collisional belt: regionally symmetric cooling patterns and their relation to extensional faults in the Anatolide belt of Western Turkey. Geological Magazine 140, 421–441.

Ring, U., Susanne, L., Matthias, B., 1999b. Structural analysis of a complex nappe sequence and late orogenic basins from the Aegean Island of Samos, Greece. Journal of Structural Geology 21, 1575–1601.

Ring, U., Willner, A.P., Lackman, W., 2001. Stacking of nappes with different pressure-temperature paths: An example from the Menderes nappes of western Turkey: American Journal of Science 301, 912-944.

Rojay, B., Toprake, V., Demirci, C., Süzen, L., 2005. Plio-Quaternary evolution of the Küçük Menderes Graben southwestern Anatolia, Turkey. Geodinamica Acta 18, 317–331.

Sarıca, N., 2000. The Plio-Pleistocene age of Buyuk Menderes and Gediz grabens and their tectonic significance on N-S extensional tectonics in west Anatolia: Mammalian evidence from the continental deposits: Geological Journal 35, 1–24.

Satır, M. Friedrichsen, H., 1989. The origin and evolution of the Menderes Massif, W-Turkey: A rubidium/strontium and oxygen isotope study: Geologische Rundschau 75/3, 703-714.

Satır, M. Taubald, H., 2001. Hydrogen and oxygen isotope evidence for fluid-rock interactions in the Menderes Massif, western Turkey: International Journal of Earth Sciences 89, 812-821.

Şen, F., 2004, Karadut ve cevresinde Gediz grabeni' nin stratigrafisi ve yapisi [B.Sc. thesis]: İstanbul, İstanbul University, (in Turkish), 110 p.

Şen, S., de Bonis, L., Dalfes, N., Geraads, D., Koufos, G., 1994. Les gisements de mammife`res du Mioce`ne supe´rieur de Kemiklitepe, Turquie: 1. Stratigraphie et magnetostratigraphie. Bull. Mus. Natl. Hist. Nat., Paris, 4e`me Ser., Section 16, 5–17.

Şengör, A.M.C., 1979. The North Anatolian transform fault: its age, offset and tectonic significance. Journal of the Geological Society of London 136, 269-282.

Şengör, A.M.C., 1986. The duel nature of the Alpine-Himalayan system; progress, problems and Prospects: Tectonophysics 127, 177-195.

Şengör, A.M.C., 1987. Cross-faults and differential stretching of hanging walls in regions of low-angle normal faulting: examples from Western Turkey. In: Coward, M.P., Dewey, J.F., Hancock, P. (Eds.), Continental Extensional Tectonics. Journal of Geological Society of London 575–589.

Şengör, A.M.C., Görür, N., Saroglu, F., 1985. strike-slip deformation basin formation and sedimentation: Strike-slip faulting and related basin formation in zones of tectonic escape: Turkey as a case study. In: Biddle, K. T. & Christie-Blick, N. (eds) Strike - slip Faulting and Basin Formation. Society of Economic Paleontologists and Mineralogist Special Publication 37, 227-64.

Şengör, A.M.C., Satır, M., Akkök, R., 1984. Timing of tectonic events in the Menderes Massif, Western Turkey: implications for tectonic evolution and evidence for Pan-African basement in Turkey. Tectonics 3, 693–707.

Şengör, A.M.C., Yılmaz, Y., 1981. Tethyan Evolution of Turkey: A Plate Tectonic Approach. Tectonophysics 75, 181–241.

Seyitoğlu, G., 1997a. Late Cenozoic tectono-sedimentary development of the Selendi and Uşak-Güre basins: a contribution to the discussion on the development of east-west and north trending basins in Western Turkey. Geological Magazine 134, 163–175.

Seyitoğlu, G., 1997b. The Simav graben: An example of young E-W trending structures in the late Cenozoic extensional system of Western Turkey. Turkish Journal of Earth Science 6, 135–141.

Seyitoğlu, G., Alçiçek, M.C., Işık, V., Alçiçek, H., Mayda, S., Varol, B., Yılmaz, İ., Esat, K., 2009. The stratigraphical position of Kemiklitepe fossil locality (Uşak-Eşme) revisited: Implications for the Late Cenozoic sedimentary basin development and extensional tectonics in Western Turkey. Neues Jahrbuch für Geologie und Paläontologie 251, 1–15.

Seyitoğlu, G., Anderson, D., Nowell, G., Scott, B., 1997. The evolution from Miocene potassic to Quaternary sodic magmatism in Western Turkey: implications for enrichment processes in the lithospheric mantle. Journal of Volcanology and Geothermal Research 76, 127–147.

Seyitoğlu, G., Çemen, İ., Tekeli, O., 2000. Extensional folding in the Alaşehir graben, western Turkey. Journal of the Geological Society of London, 157, 1097-1100.

Seyitoğlu, G., Isik, V., Çemen, I., 2004. Complete Tertiary exhumation history of the Menderes massif, western Turkey: an alternative working Hypothesis: Terra Nova 16, 358-364.

Seyitoğlu, G., Scott, B. C., 1996. The cause of north-south extensional tectonics in western Turkey: Tectonic escape vs. Back-arc spreading vs. Orogenic collapse. Journal of Geodynamics 22, 145-153.

Seyitoğlu, G., Scott, B.C., 1991. Late Cenozoic crustal extension and basin formation in west Turkey. Geological Magazine, 128, 155–166.

Seyitoğlu, G., Scott, B.C., 1994a. Late Cenozoic basin development in west Turkey: Gördes basin tectonics and sedimentation. Newsletter Stratigraphy 131, 133–142.

Seyitoğlu, G., Scott, B.C., 1994b. Neogene palynological and isotopic age data from Gördes basin, West Turkey. Newsletter Stratigraphy 31, 133-142.

Seyitoğlu, G., Scott, B.C., Rundle, C.C., 1992. Timing of Cenozoic extensional tectonics in west Turkey. Journal of the Geological Society of London 149, 533-538.

Seyitoğlu, G., Tekeli, O., Çemen, I., Şen S., Işık, V., 2002. The role of the flexural rotation/rolling hinge model in the tectonic evolution of the Alaşehir graben, western Turkey. Geological Magazine 139, 15-26.

Sözbilir, H., 2001. Extensional tectonics and the geometry of related macroscopic structures: field evidence from the Gediz Detachment, Western Turkey. Turkish Journal of Earth Science 10, 51–67.

Sözbilir, H., 2002. Revised stratigraphy and facies analysis of the Palaeocene-Eocene supra-allochthonous sediments and their tectonic significance (Denizli, SW Turkey). Turkish Journal of Earth Science 11, 1–27.

Spakman, W., Wortel, M. J. R., Vlaar, N. J., 1988. The Hellenic subduction zone: A tomographic image and its geodynamic implications. Geophysical Research Letters 15, 60-63.

Stampli, S. M., 2000. Tethyan Oceans, Geological Society Special Publications 173, 1-23.

Tankut, A., Dilek, Y., Önen, P., 1998. Petrology and geochemistry of the Neo-Tethyan volcanism as revealed in the Ankara melange, Turkey. Journal of Volcanology and Geothermal Research 85, 265-284.

Taymaz, T., Jackson, J.A., McKenzie, P., 1991. Active Tectonics of North and Central Aegean Sea. Geophysical Journal of International 106, 433-490.

Wernicke, B. P, 1985. Uniform-sense normal simple shear of the continental lithosphere. Canadian Journal of Earth Sciences 22, 108-125.

Wernicke, B. P, 1988. On the role of isostasy in the evolution of normal fault systems: Geology 16, 848-851.

Wernicke, B. P., 1981. Low angle normal faults in the Basin and Range province: nappe tectonics in an extending Orogen. Nature 291, 645-648

Wernicke, B., 1992. Cenozoic extensional tectonics of the US Cordillera: Geological Society of America, The Geology of North America, v. G-3, p. 553-581.

Wernicke, B., Axen, G. J., Snow, J. K., 1988. Basin and Range extensional tectonics at the latitude of Las Vegas, Nevada, Geological Society of America Bulletinn 100, 1738-1757.

Westaway, R., Pringle, M., Yurtmen, S., Demir, T., Bridgland, D., Rowbotham, G., Maddy, D., 2004. Pliocene and Quaternary regional uplift in Western Turkey: the Gediz River terrace staircase and the volcanism at Kula. Tectonophysics 391, 121–169.

Whitney, D.L. and Bozkurt, E., 2002. Metamorphic history of the southern Menderes massif, western Turkey. Geological Society of America Bulletinn 114, 829-838.

Wright, L.A., Troxel, B., 1973. Shallow fault interpretation of Basin and Range Structure, Southwestern Great Basin, in De Jong, K. A., and Scholten, R., (eds.), Gravity and Tectonics: New York, John Wiley and Sons, 397-407.

Yağmurlu, F., 1984, Akhisar doğusunda kömür içeren Miyosen tortulların stratigrafisi, depolanma ortamları ve tektonik özellikleri. [Stratigraphy, depositional environment and tectonic features of the coal-bearing Miocene sediments in the east of Akhisar]. Bulletin of the Geological Society of Turkey 5, 3–20.

Yılmaz, Y., Genç, Ş.C., Gürer, F., Bozcu, M., Yılmaz, K., Karacık, Z., Altunkaynak, Ş., Elmas, A., 2000. When did the Western Anatolian grabens begin to develop? In: Bozkurt, E. Winchester, J.A. & Piper J.A.D. (eds), Tectonics and Magmatism in Turkey and the Surrounding Area. Journal of Geological Society of London 173, 131–162.